

**Development of a portable Raman and  
Near Infrared Spectrometer for quality  
assessment of Medicinal Plants**

*Thesis Submitted By*

**DILIP SING**

*Doctor of Philosophy (Engineering)*

**Department of Instrumentation and Electronics Engineering  
Faculty Council of Engineering & Technology  
Jadavpur University  
Kolkata -700032  
2021**

**JADAVPUR UNIVERSITY**

**KOLKATA – 700 032**

**Index Number: D7/E/351/19**

Title of the Thesis

Development of a portable Raman  
and Near Infrared Spectrometer for  
quality assessment of Medicinal  
Plants

Name, Designation &  
Institution of the Supervisors

Prof. Rajib Bandyopadhyay  
Professor  
Dept. of Instrumentation &  
Electronics Engg., Salt Lake Campus,  
Jadavpur University,  
Kolkata-700106, India

Prof. Pulok K. Mukherjee,  
Director  
Institute of Bioresources and  
Sustainable Development (IBSD),  
Takyelpat, Imphal,  
Manipur- 795001, India

## List of Publications

### I. Papers published in International Journals: 02

1. **Dilip Sing**, Subhadip Banerjee, Shibu Narayan Jana, Ranajoy Mallik, Sudarshana Ghosh Dastidar, Kalyan Majumdar, Amitabha Bandyopadhyay, Rajib Bandyopadhyay, and Pulok K. Mukherjee. “Estimation of Andrographolides and Gradation of *Andrographis Paniculata* Leaves Using Near Infrared Spectroscopy Together With Support Vector Machine.” *Frontiers in Pharmacology*, vol. 12, pp. 1–8, May, 2021. <https://doi.org/10.3389/fphar.2021.629833>.
2. **Dilip Sing**, Shibu Narayan Jana, Subhadip Banerjee, Ranajoy Mallik, Kalyan Majumdar, Pallab Kanti Halder, Amitabha Bandyopadhyay, Nanaocha Sharma, Rajib Bandyopadhyay, and Pulok K. Mukherjee. “Rapid Estimation of Piperine in Black Pepper: Exploration of Raman Spectroscopy.” *Phytochemical Analysis*, pp.1–10, July, 2021. <https://doi.org/10.1002/pca.3080>.

### II. Papers published in International and National/Conference proceedings: 07

1. **Dilip Sing**, Ranajoy Mallik, Shibu Narayan Jana, Bipan Tudu, Kalyan Majumdar, Rajib Bandyopadhyay, “Quantification of piperine in *Piper Nigrum* using a portable Raman Spectrometer”, 7th Asian NIR Symposium 2020. 12-15th Feb,2020, Khonkaen, Thailand.
2. **Dilip Sing**, Subhadip Banerjee, Kalyan Majumdar, Rajib Bandyopadhyay, Pulok K. Mukherjee, “Development of a portable near infrared spectrometer for quality assessment of *Andrographis paniculata*”, 7th Asian NIR Symposium 2020. 12-15th Feb, 2020, Khonkaen, Thailand.
3. **Dilip Sing**, Ranajoy Mallik, Subhadip Banerjee, Shibu Narayan Jana, Kalyan Majumdar, Rajib Bandyopadhyay “In-situ discrimination of *Piper Nigrum* seeds based on piperine content: Application of Raman Spectroscopy” PSE-NPS 2020 Summit, 16-18th Jan, 2020, Khulna University, Khulna, Bangladesh.
4. **Dilip Sing**, Subhadip Banerjee, Rajib Bandyopadhyay and Pulok K. Mukherjee “Non-invasive quality estimation of *Piper Nigrum* using a developed a portable Raman Spectrometer”, *Contemporary Trends in Optics 2019 (CoOpt-2019)*, 20-23rd May, 2019, Indian Institute of Science Education and Research Kolkata, Kolkata, India.
5. **Dilip Sing**, Somdeb Chanda, Kallol Bera, Rajib Bandyopadhyay, Subhadip Banerjee, Shibu Narayan Jana, and Pulok K. Mukherjee, “In situ non-invasive measurement of Andrographolide in *Andrographis paniculata* using spectroscopic

methods,” The 6 International Congress of the Society for Ethnopharmacology, India (SFEC 2019), February 8-10, 2019, Manipal, India.

6. **Dilip Sing**, Somdeb Chanda, Subhadip Banerjee, Bipan Tudu, Kalyan Majumdar, Rajib Bandyopadhyay and Pulok K. Mukherjee, “Exploration of near infrared spectroscopy for *Andrographis paniculata*: Discrimination between samples with different andrographolide content”, The Sixth Asian NIR Symposium (ANS2018), June 21- 24, 2018, Kunming City, China.
7. **Dilip Sing**, Somdeb Chanda, Subhadip Banerjee, Shibu Narayan Jana, Bipan Tudu, Rajib Bandyopadhyay and Pulok K. Mukherjee, “Development of a portable Raman Spectrometer for quality measurement of piperine in *Piper Nigrum*,” National Symposium on “Promotion and Development of Indian Medicinal Plants” Special Reference - Brahmi, September 7- 8, 2018, Kolkata, India.

### III. Book chapters contributed: 01

Chapter Title: "Application of NIR and Raman Spectroscopy for quality evaluation and gradation of medicinal plants: Possibilities and challenges" Authors: Rajib Bandyopadhyay, **Dilip Sing**, Sudarshana Ghosh Dastidar, Subhadip Banerjee, Pulok Kumar Mukherjee, 2nd edition of the book entitled “Evidence-Based Validation of Herbal Medicine” edited by Prof. Pulok K. Mukherjee, Elsevier, USA

### IV. List of Patents: Nil

### V. List of presentations in National/ International/ Conferences/ Workshop: 06

1. **Dilip Sing**, Ranajoy Mallik, Shibu Narayan Jana, Bipan Tudu, Kalyan Majumdar, Rajib Bandyopadhyay, “Quantification of piperine in *Piper Nigrum* using a portable Raman Spectrometer”, 7th Asian NIR Symposium 2020. 12-15th Feb, 2020, Khonkaen, Thailand.
2. **Dilip Sing**, Subhadip Banerjee, Kalyan Majumdar, Rajib Bandyopadhyay, Pulok K. Mukherjee, “Development of a portable near infrared spectrometer for quality assessment of *Andrographis paniculata*”, 7th Asian NIR Symposium 2020. 12-15th Feb, 2020, Khonkaen, Thailand.
3. **Dilip Sing**, Ranajoy Mallik, Subhadip Banerjee, Shibu Narayan Jana, Kalyan Majumdar, Rajib Bandyopadhyay “In-situ discrimination of *Piper Nigrum* seeds based on piperine content: Application of Raman Spectroscopy” PSE-NPS 2020 Summit, 16-18th Jan, 2020, Khulna University, Khulna, Bangladesh.
4. **Dilip Sing**, Subhadip Banerjee, Rajib Bandyopadhyay and Pulok K. Mukherjee “Non-invasive quality estimation of *Piper Nigrum* using a developed a portable Raman Spectrometer”, Contemporary Trends in Optics 2019 (CoOpt-2019), 20-23rd May, 2019, Indian Institute of Science Education and Research Kolkata, Kolkata, India.

5. **Dilip Sing**, Somdeb Chanda, Kallol Bera, Rajib Bandyopadhyay, Subhadip Banerjee, Shibu Narayan Jana, and Pulok K. Mukherjee, “In situ non-invasive measurement of Andrographolide in *Andrographis paniculata* using spectroscopic methods,” The 6 International Congress of the Society for Ethnopharmacology, India (SFEC 2019), February 8-10, 2019, Manipal, India.
6. **Dilip Sing**, Somdeb Chanda, Subhadip Banerjee, Shibu Narayan Jana, Bipan Tudu, Rajib Bandyopadhyay and Pulok K. Mukherjee, “Development of a portable Raman Spectrometer for quality measurement of piperine in Piper Nigrum,” National Symposium on “Promotion and Development of Indian Medicinal Plants” Special Reference - Brahmi, September 7- 8, 2018, Kolkata, India.

## **“Statement of Originality”**

I, **Dilip Sing**, registered on 04/06/2019 do hereby declare that this thesis entitled **“Development of a portable Raman and Near Infrared Spectrometer for quality assessment of Medicinal Plants”** contains literature survey and original research work done by the undersigned candidate as part of Doctoral studies.

All information in this thesis have been obtained and presented in accordance with existing academic rules and ethical conduct. I declare that, as required by these rules and conduct, I have fully cited and referred all materials and results that are not original to this work.

I also declare that I have checked this thesis as per the “Policy on Anti Plagiarism, Jadavpur University, 2019”, and the level of similarity as checked by iThenticate software is 5%.

Dilip Sing  
Index No. D-7/E/351/19  
Date: 30/09/2021

Certified by Supervisors

Prof. Rajib Bandyopadhyay  
Professor  
Dept. of Instrumentation & Electronics  
Engg., Salt Lake Campus,  
Jadavpur University,  
Kolkata-700106, India

Prof. Pulok K. Mukherjee,  
Director  
Institute of Bioresources and  
Sustainable Development  
(IBSD), Takyelpat, Imphal,  
Manipur- 795001, India

## CERTIFICATE FROM THE SUPERVISORS

This is to certify that the thesis entitled “**Development of a portable Raman and Near Infrared Spectrometer for quality assessment of Medicinal Plants**” submitted by Shri **Dilip Sing**, who got his name registered on 04/06/2019 for the award of Ph. D. (Engg.) degree of Jadavpur University is absolutely based upon his own work under the supervision of Prof. Rajib Bandyopadhyay, Dept. of Instrumentation & Electronics Engg., Salt Lake Campus, Jadavpur University, Kolkata-700106, India and Prof. Pulok K. Mukherjee, Director, Institute of Bioresources and Sustainable Development (IBSD), Takyelpat, Imphal, Manipur- 795001, India and that neither his thesis nor any part of the thesis has been submitted for any degree/diploma or any other academic award anywhere before.

Prof. Rajib Bandyopadhyay  
Professor  
Dept. of Instrumentation & Electronics  
Engg., Salt Lake Campus,  
Jadavpur University,  
Kolkata-700106, India

Prof. Pulok K. Mukherjee,  
Director  
Institute of Bioresources and  
Sustainable Development  
(IBSD), Takyelpat, Imphal,  
Manipur- 795001, India

**DEDICATED TO  
MY PARENTS  
MR. JUGAL SING  
&  
MRS. SATADAL SING**



## **Acknowledgements**

*It is my great privilege to record deep sense of gratitude and indebtedness to **Prof. Rajib Bandyopadhyay**, Department of Instrumentation & Electronics Engineering, Jadavpur University, Kolkata and **Prof. Pulok K. Mukherjee**, Director, Institute of Bioresources and Sustainable Development (IBSD), Imphal, Manipur for providing me a very helpful and invaluable guidance in every phase of the program, without which completion of this thesis would not have been possible. I would also like to take this opportunity to express heartiest regards and gratitude towards **Mr. Kalyan Majumdar** for his guidance in design, development, and calibration of prototype. In addition, I also thankful to Prof. Bipan Tudu, for his support to pursue this Ph.D. Also, I am deeply indebted to Dr. Nabarun Bhattacharyya, Senior Director and Centre Head, Centre for Development of Advanced Computing (C-DAC) and Dr. Amitabha Bandyopadhyay, Retired Scientist, Indian Council of Agricultural Research, Delhi for their unstinted support and guidance in implementation and field-trial activities taken up under the programme.*

*This PhD project was carried out in collaboration of Department of Instrumentation & Electronics Engineering (IEE), and School of Natural Product Studies (SNPS) of Jadavpur University West Bengal, India with Institute of Bioresources and Sustainable Development (IBSD), Imphal, Manipur. My sincere gratitude goes to all those organizations and personnel who actively helped in field trial and evaluation activities. Those who deserve special mention in this regard are Dr. Somdeb Chanda, and Mr. Gautam Majumdar of Dept of IEE, Jadavpur University for their support and encouraging me during my PhD journey. Also, special acknowledgement goes to the **Tata Trust**, Rashtriya Uchchatar Shiksha Abhiyan (**RUSA**) 2.0 of Jadavpur University, and National Medicinal Plants Board (**NMPB**) of Govt. of India for funding the work.*

*Mr. Subhadip Banerjee, and Mr. Shibu Narayan Jana of School of Natural Product Studies of Jadavpur University have been integral part of the studies and experimentation in this work. I record my heart-felt gratitude for their diligent and valuable assistance. Mr. Kallol Bera, Mr. Ranjoy Mallik, Ms. Sudarshana Ghosh Dastidar, of Jadavpur University have immensely contributed in electronic and mechanical assembly jobs associated with the program as and when necessary and my sincere thanks and gratitude goes to them. Besides, I also want to extend my heartfelt gratitude to those whom I have not mentioned here but offered help during my PhD life.*

*Last but not the least, this work involved lot of travels for field experimentations and long hours at the laboratories for study, drafting of publications etc. I take this opportunity to express my deep sense of gratitude to **my family members** for their inspiration and encouragement throughout this work.*

Dilip Sing

Department of Instrumentation and Electronics Engineering

Jadavpur University, Salt Lake Campus,

Kolkata –700106,

West Bengal, India

September, 2021

# Abstract

Medicinal plants are the integral components of alternative medical care in the world and the herbal medicines manufactured from these plants serve the primary healthcare needs of the majority of the world's population. There are varied problems in this sector primarily due to absence of knowledgebase on the chemotypic diversity of medicinal plants.

One of the most important attributes of these plant species is the chemotypic variation with respect to the major bioactive therapeutic compounds and the most important synergistic compounds that enhance the potential of the primary compounds. The conventional methods of measurement using High-performance liquid chromatography (HPLC), Thin-layer chromatography (TLC), Liquid chromatography–mass spectrometry (LCMS), and Gas chromatography–mass spectrometry (GCMS) are very accurate and precise, but are complex, expensive and requires skilled manpower as most of the measurements are based on chemical methods and lab based. It cannot be used in the field or in the industry for day-to-day use. In this respect, the portable measurement systems based on Raman and Near Infrared (NIR) Spectroscopy are promising and, if tuned properly, can be used for many such applications.

The basic goal of the thesis is to develop sensor systems for detection and quantification of the major active groups of compounds in a few medicinal plants such as *Andrographis paniculate* (Kalmegh), *Piper nigrum* (black pepper) plants.

The design and development of a portable Raman and NIR spectrometer with customized GUI is presented in this research work. The integrated Raman spectrometer consists of laser power supply, optical head and detector and a customized GUI was developed to estimate the piperine content in black pepper for assessing its quality. The portable NIR has a light source and optical components and detector, and a GUI for the quantitative estimation of andrographolides in *Andrographis paniculata* for its gradation and quality assessment

In this work, a methodology is proposed for determining the content of piperine in black pepper berries using Raman spectroscopy. In this study, we present a simple, rapid and green analytical method based on Raman spectroscopy for the quantitative assessment of piperine. To assess the potential of the technique, we report the complete vibrational characterisation of the piperine with density functional theory (DFT) calculations. The theoretical peaks were obtained at  $1097\text{ cm}^{-1}$ ,  $1388\text{ cm}^{-1}$ ,  $1528\text{ cm}^{-1}$ ,  $1578\text{ cm}^{-1}$ , and at  $1627\text{ cm}^{-1}$ , and this result was verified in a Raman spectrometer followed by a preliminary experiment. Twenty black

pepper samples were analysed using high-performance liquid chromatography (HPLC) and used as reference data for Raman analysis. The Raman shift spectra were analysed using partial least squares (PLS) and good prediction accuracy with correlation coefficient of prediction ( $R_p^2$ )= 0.93, root mean square error of prediction (RMSEP) = 0.13 and residual prediction deviation (RPD) = 3.9 obtained. The results demonstrate the efficacy of the Raman technique for the estimation of piperine in the dry fruit of *Piper nigrum*. Thus, this method can be suitably applied for in situ quality detection of inward medicinal plant leaves in medicinal plant industry.

In this study, a methodology has been proposed to grade *Andrographis paniculata* samples using NIR spectroscopy and SVM classifier based on the content of marker molecules, andrographolides. Relative accuracies of estimating the andrographolides by NIR spectra of methanol extracts of the samples, and powdered leaf samples were compared taking the estimates obtained from HPLC analysis as the standard. The accuracy of estimation based on extracts was a little higher than the powder leaf samples. But it did not change the grading pattern of the samples. Support vector machine was used to grade the samples into three classes—Class I (best quality), Class II (intermediate quality) and Class III (poor quality). The average classification accuracy of tenfold cross validation of SVM was obtained as 83%. Thus, NIR based estimation of powdered leaf samples combined with SVM classifier can be a low-cost solution to grade the samples rapidly. A small range portable NIR instrument would serve as a field-lab deployable instrument for gradation of *Andrographis paniculata* samples by the industry.

# Abbreviations

1d	First derivative
2d	Second derivative
ADC	Analog to Digital Converter
B	Bending
CARS	Competitive adaptive reweighted sampling
CMOS	Complementary metal oxide semiconductor
CVA	Change Vector Analysis
CWL	Centre Wavelength
DFT	Density Functional Theory
DLL	Dynamic link library
DM	Dichroic Mirror
DT	Diffuse transmittance
DR	Diffuse reflectance
EMSC	Extended multiplicative scatter correction
FIR	Far infrared
FT-NIR	Fourier transform near infrared
FWHM	Full width at half maximum
GCMS	Gas Chromatography Mass spectroscopy
GUI	Graphical user interface
HPLC	High Performance Liquid Chromatography
ICH	International Conference on Harmonization
InGaAs	Indium gallium arsenide
IP	Indian Pharmacopoeia
IR	Infrared
KELM	Kernel extreme learning machine
KNN	K-Nearest neighbour
LC-MS	Liquid Chromatography Mass Spectroscopy
LDA	Linear Discriminant Analysis
LOD	Limit of Detection
LOQ	Limit of Quantification
MC	Mean Centering
MIR	Mid infrared
MLR	Multiple linear regression
MSC	Multiplicative Scatter Correction
MW-PLS-DA	Moving window partial least-squares discriminant
NIR	Near infrared
NIST	National Institute of Standards and Technology
OPA	Off-Axis Parabolic Mirror
PC1	First Principle Component
PC2	Second Principle Component
PCA	Principal Component Analysis

PLS-DA	Partial Least Squares Discriminant Analysis
PLSR	Partial Least Squares Regression
QC	Quality control
Rc2	Correlation Coefficient of Calibration
RFL	Reflected focal length
RMSEC	Root Mean Square Error of Calibration
RMSEP	Root Mean Square Error of Prediction
Rp2	Correlation Coefficient of Prediction
RPD	Residual Prediction Deviation
RP-HPLC	Reversed-phase High Performance Liquid Chromatography
RQ	Research questions
RSD	Relative standard deviation
S	Stretching
S-G	Savitzky-Golay smoothing
SI	Separability Index
SPXY	Sample set partitioning based on joint x-y distances
TEC	Thermo-Electric cooling
TM	Traditional Medicine
USDA	United States Department of Agriculture
UV/Vis	Ultraviolet/visible

## List of figures

Figure 1. 1 Challenges faced in the quality control of herbal drug preparations. _____	5
Figure 1. 2 Quality control methods in evaluating herbal medicinal products. _____	6
Figure 1. 3 Importance of marker analysis in drug development from natural resources _____	7
Figure 1. 4 Photograph of LCMS _____	8
Figure 1. 5 Photograph of HPLC _____	8
Figure 1. 6 Photograph of GCMS _____	8
Figure 1. 7 Illustration of Raman and Rayleigh scatter rays from a sample molecule _____	11
Figure 1. 8 Graphical representation of Rayleigh scattering, Stokes, and anti-Stokes Raman _____	11
Figure 1. 9 Electromagnetic spectrum and transmission characteristics _____	13
Figure 1. 10 Pathways of light through a sample _____	14
Figure 2. 1 Block diagram of the laser power supply _____	41
Figure 2. 2 Measured laser current versus calculated current _____	45
Figure 2. 3 Three dimensional model of the Laser power supply circuit. (top view) _____	46
Figure 2. 4 3D model of the complete laser power supply with housing (View-1). _____	46
Figure 2. 5 3D model of the complete laser power supply with housing (View-2). _____	46
Figure 2. 6 Prototype of proposed laser power supply circuit. _____	47
Figure 2. 7 Photograph of Laser power supply of a Raman Spectrometer _____	47
Figure 2. 8 PC-based GUI for the laser power supply. _____	48
Figure 2. 9 Optical assembly of the Raman spectrometer with all its components. The beam path is shown with coloured arrows. (Laser not shown) _____	51
Figure 2. 10 3D model of the proposed optical assembly _____	52
Figure 2. 11 Photograph of the Optical setup. _____	52
Figure 2. 12 Optical component layout of the detector _____	53
Figure 2. 13 Block diagram of the optical head. _____	54
Figure 2. 14 3D model of the optical head of portable Raman spectrometer _____	55
Figure 2. 15 Inside Photograph of the prototype Raman spectrometer with its associated components _____	55
Figure 2. 16 3D model of the portable Raman spectrometer _____	55
Figure 2. 17 Photograph of the developed prototype portable Raman spectrometer _____	55
Figure 2. 18 GUI of the SpecEvaluationUSB2 software from Hamamtsu Photonic _____	57
Figure 2. 19 Illustration of the concept of wrapper dll to be used along with the original dll. _____	59
Figure 2. 20 GUI developed for the Raman spectrometer using MATLAB App designer. _____	60
Figure 2. 21 Standalone GUI for Piperine content estimation _____	62
Figure 2. 22 Raman spectra of Benzene obtained from the developed Raman spectrometer _____	64
Figure 2. 23 Raman spectra of Chloroform obtained from the developed Raman spectrometer _____	66

Figure 2. 24 Raman spectra of Glacial acetic acid obtained from the developed Raman spectrometer.	67
Figure 2. 25 Raman spectra of piperine obtained from the developed Raman spectrometer	69
Figure 3. 1 Block diagram of regression modeling for chemical analysis using Raman spectroscopy.	72
Figure 3. 2 Two dimensional Ball and Stick Model of Piperine	77
Figure 3. 3 B3LYP/6–31G(d) optimized geometry of Piperine molecule.	77
Figure 3. 4 The raw and baseline corrected Raman spectra of black pepper.	80
Figure 3. 5 PCA plot with first two PC.	81
Figure 3. 6 LDA plot with first two components.	82
Figure 3. 7 RMSE comparison of calibration results for 15 samples obtained SNV for component number 1 to 10	83
Figure 3. 8 Scatter diagram of calibration set by PLS using preprocessing of SNV.	84
Figure 3. 9 Scatter diagram of prediction set by PLS using preprocessing of SNV	85
Figure 3. 10 Scatter plot of actual versus measured piperine values for the calibration set.	86
Figure 3. 11 Scatter plot of actual versus measured piperine values for the prediction set.	87
Figure 4. 1 3D model of the proposed optical assembly of the NIR spectrometer.	98
Figure 4. 2 Developed prototype of the Optical assembly of the NIR Spectrometer.	99
Figure 4. 3 Closer view of the arrangement of optical components in the developed NIR spectrometer.	99
Figure 4. 4 Block diagram of the optical assembly of developed NIR spectrometer.	99
Figure 4. 5 Block diagram illustrating communication between	102
Figure 4. 6 Layout of the GUI created using MATLAB App Designer.	102
Figure 4. 7 GUI developed for the NIR spectrometer using	103
Figure 4. 8 Perdition tab of developed GUI for NIR spectroscopy	104
Figure 4. 9 Flow diagram of the process involved in real-time prediction of	105
Figure 4. 10 Lattepanda delta 432 single board PC (left).	106
Figure 4. 11 Touch display connected to single board PC	106
Figure 4. 12 Internal arrangement of the proposed NIR spectrometer setup inside the enclosure.	107
Figure 4. 13 Top view of the proposed NIR spectrometer setup inside the enclosure.	107
Figure 4. 14 3D model of the NIR spectrometer proposed setup with the enclosure and the touch display	108
Figure 4. 15 Top view of the actual prototype of the NIR spectrometer setup inside the enclosure	108
Figure 4. 16 Internal arrangement of the actual prototype of the developed NIR spectrometer setup inside the enclosure.	108
Figure 4. 17 Actual prototype of the developed NIR spectrometer with the enclosure and graphical user interface.	108
Figure 5. 1 HPLC chromatogram of (a) Andragrapholides Standard (b) Andrographis paniculata extract sample.	117
Figure 5. 2 Experimental workflow of (a) chemical analysis. (b) training, (c) testing.	119
Figure 5. 3 Wavelength versus absorbance of the original spectra without any pre-processing.	120



Figure 5. 4 Chemical structure of andrographolides. _____	120
Figure 5. 5 Loading plot of the first 4 PCs of MSC preprocessed spectra of <i>Andrographis paniculata</i> . _____	121
Figure 5. 6 PCA plot with first two PC. _____	121
Figure 5. 7 LDA plot with first two components. _____	122
Figure 5. 9. Wavelength versus absorbance plot of the raw spectra. _____	126
Figure 5. 10 Wavelength versus absorbance plot of the SNV pre-processed spectra. _____	126
Figure 5. 11 Wavelength versus absorbance plot of the MSC pre-processed spectra. _____	127
Figure 5. 12 Loading plots of the first four principal components of the raw spectra. _____	127
Figure 5. 13 Loading plots of the first four principal components of _____	128
Figure 5. 14 PCA analysis plot. _____	129
Figure 5. 15 RMSECV vs. Number of components plot. _____	130
Figure 5. 16 Scatter plot of PLSR of raw data. _____	131
Figure 5. 17 Scatter plot of SVM of raw data. _____	131

## **List of tables**

Table 1. 1 Estimated Annual Values of Herbal Medicines and Some Health Foods _____	3
Table 1. 2 Examples of recent research activities on NIR spectroscopy and Raman spectroscopy for analysis of medicinal plant and various chemometric tools used therein. _____	18
Table 2. 1 Comparison of different Raman systems available in the market .....	38
Table 2. 2 The components used for the laser power supply .....	42
Table 2. 3. List of components used to develop a portable Raman Spectrometer .....	49
Table 2. 4 Important specifications for the developed portable Raman spectrometer.....	56
Table 2. 5 Comparison of Raman shift ( $\text{cm}^{-1}$ ) of Benzene in the developed spectrometer with other reports .....	63
Table 2. 6 Comparison of Raman shift ( $\text{cm}^{-1}$ ) of Chloroform in the developed spectrometer with other reports.....	65
Table 2. 7 Comparison of Raman shift ( $\text{cm}^{-1}$ ) of Glacial acetic acid in the developed spectrometer with other reports .....	66
Table 2. 8 Comparison of Raman shift ( $\text{cm}^{-1}$ ) of piperine in the developed spectrometer with other reports .....	68
Table 3. 1 Statistics about piperine content in the measured black pepper samples used for calibration and prediction sets. ....	74
Table 3. 2 Experimental and theoretical vibrational Raman data of piperine with the proposed assignments.....	78
Table 3. 3 Test result of five black pepper samples.....	84
Table 3. 4 Statistics about piperine content in the measured black pepper samples used for calibration and prediction sets. ....	85
Table 3. 5. Test results for the five black pepper samples.....	86
Table 3. 6 Comparison of evaluation performance between our low cost spectrometer and the spectrometer used by Sing et al. referred above.....	88
Table 4. 1 Comparison of different NIR systems available in the market.....	94
Table 4. 2 List of components used to develop a portable NIR Spectrometer _____	97
Table 4. 3 Measurement parameters to be set for acquiring spectral data _____	101
Table 4. 4 Instrumental and operational key performance attributes of developed portable NIR spectrometer.....	109
Table 5. 1 Result of HPLC and NIR and the grades of the 18 samples.....	122
Table 5. 2 Result of 10-fold cross-validation method.....	124
Table 5. 3 Statistics about andrographolide content in the <i>Andrographis paniculata</i> _____	125
Table 5. 4 Performance of partial least square regression (PLSR) and support vector machine (SVM) full-band models using different preprocessing methods for andrographolide content in the <i>Andrographis paniculata</i> using developed NIR spectrometer. _____	131

# **Table of Contents**

Short Bibliography	i
List of Publications	ii-iii
Statement of originality	iv
Certificate from the Supervisors	v
Acknowledgements	vi-viii
Abstract	ix-x
List of Abbreviations	xi-xii
List of Figures	xiii-xv
List of Tables	xvi
Table of content	xix-xxiii

## **Chapter 1: Introduction & Scope of the thesis 1-35**

1.1 Introduction.....	2
1.2 Benefits of medicinal plants.....	2
1.2.1 Economic Benefits .....	2
1.2.2 Health Benefits.....	3
1.3 Summarized facts of Indian medicinal plants .....	4
1.4 Quality control of medicinal plants: Challenges and solutions .....	5
1.4.1 Standardization of chemical aspects using marker analysis .....	6
1.5 Existing methods for quality estimation of medicinal plants.....	7
1.5.1 Chemical assessment of quality .....	7
1.5.2 Quality assessment using spectroscopy .....	8
1.6 Objectives of the thesis work.....	10
1.7 Brief theory on NIR and Raman spectroscopy .....	11
1.7.1 Brief theory of Raman spectroscopy.....	11
1.7.2 Brief theory of NIR spectroscopy .....	12
1.7.2.2 Origin of absorption bands in NIR .....	13
1.7.2.2 Diffuse reflectance (DR) measurement mode .....	14
1.7.2.3 Diffuse transmittance (DT) measurement mode .....	15
1.8 Literature review .....	16
1.8.1 Raman spectroscopy .....	16

1.8.2 NIR spectroscopy .....	17
1.9 Brief description on Chemometrics .....	20
1.9.1 Pre-processing techniques.....	20
1.9.1.1 Scatter correction .....	21
1.9.1.2 Standard Normal Variate (SNV) .....	21
1.9.1.3 Multiplicative Scatter Correction (MSC) .....	21
1.9.1.4 Mean Centering (MC) .....	22
1.9.1.5 Smoothing.....	22
1.9.1.6 SavitzkyGolay (SG) smoothing.....	22
1.9.1.7 Derivatives.....	22
1.9.2 Clustering, classification and regression techniques: .....	23
1.9.2.1.1 Principal component analysis (PCA).....	23
1.9.2.1.2 Linear discriminant analysis (LDA) .....	23
1.9.2.2 Classification techniques .....	24
1.9.2.2.1 K-Nearest Neighbour (KNN) .....	24
1.9.2.2.2 Support Vector Machine (SVM) .....	24
1.9.2.2.3 Naïve Bayes .....	24
1.9.3 Regression.....	24
1.9.3.1 Partial least squares regression (PLSR).....	25
1.9.3.2 Support Vector Regression (SVR).....	25
1.10 Research questions.....	26
1.11 Thesis structure .....	26

**Chapter 2: Development of a portable Raman spectrometer 36-69**

2.1 Introduction.....	37
2.2 Commercially available Raman spectrometer .....	37
2.3 Development of the portable Raman spectrometer.....	40
2.3.1 Laser Power supply .....	41
2.3.1.1 Working principle of the Laser power supply .....	41
2.3.1.2 Components of the laser power supply.....	42
2.3.1.3 Design and calibration of the electronic circuitry.....	44
2.3.1.4 Developing the graphical user interface for the Laser power supply .....	47
2.3.2 Optical Assembly .....	48

2.3.2.1 Components of the Optical Assembly .....	48
2.3.2.2 Designing of the Optical Assembly .....	50
2.3.3 Detector.....	52
2.3.4 Working principle of the Optical Assembly .....	54
2.3.5 Developing GUI in Visual Studio and MATLAB App Designer.....	56
2.3.5.1 Need of customized GUI for Hamamatsu Raman spectrometer .....	57
2.3.5.2 Designing the GUI.....	58
2.3.5.3 Modules of the GUI.....	60
2.4 Result and discussion for verification and validation of the developed instrument .....	62
2.4.1 Benzene.....	63
2.4.2 Chloroform.....	64
2.4.3 Glacial acetic acid.....	66
2.4.4 Piperine .....	68
2.5 Conclusion .....	69

**Chapter 3: Quality assessment of black pepper with the procured and developed Raman spectrometers** **70-91**

3.1 Introduction.....	71
3.2 Experiment I: Feasibility study of using commercially available Raman spectroscopy for quantification of black pepper .....	73
3.2.1 Material and methods.....	74
3.2.1.1 Chemical and reagent .....	74
3.2.1.2 Plant Material .....	74
3.2.1.3 Extraction.....	75
3.2.1.4 High performance liquid chromatography (HPLC) fingerprints.....	75
3.2.1.5 Method validation.....	75
3.2.1.6 Raman spectral data collection .....	76
3.2.2 Results and discussion .....	76
3.2.2.1 The Piperine Molecule and Its Assignment of Raman Peaks.....	76
3.2.2.2 Data pre-processing .....	80
3.2.2.3 Qualitative analysis using PCA and LDA .....	80
3.2.2.4 Quantitative analysis using PLSR .....	82
3.3 Experiment II: Qualitative estimation of black pepper using our developed portable Raman spectrometer.....	85

3.3.1 Black pepper samples .....	85
3.3.2 Result and discussion.....	86
3.4 Comparison study between commercially available spectrometer and our developed spectrometer.....	87
3.5 Conclusion .....	88

**Chapter 4: Development of a portable NIR spectrometer 92-112**

4.1 Introduction.....	93
4.2 Commercially available NIR spectrometers .....	94
4.3 Development of low-cost portable NIR spectrometer using off-the-shelf optical components and detector.....	96
4.3.1 Optical Assembly of NIR spectrometer .....	96
4.3.1.1 Components of optical assembly .....	96
4.3.2 Designing of the Optical Assembly .....	98
4.3.3 Working principle of the optical assembly of NIR spectrometer .....	99
4.4 Development of customized GUI for the NIR spectrometer .....	100
4.5 NIR spectrometer to work as a standalone instrument .....	106
4.6 Conclusion .....	109
References.....	111

**Chapter 5: Quality assessment of *Andrographis paniculate* with the procured and the developed NIR spectrometer 113-136**

5.1 Introduction.....	114
5.2 Experiment I: Feasibility study of using commercially available NIR spectroscopy for quantification of <i>Andrographis paniculata</i> .....	115
5.2.1 Material and Methods .....	115
5.2.1.1 Plant Material .....	115
5.2.1.2 Chemical Analysis .....	116
5.2.2 Experimental Setup and NIR Spectra Acquisition.....	118
5.2.3 Result and Discussion .....	119
5.2.3.1 Interpretation of Spectroscopic Characterization .....	119
5.2.3.2 Plot of PCA.....	121
5.2.3.3 Plot of LDA .....	122
5.2.3.4 SVM model.....	122

5.3 Experiment II: Qualitative estimation of <i>Andrographis paniculata</i> using our developed portable NIR spectrometer .....	124
5.3.1 Material and methods.....	124
5.3.1.1 Plant Material .....	124
5.3.1.2 NIR spectral data collection .....	124
5.3.2 Results and Discussion .....	126
5.3.2.1 NIR spectra of andrographolides .....	126
5.3.2.2 Exploratory Analysis using PCA.....	128
5.3.2.3 Quantitative analysis using PLSR and SVM.....	129
5.4 Comparison study between commercially available spectrometer and our developed spectrometer.....	132
5.5 Conclusion .....	133
References.....	134

**Chapter 6: Conclusion and future scope 137-142**

6.1 Introduction.....	138
6.2 Summary of findings.....	139
6.2.1 Development of a portable Raman spectrometer.....	139
6.2.2 Estimation of piperine in black pepper .....	139
6.2.3 Development of a portable NIR spectrometer .....	139
6.2.4 Assessment of andrographolides in <i>Andrographis paniculata</i> .....	140
6.3 Limitations during development of instruments and models.....	140
6.4 Future scopes of research.....	141
6.5 Final remark.....	141

# **Chapter 1**

## **Introduction and scope of the thesis**



## 1.1 Introduction

Medicinal plants are integral part of human life since their discovery from prehistoric times. As per the statistics of the World Health Organization (WHO), 80% of the global population depends on plant-based medicines [1–3]. Over the last few years, a remarkable increase in acceptance and attention of people is noticed in herbal products in the developing and the developed nations. Apart from the medicine shops, currently the plant-based products can be found in places like food stores, shopping mall, and in other public market places [4].

The medicinal plants can be defined as those plants/herbs, whose whole or segment of plants or extracts from herbs/plants is implemented in healthcare or in fighting illness. Many countries have traditions related to traditional medicine, such as China (Traditional Chinese Medicine), India (Ayurveda, Unani, Homeopathy, Siddha,), Japan, Middle East, Tibet, Korea, Russia, and South America. Although many countries like India, China, Korea, Vietnam and Thailand have officially recognized the use of TM (Traditional Medicine), there are still many countries that are yet to include it in their own formal healthcare system. The reason may be the complexity of the healthcare system, lack of scientific approach in their use and the need for effective and widely-publicized treatment for various diseases. However, there is a significant requirement of both the codified TM and uncoded traditional medicines for the treatment of numerous critical and chronic diseases in the world.

## 1.2 Benefits of medicinal plants

The impact of traditional medicines in the economic front as well as for the treatment of diseases and the well-being of the human health has resulted in a significant public demand for enhanced accountability of these medicines. Effective quality assessment of medicinal plants and related products is now very much essential to fulfil the basic requirement of the consumers. The economic and health benefits of medicinal plants are stated below:

### 1.2.1 Economic Benefits

The expanding value of medicinal plants can be comprehended from the economic viewpoint when the following evidences are contemplated:

- More than hundred billion USD is the annual market share around the world.

- (2-5) billion USD is the figure of medicinal plant business for India and China per year
- Germany earns more than 1 billion USD yearly
- Approximately seven thousand species is traded in China and India individually.
- Morocco exports around sixty tons of medicinal plants per annum
- The revenue of China, India, and Europe has increased two times, three times and twenty five percent respectively in the last 5 years.

However, the estimated annual values of herbal medicines and some health foods are given in Table 1.1.

Table 1. 1 Estimated Annual Values of Herbal Medicines and Some Health Foods [5]. The currency is in USD

Worldwide revenue of herbal product	Eighty-three billion (2008)
Trade of plant-based medicine (India)	One billion (2006)
Price of natural products exports (India)	One hundred twenty-eight million (2010)
Revenue of United Kingdom imports of Indian herbal medicine	Five million (2009)
Revenue of medicinal plant at Bozhou market, China	Seven hundred thirty-five million (2011)
Market shares of Canadian ginseng	Sixty eighty million (2001)
Turmeric import by United States	Four million (2008)

### 1.2.2 Health Benefits

The major benefit of treatment with medicinal herbal/plants is that it is regarded as safe with nearly zero side effects. Natural products show superior treatments in comparison with the chemically processed medicines and synthetic products because the natural products are in good harmony with nature, our body and mind. Unlike other pharmaceuticals and therapies,

these medicinal plants are recognised to treat disease at its source, helping people to stay healthy and fit in the long run.

The benefits can be summarized as:

- They take a holistic path and support for digestion and appropriate integration
- They are not symptom targeted, but rather work as a preventative care that boosts the immunity and improves overall health and fitness.
- They are comparable to allopathic treatments for many diseases and, in certain cases, have been shown to be very effective in the treatment of cancer and autoimmune illnesses.
- They are non-toxic and safe because they are self-sufficient and nourishing in nature.
- These herbal medicines are intended to promote general health and harmony between the mind, body, and spirit.
- Plant based products and treatments can be used to treat a variety of metabolic and chronic illnesses with a little or no side effects.

### **1.3 Summarized facts of Indian medicinal plants**

Important information on medicinal plants of India is mentioned below [6]:

- Due to widespread usage of medicinal plants, India is one of seventeen super biodiversity nations
- Contributes approximately seven percentage of global biodiversity
- It has fifteen Agro-climatic regions
- Medicinal herbs can be found in a variety of environments, from the mountain to the sea, dry to rain forest.
- More than seven thousand plants species have been identified as medicinal plants out of eighteen thousand flowering plants species in India
- Ayurveda is a three-thousand-year-old natural product based medical system that was originated in India and now has gained broad popularity around the world.
- More than ninety percentage of the preparations in the Siddha, and Unani system of medicine are plant-based.

- Approximately twenty-two percentage of the production of medicinal plants is obtained through cultivation and the rest is obtained from the forests

#### 1.4 Quality control of medicinal plants: Challenges and solutions

The content and pattern of secondary metabolites in all plants are now well understood to be influenced by ecological, genetic, and photoperiodicity parameters and these secondary metabolites play crucial roles in curing diseases. Thus assessment of the content of these secondary metabolites is the need of the hour. Even though these herbal product formulations are in use since prehistoric times, it is ethical to clinically evaluate them first and then gather relevant pharmacological information. All of this knowledge is required for standardisation of quality products [7].

The issues encountered in quality control of herbal product formulations are shown Figure 1.1.



Figure 1. 1 Challenges faced in the quality control of herbal drug preparations.

However, Quality Control (QC) of traditional medicines (TM) in India was assessed from the beginning by religious experts or medicine men employing the herb for ailments, and afterwards by physicians known as vaidyas and hakims. Modern concepts, on the other hand, necessitate a shift in these methods. For instance, QC of TM, as well as traditional techniques of production, are now being investigated and documented, and this evidence is then

appropriately interpreted. Various methods of quality control of herbal medicines are presented in Figure 1.2.

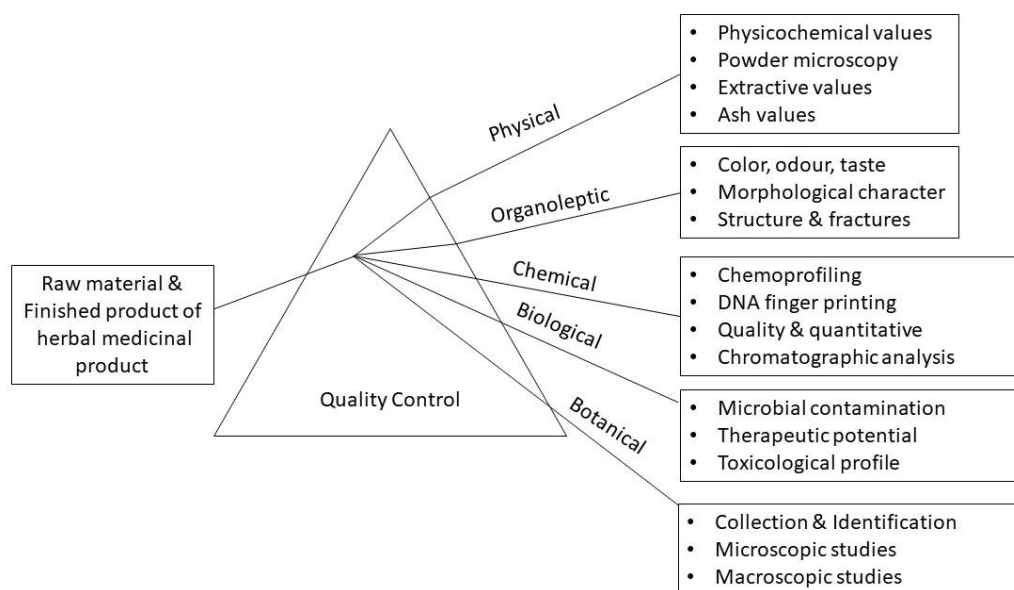


Figure 1. 2 Quality control methods in evaluating herbal medicinal products.

#### 1.4.1 Standardization of chemical aspects using marker analysis

Three parameters, namely authentication, purity, and assay are desirable for standardisation and QC of TM. As the name implies, authentication is concerned with the fact that the material is genuine, that is it conforms to the stated identity. Purity refers to determining whether or not the plant material contains any impurities, and it can be determined by traditional pharmacognostic methods such as microscopy, ash values, and additional assays, such as extractive values. Chemical and biological profiling is used in the test stage of standardisation to examine chemical and biological effects and determine effective levels. This could also be used to determine the safety of the product. The drug activity is tested in biological tests using a pharmacological model, although this is rarely done because biological testing is extremely subjective, vulnerable to a lot of variation in responses, and animal testing is subject to tight regulatory regulations. As a result, developing standardisation processes for quality control using biological assays is important, yet challenging [8].

Chemical approaches, on the other hand, are adaptable and can be useful in standardisation, and they are still the most widely utilised technical method. For qualitative evaluation,

fingerprints can be developed. The concentrations of secondary metabolites, which are thought to be the active ingredients of herbal medications, are investigated and used to provide standardisation processes in terms of quantitative assessment. The substances in question are known as 'marker' compounds. Some of these marker chemicals are therapeutically active, while others are not, but all should be present in large quantities when utilised[9][2]. Marker analysis can be used to measure potency, predict active ingredients, and assure the standardization of herbal final products, among other parameters. They may also aid in the detection of contaminants and the observation of decomposition, both of which are important in the study of pharmacological stability and determining the shelf-life of a product[10]. Figure 1.3 depicts a number of benefits of marker analysis.



Figure 1. 3 Importance of marker analysis in drug development from natural resources

## 1.5 Existing methods for quality estimation of medicinal plants

### 1.5.1 Chemical assessment of quality

There is a steady increase in demand by the consumers for good quality products from medicinal plants. As a result, grading and sorting operations are critical in achieving the quality standardizations and supplying clients with quality herbal products. This, together with the fact that instruments and machines are more consistent than humans [11–13], the

scarcity of labour in developed countries, and the opportunity to reduce labour costs [14], has ushered great opportunities for mechanization and automation in the industries dealing with medicinal plants.

As the quality assessment is the key factor for sales of herbal product in business, a field-deployable, non-invasive, high-performance quality evaluation system would be of great use to: -

- Enhance the efficiency of sorting and grading processes.
- Augment the speed and precision of the method.
- Reduce the costs of processing medicinal plant products.

The instrumental methods currently employed are mostly based on Gas Chromatography Mass spectroscopy (GC-MS), Liquid Chromatography Mass Spectroscopy (LC-MS) and High-Performance Liquid Chromatography (HPLC) to assess the quality of medicinal plants and herbal medicines. Figure 1.4 to Figure 1.6 shows the photographs of the instruments.



Figure 1. 4 Photograph of LCMS



Figure 1. 5 Photograph of HPLC



Figure 1. 6 Photograph of GCMS

### 1.5.2 Quality assessment using spectroscopy

The sophisticated instruments (HPLC, LCMS, GCMS) are in use for several decades and have gained the confidence and trust of the scientists, but the following limitations restrict their regular use in the industries dealing with medicinal plants:

- Very expensive.
- Laboratory based.
- Take long time for analysis.

- Complicated sample pre-treatment.
- Requirement of highly skilled labourers.
- Product wastage due to improper sorting and other human errors.

Due to the above factors, scientists have been exploring the spectroscopic techniques for assessing the biomarkers of the plant products. In general, the spectrometers are laboratory based and expensive, but since these methods are based on the vibrations at the molecular level, the estimations are, in general, accurate and precise. Recently, there has been significant development towards low-cost and portable spectrometers, and these new generation spectrometers are being used for several applications. In particular, Near Infra-Red and Raman Spectroscopy have shown a lot of promise towards this and low-cost but accurate instruments are now available. Unfortunately, in medicinal plant industries, there are only a few reports of their usage and here in this chapter, research reports on applications of these two spectroscopic techniques are presented in detail. Following are the important advantages of the two spectroscopic methods:

- Speed-results in seconds, or even continuously, rather than in hours or days.
- Accuracy - equivalent to any reference methods.
- Precision (reproducibility) - equal or superior to reference methods.
- Low cost per test-low labour costs, no chemicals (to purchase or dispose of).
- Flexibility in sample presentation to the instrumentation – no other analysis method offers the flexibility of accepting whole - or ground-state material in amounts of up to a kilogram of material without affecting the sample
- Flexibility in testing- many (up to 12) constituents can be tested simultaneously.
- Environmentally clean-no chemical
- Easy and cheap to install- no drainage or exhaust needed.
- Little or no sample preparation.
- Stand-alone instruments, with no peripherals.
- Small instrument size.
- Durability-instruments work well for 10+ years.
- Simple and safe to operate
- Calibration transferability among instruments of the same model (and even different models).
- Networking - many instruments, even remote from each other, could be linked.



- Continuous on-line interactance analysis (using fibre optics probe) by NIRS and Raman Spectroscopy obviate the need for taking samples.

There are also some drawbacks in NIR and Raman spectroscopy. These are:

- Each product and constituent require its own calibration – however, many modern instruments can now be calibrated at the factory and the user has to verify performance.
- The need to monitor accuracy and reproducibility (also needed in reference analysis).
- Instruments are expensive to purchase, but quickly pay for themselves in cost saving in labour, installation, time and chemicals.
- Scepticism- many people lack faith in the technology.
- Lack of knowledge as to how to operate instruments most efficiently.
- The crucial need for education in NIR technology at a university undergraduate level.

### 1.6 Objectives of the thesis work

In this thesis work, the quality assessment of two important medicinal plants (Kalmegh and black pepper) was taken up and two spectroscopic methods employing near infrared and Raman techniques were explored. The objectives of the thesis work were:

- 1) Development of a portable Raman spectrometer
- 2) Development of a portable NIR spectrometer
- 3) In situ quality assessment of two important medicinal plants
  - a) Kalmegh (*Andrographis paniculata*) by measuring concentration of the active molecule Andrographolide using portable NIR spectrometer and
  - b) Piperine in black pepper seeds (*Piper nigrum*) using Raman spectrometer.
- 4) Development of machine learning and deep learning techniques to extract accurate and more useful data from the spectra of NIR and Raman spectrometer.

## 1.7 Brief theory on NIR and Raman spectroscopy

### 1.7.1 Brief theory of Raman spectroscopy

Scattering of light occurs with release of electromagnetic radiations, which is produced due to oscillating dipole induced in a molecule by the electric field of the incident radiation. In case of Raman scattering, the induced dipole moment occurs because of the change in the molecular polarizability, which is the change of electron density of a molecule due to the deformability of the electron cloud around the molecule by an exterior electric field. This momentary change of dipole moment of the molecule produces electromagnetic radiations that are mostly elastically scattered light with a very little amount of non-elastically scattered light. The elastic scattering of light is known as Rayleigh scattering and the non-elastic scattering of light is known as Raman scattering (Figure 1.7).

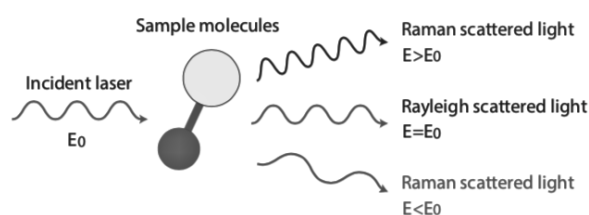


Figure 1. 7 Illustration of Raman and Rayleigh scatter rays from a sample molecule

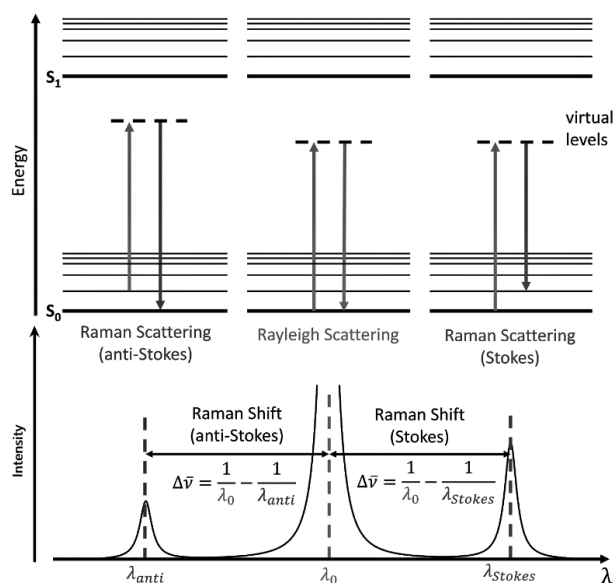


Figure 1. 8 Graphical representation of Rayleigh scattering, Stokes, and anti-Stokes Raman scattering. The dashed lines show the “virtual state.”  $\Delta\bar{\nu}$  is the change in wavenumber.

Two possible events give rise to two types of Raman scattering as shown in figure 1.8. Molecules initially in the ground state settling into higher vibrational energy state after returning from virtual state produce Raman stokes which have energy (and frequency) lesser than the incident energy. Molecules initially in a higher vibrational energy state settling to the ground state after transition from the virtual state produce Raman anti-stokes whose energy (and frequency) are more than the incident energy. The intensity of stokes and anti-stokes depends on two parameters viz. absolute temperature of the molecule and variation of energy due to change of states. At room temperature, the intensity ratio of the stokes relative to anti-stokes is governed by the Boltzmann's law which shows that the intensity of Raman stokes scattering is more than anti-stokes, because the majority of molecules can be located in the ground state at room temperature.

The intensity of Raman scattered radiation is related to various parameters by the relation

$$I_R \propto \nu^4 I_o N \left( \frac{\partial \alpha}{\partial Q} \right)^2$$

Here,  $I_o$  - power of laser source,

$N$  - no of scattering molecules in the specified state,

$\nu$  - frequency of laser,

$\alpha$  - polarizability of the molecule, and

$Q$  - the vibrational amplitude.

### 1.7.2 Brief theory of NIR spectroscopy

Although William Herschel is credited with discovering near-infrared energy in the late nineteenth century, but the first practical implementation did not occur until nineteen fifty. The electromagnetic spectrum is shown in Figure 1.9. Infrared is subdivided into three regions, namely: the near (780-2500 nm), mid (10 to 2.5  $\mu\text{m}$ ) and far (1mm-10 $\mu\text{m}$ ) infrared regions, and are abbreviated as NIR, MIR and FIR, respectively. NIR spectroscopy is result of molecular overtone and combination of fundamental IR vibrations

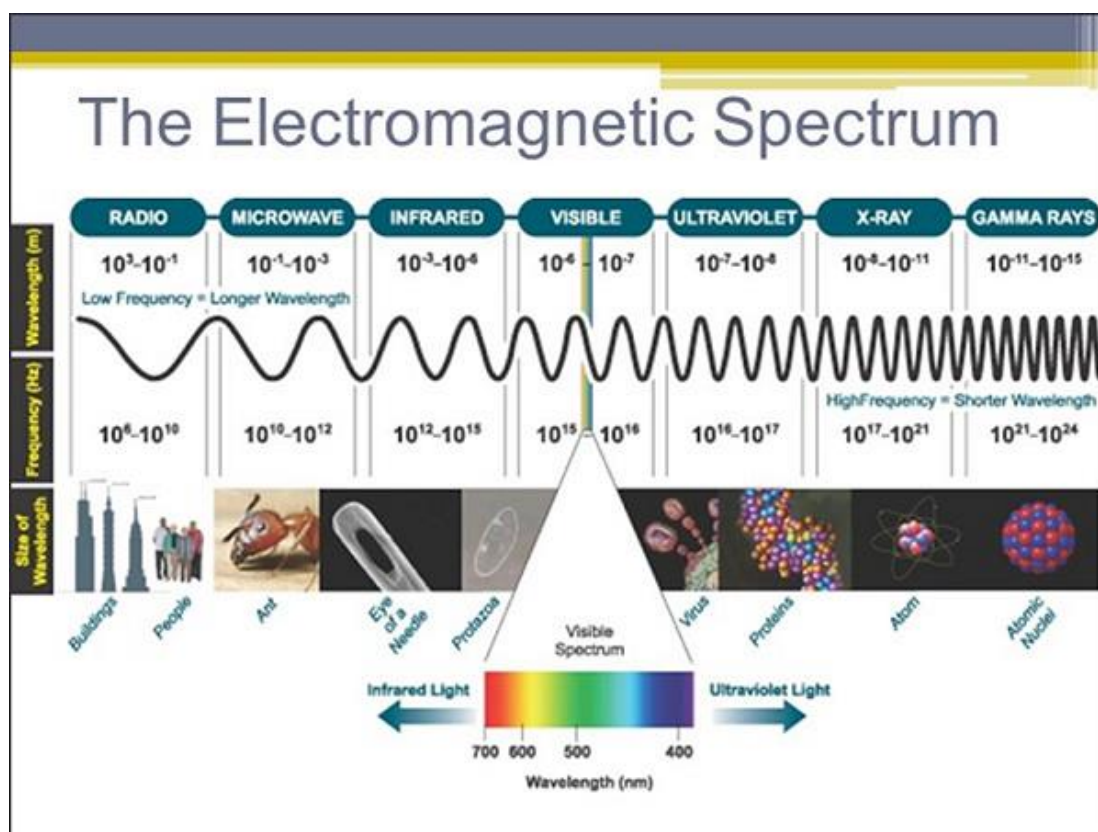


Figure 1. 9 Electromagnetic spectrum and transmission characteristics

### 1.7.2.2 Origin of absorption bands in NIR

Molecules will interact with only those frequencies of the NIR light for which the energy is exactly equal to the energy difference between two vibrational energy levels and accordingly some frequencies will be fully absorbed, while others are partially or not absorbed at all. The absorption spectra of the analyte are dependent on the correlation of intensity of absorbed radiation against frequency of incident light. Absorption is only feasible if the vibrational motion of the atoms that form the molecular bond gives rise to a change in the dipole moment and hence it is essential that the electric field of the electromagnetic wave from the NIR source is able to interact with the electric field of the molecules. There are a few kinds of absorption bands. The combination bands in polyatomic molecules give rise to transitions that involve two simultaneous vibration modes. The functional groups C-H, N-H and several others give rise to the overtone absorption bands. The spectral features in NIR region are dominated by combination and overtones absorption bands [15]. For combination bands to occur, unlike MIR, only and only one of the combining vibrations should stay active to cause

the dipole change in NIRS which makes it a unique characteristic as the vibrations which were not visible in MIR are now in fact observable in the NIR spectral range.

### 1.8.2.1 Sample preparation and measurement modes in NIR spectroscopy

The different pathways that light energy can take through or from a sample are illustrated in Figure 1.10. Some light energy (1) is reflected directly from the surface and carries no information (specular reflection). Some of the energy (5) gets completely scattered within the sample to the extent that it never emerges. Some energy (4) passes right through the sample in transmittance mode to reach the detector and is used in NIR transmittance spectroscopy while other energy is diffusely reflected (2, 3) or transmitted (6) from within or through the sample, but does not reach the detector. The energy that is used by NIRS (2 and 4) is diffusely reflected from within, or transmitted through the sample, and reaches the detector(s).

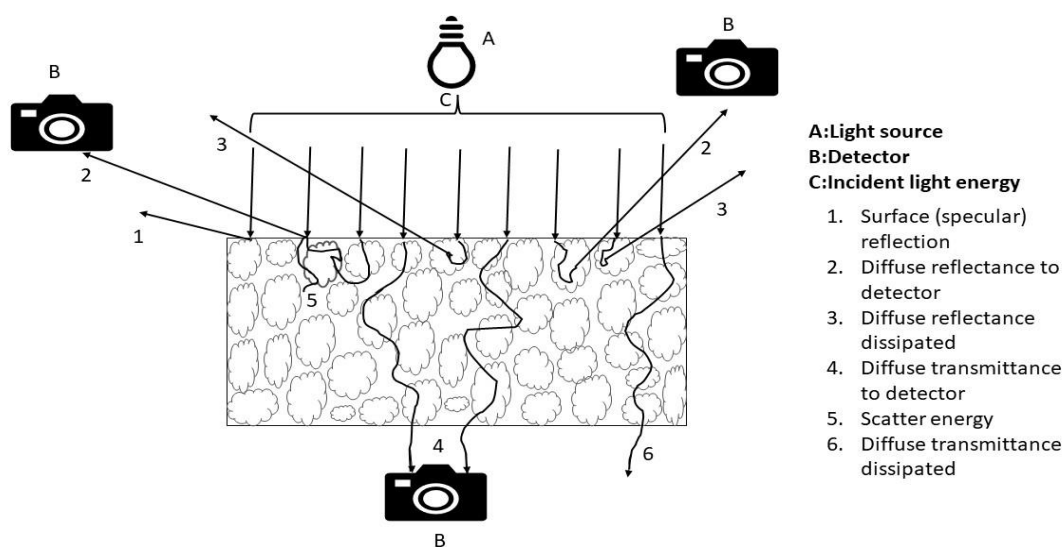


Figure 1. 10 Pathways of light through a sample

### 1.7.2.2 Diffuse reflectance (DR) measurement mode

The ratio between the intensity of light from two surfaces viz. one from diffused surface ( $I_0$ ) and another from sample ( $I_s$ ) is known as the reflectance of a certain material, which is usually denoted by absorbance parts  $\log(1/R)$ . The absorbance spectra is taken using this way shows

a linear relationship with the concentration of sample in accordance with the Beer-Lambert's Law[16] . In 1908, Mie put forth a theory describing the elastic scattering phenomenon and its association with the radiation frequency [17] .

$$\frac{I_{\theta scat}}{I_o} = \frac{\lambda^2}{8\pi^2 R^2} = i_1 + i_2 \quad (1)$$

where,

$\lambda$  is a single wavelength,

$I_{\theta scat}$  is intensity of scattered light of path length R and angle  $\pi$  with respect to the mid-point of the scattering molecule.

$i_1, i_2$  are complex functions of the angle of the scattered light.

This expression demonstrates that wavelength and intensity of scattered light are directly dependent and hence can be a possible explanation for the baseline up scaling observed in the NIR absorbance of solid samples. However, the Mie theory had a lot of shortcomings such as it could not explain the multiple scattering phenomenon.

In 1931, Kubelka and Munk found the solution to the radiation transfer equation. The below mentioned equation relates the diffuse reflectance to the ratio of the absorption coefficient (K) and scattering coefficient (S). This is a widely accepted explanation for the diffuse reflectance and can be experimentally tested [18] .

$$f(R_\infty) = \frac{k}{s} = \frac{1-2R_\infty+R_\infty^2}{2R_\infty} \quad (2)$$

### 1.7.2.3 Diffuse transmittance (DT) measurement mode

The fact that allows the NIR light to breach the solid with a minimum amount processing is that the interaction of near infrared light with solid particles is characterised by a low absorption combined with a strong scattering. Compared to the MIR and UV spectroscopy the diffuse transmission measurements of solid samples are distinctive for the NIRS. The transmittance of a sample can be explained in the form of the Beer-Lambert Law [19] :

$$A = \log \frac{1}{T} = \log \frac{I_o}{I_s} = abc$$

For single wavelength,

$I_o$ –Intensity of transmitted light without sample

$I_s$ –Intensity of transmitted light with sample

$A$  – Beer-Lambert optical absorbance

$a$  – absorption coefficient,  $\text{cm}^{-1}$

$b$  – Path length (or material width), cm

$c$  – Concentration of absorbing sample

$T$  – Transmittance ratio

## 1.8 Literature review

### 1.8.1 Raman spectroscopy

Raman spectroscopy has gained excellent achievements in several areas like material science [22], chemistry [23], geology [24], biology [25], medicine [26], and real life applications such as quality assessment of essential oil [20], wood [21], etc. Use of Raman Spectra for detection and estimation of specific chemical constituents has proved its worth in diverse fields of application. It has been used for analysing biomaterials and chemical compounds such as cellulose and cellulose nanofibers from *Citrullus colocynthis* seeds [27], monitoring of plant health and development in *Solanum lycopersicum* (tomato) leaves [28], discrimination of piperine and flavopiperine content in pau-pereira [29], monitoring the extraction of anethole and fenchone from fennel seed [30], quantification of 10-deacetylbaicalin III (10-DAB) in yew plant [31], authenticity of vegetable oils and essential oils [32]. The two noteworthy review articles [33, 34] present several such applications.

### 1.8.2 NIR spectroscopy

The efficacy of near infrared spectroscopy for qualitative assessment of agricultural product was established by Karl Norris and his co-workers. They determined the defection rate in eggs [35], the degree of ripeness of fruits [36] and the amount of moisture in grain and seeds [37]. Norris developed the first moisture meter [38, 39]; and is known as pioneer of recent near infrared spectroscopy. Dickey-John developed the first commercial application near infra-red set up, Grain Analysis Computer, with tungsten-halogen lamp for light source in the year of nineteen seventy-one [40]. Alongside advancements in instrumental accuracy and capabilities such as computing and analytical approaches, as well as spectral data collection and pre-processing, NIR spectroscopy has greatly proven its versatility for qualitative and quantitative analysis. Because of its non-destructive approach and wide range of applications in practically all branches of science, this methodology has become the largest rising analysis tool [41–44].

A discriminate study was conducted on leaves using near infrared spectroscopy [45]. In another study, Indian borage, *Hibiscus rosa-sinensis*, *Ocimumtenui florum*, *Solanum trilobatum* and *Piper betel* were selected as sample for discrimination purposes using the same technology [46, 47].

Measurement of quality attributes of horticultural produce is presented in [48]. Different spectrophotometer designs and three measurement modes of NIR spectroscopy: the reflectance, transmittance and interactance modes are compared. In order to estimate the absorbed and scatter light of vegetable tissue both near infrared multi and hyperspectral imaging method were used [49].

Internal and external quality measurement of citrus fruit is done by measurement of soluble solid content and titratable acidity due to their chemical structure; thereby their concentration can be determined by NIR spectroscopy. It also provides non-invasive measurement for determining the chemical composition carbohydrate content etc. of the fruit [49][50].

Pioneering work had been done by Lai et. al [51] for assessment of TMC. Andrographolide, deoxyandrographolide, dehydroandrographolide, neoandrographolide, moisture, ash content, and alcohol-soluble extract of *Andrographis paniculata* have been estimated using NIR spectroscopy. The results showed that the calibration models that were developed were good



and could be useful to estimate the seven marker molecules in *Andrographis paniculata* for QC of TCM [51].

A study was conducted for determining the quality of the tea leaves by estimating the total polyphenol content in the tea leaves. The tea leaves are dried and then grinded and the sample is transferred to the NIR spectrometer. For measuring the polyphenol percentage in situ, the regression model is developed using PLS regression algorithm using 55 samples [52, 53].

NIR spectroscopy has been widely employed for food quality assessment. The viability of seeds is important for determination of their quality. Seed having high capability of germination has high productivity thereby the quality is good. FT-NIR spectroscopy is employed for determining the viability of soybean seeds. Partial least-squares discriminant analysis (PLS-DA) was used for classifying the soybean seeds. The variable importance in projection (VIP) technique was used to determine the significant variables. The most effective wavelengths were selected by the VIP method. 146 optimal variables from the full set of 1557 variables were selected [54, 55].

Table 1.2 lists some of the medicinal plants that have been used for analysis using these vibrational spectroscopic methods, the purpose of the analysis and the chemometric methods involved in their analysis.

Table 1. 2 Examples of recent research activities on NIR spectroscopy and Raman spectroscopy for analysis of medicinal plant and various chemometric tools used therein.

Serial No.	Name of the medicinal plant	Major purpose	Instrument/methodology	Data analysis methods	Reference
1	Indian borage (Karpooravalli), <i>Hibiscus rosa-sinensis</i> ( <i>Hibiscus sp.</i> ), <i>Ocimumtenuiflorum</i> , <i>Solanum trilobatum</i> and <i>Piper betle</i>	Identification	NIR Spectroscopy	PCA	[56]
2	<i>Angelica dahurica</i> , <i>Typhoniumflagelliforme</i> ,	Identification	NIR Spectroscopy	PCA, LDA, PLS-DA,	[57]

	and <i>Dioscorea opposita</i> collected from different geographical regions of China			MW-PLS-DA	
3	<i>Camellia sinensis</i>	Identification	NIR Spectroscopy	PCA, LDA, MLR,	[58]
4	<i>Rhodiola sp.</i> ( <i>Rhodiola crenulata</i> , <i>Rhodiola fastigiata</i> , <i>Rhodiola kirilowii</i> , <i>Rhodiola brevipedunculata</i> )	Identification	NIR Spectroscopy	SNV, SPXY, CARS, KELM, PLS-DA	[59]
5	<i>Trichosanthes kirilowii</i> (fresh ripe fruits)	Identification	NIR Spectroscopy	KNN, PCA, PLS-DA, SVM-DA	[60]
6	<i>Garcinia cambogia</i>	Identification, quantification	NIR Spectroscopy	PLSR	[61]
7	<i>Salvia officinalis</i> , <i>Thymus serpyllum</i> , <i>Lavandula x hybrida</i> , <i>Melissa officinalis</i> and <i>Mentha piperita</i>	Quality evaluation	NIR Spectroscopy	MLRA, PCA, CVA	[62]
8	<i>Crocus sativus</i>	Quality assessment, quantification	NIR Spectroscopy	SI-PLS, CARS, SNV, MSC, PCA, PLS-DA	[63]

9	<i>Gentianascabra</i>	Quantification	NIR Spectroscopy	MPLSR, SMLR	[63]
10	<i>Carumcarvi</i> L.	screening tool for quality control	Raman Spectroscopy		[64]

## 1.9 Brief description on Chemometrics

In NIR region, the molecular overtone and combination bands (O-H, C-H, C-HO, and N-H) have extensive response. Therefore, assignment of certain features to specific chemical components becomes difficult. In this regard, chemometric techniques becomes a necessity in order to facilitate the extraction of desired spectral information from the sample.

Chemometrics is the process of applying several mathematical and statistical algorithms on the spectral data [65]. Chemometrics plays an important role in extracting useful information from the NIR spectra of a sample under investigation. Various multivariate techniques are utilized in chemometrics for developing models. The reference chemical values obtained by other analytical techniques have been used in this process.

The chemometric techniques used in NIR can be broadly classified into the following categories: -

- Pre-processing
- Clustering and Classification
- Regression

### 1.9.1 Pre-processing techniques

The data acquired from the NIR spectrometer contains various uninformative content along with the actual information of the sample [65]. To avoid the suppression of main information contained in this data by the uninformative content, the spectral pre-processing techniques are used. It employs a series of steps in sequential manner for removing the spectral noise and thereby enhancing the signal to noise ration [66]. The size of the particle and the sample shape bring about multiplicative and/or additive scattering effects on the spectra; thus, decreasing the signal to noise ratio of the spectra. The effect of scattering is more on bigger particles than on smaller ones and differs from material to material due to different path

length. While multiplicative effect disturbs the slope of each spectrum, additive effect leads to shifts in the baseline with respect to a reference.

Spectral pre-processing has been categorically divided into 3 types on the basis of their operation: -

### 1.9.1.1 Scatter correction

A sample may contain non-uniform sized particles which alters the scattered NIR photon's path length [66]. This phenomenon, particle size effect is corrected by this technique and the commonly used techniques are mentioned below:

### 1.9.1.2 Standard Normal Variate (SNV)

Standard Normal Variate is a type of scatter correction method. Undesired spectral variations due to light scattering effects and variations in effective path length can be removed by this method [67]. It operates row-wise and is calculated as:

$$x_{ij} = \frac{x_{ij} - x_i}{s_i} \quad (3)$$

- where,  $x_{ij}$ - absorbance of  $j$ -th wavelength for the  $i$ -th sample,
- $x_i$  - average absorbance of the original  $i$ -th spectrum,
- $s_i$ - standard deviation of the absorbance of the  $i$ -th spectrum.

### 1.9.1.3 Multiplicative Scatter Correction (MSC)

In Multiplicative Scatter Correction (MSC), the noise of each sample is estimated relatively to a reference sample, usually the average spectrum [67]. MSC correction for each  $x_{ij}$  is calculated as:

$$x_{ij} = \frac{x_{ij} - a}{b} \quad (4)$$

- where,  $x_{ij}$  is the intensity of the  $i$ -th spectrum and the  $j$ -th wavelength,
- while,  $a$  and  $b$  are estimated for each sample by ordinary least-squares regression of spectrum  $x_i$  versus the reference one (here, the average spectrum), over the available wavelengths.

#### **1.9.1.4 Mean Centering (MC)**

In Mean-centering, the mean value of each variable is subtracted from each instance of that variable [68].

#### **1.9.1.5 Smoothing**

This technique removes the environmental or noise due to the instrument contained in the spectral data [66]. The signal-to-noise ratio of a spectrum is enhanced by this process.

#### **1.9.1.6 Savitzky Golay (SG) smoothing**

The spectral data is iterated in a sequential manner using a moving window. The moving window is mainly responsible for controlling the strength of the filtering operation in this algorithm. The spectrum is fitted inside the window and is then replaced with a polynomial having low-degree. Though the large windows are more effective for eliminating the noise than smaller windows, but they may also remove some peaks from the spectrum. So, the window size and degree of the polynomial needs to be tuned individually for achieving optimal removal of noise [66]. This filter also reduces high frequency noise present in a signal [69].

#### **1.9.1.7 Derivatives**

It helps in removing the background information and thereby increase the resolution of the spectra [70].

##### **1.9.1.7.1 First derivative**

By first derivative method, a discrete differentiation is employed on the spectral data. The baseline is ignored and overlapping bands are separated through this. It further helps in removing horizontal baselines of varying levels present in the data [71].

##### **1.9.1.7.2 Second derivative**

Second derivative and other higher order pre-processing takes place by repetitive discrete differentiation of the spectral data. The baseline is ignored and overlapping bands are separated through this. It also helps in removing varying levels and slopes present in the data [71]

### **1.9.1.7.3 Savitzky Golay derivation**

It reduces low frequency signal caused due to offsets and slopes using differentiation method [69].

## **1.9.2 Clustering, classification and regression techniques:**

Clustering is the process of grouping a population or set of variables into several categories. It keeps the identical variables in same category (known as a cluster). To put it another way, the goal is to separate groups with similar characteristics and allocate them to clusters. Classification is the process of categorically dividing the samples into distinct classes based on the spectral data acquired from the samples. Classification may be: 1) supervised or 2) unsupervised. The classification techniques are used to grade or sort the samples. The regression techniques are used to predict a numerical value when a set of variables are given as input. This regression techniques are used to obtain the concentration of a secondary metabolite of a medicinal plant when the spectrum of the sample is available.

### **1.9.2.1 Important clustering techniques: -**

#### **1.9.2.1.1 Principal component analysis (PCA)**

PCA reduces the high-dimensional data into a lower dimension. This is achieved by projection of the input data on the orthogonal axes along the direction of maximum variance. The dimensionality reduction is achieved by considering the PCs which account for maximum variance and minimum correlation in the data set. Thus, the correlation between the features is reduced in the original data set and is transformed into a set of uncorrelated principal components. Thereby, PCA is a powerful tool for visualizing high dimensional data in two- or three-dimensional coordinate system [72].

#### **1.9.2.1.2 Linear discriminant analysis (LDA)**

LDA focuses on finding optimal boundaries among classes. It aims to achieve the highest possible ratio of between-class variation to within-class variance. The major goal of this strategy is to maximise this ratio in order to achieve acceptable class separation [75]. Both the within-class information and between-class distribution is considered for LDA.

### 1.9.2.2 Classification techniques

The commonly used classification techniques used in spectroscopic data analysis are given below

#### 1.9.2.2.1 K-Nearest Neighbour (KNN)

KNN is a non-parametric machine learning algorithm which stores the training data instead of learning from it immediately. Hence it is also known as lazy learning algorithm. In KNN, 'k' stands for the number of nearest neighbours to be considered while determining the class of the test data point. Once the test data is fed, 'k' nearest neighbours are considered from the new test point by measuring the Euclidean distance from that point and the most predominant class is assigned to that point [68].

#### 1.9.2.2.2 Support Vector Machine (SVM)

SVM is a supervised machine learning algorithm. It makes use of hyperplanes which act as decision boundary to classify data into various classes. SVM also classifies non-linear data by employing kernel functions. By use of kernel functions, the non-linear data is transformed to a higher dimension where it becomes linearly separable and hyperplanes can be created to distinguish data into different classes [73].

#### 1.9.2.2.3 Naïve Bayes

It is a supervised classification technique which is based on Bayes theorem. An assumption that a particular feature of the class is independent of the other feature is made by this process. Even if the features are dependent on each other, all the features make individual contribution in deciding the class of the test dataset [74].

### 1.9.3 Regression

Regression involves predicting numerical value. Generally, the performance of any regression model is estimated by evaluating the following parameters: -

**i. Root mean square error (RMSE)**

$$\text{RMSECV or RMSEP} = \sqrt{\left(\sum_{i=1}^n (y'_i - y_i)^2 / n\right)}$$

- where  $y'_i$  is the predicted value and  $y_i$  is the measured value[75].

**ii. Correlation coefficient ( $R^2$ )**

$$R^2 = \sqrt{\left(\sum_{i=1}^n (y'_i - y_i)^2 / (y'_i - y_{\text{mean}})^2\right)}$$

- where  $y'_i$  is the predicted value and  $y_i$  is the measured value,  $y_{\text{mean}}$  is the average value[75].

**iii. Predictive residual deviation (RPD)**

$$\text{RPD} = \text{Standard deviation}/\text{RMSE}$$

A high  $R^2$ , RPD and low RMSE value is desirable for any regression model. Popular regression techniques are: -

**1.9.3.1 Partial least squares regression (PLSR)**

PLSR is a data analysis technique that finds a linear regression model. It projects both the response quantity(Y) and input quantity (X) into a new space in the direction of maximum explained variance. The covariance between the two spaces is thereby maximised. PLSR is employed for finding the basic relations between two matrices (X and Y) using a latent variable method for developing a model of the covariance structures in these two spaces [76].

**1.9.3.2 Support Vector Regression (SVR)**

It uses the same principle of maximizing the margin of the hyperplane but applies it to predict numerical values other than a class. SVR provides the flexibility to define the error( $\epsilon$ ) that is permissible in our model and finds an appropriate line/hyperplane in higher dimension to fit the data [77]. Before building a calibration model, support vector machine variables must be determined to improve the model's prediction and generalisation capacity. The RBF kernel



variable  $\sigma^2$  and the regularisation constraint  $\gamma$  must both be optimised.  $\gamma$  has to do with maximising model performance while reducing model complexity.

### 1.10 Research questions

In accordance with the scope and objectives, the thesis sets out to address the following research questions:

1. RQ1: Is it possible to develop a portable Raman and NIR spectrometer for the quality assessment of medicinal plants?
2. RQ2: Is it possible to predict the concentration of biochemical compounds in medicinal plants from the response of Raman and NIR spectrometer?
3. RQ3: What type of data analysis methods may be used for the development of correlation models?
4. RQ4: Can the developed portable Raman and NIR spectrometer system be used to aid the natural and medicinal plant industry?

### 1.11 Thesis structure

The thesis is divided into six chapters, and brief summary of the chapters are as follows:

#### Chapter 1: Introduction

The chapter presents formulation of the research problem, scope and objectives of the thesis, advantages of medicinal plant. Furthermore, the chapter also describes the fundamentals and basic theory on Raman and NIR spectroscopy and literature review on the application of spectroscopic techniques for the medicinal plants. The chapter also includes the thesis outline to illustrate the relationship between the scope of the work and the included chapters.

#### Chapter 2: Development of a portable Raman spectrometer

The chapter introduces the design and development of a portable Raman spectrometer. The details of the hardware components used and the software developed for the portable Raman spectrometer are described. Finally, the chapter shows the verification and validation of the developed instrument using standard samples like benzene, chloroform and glacial acetic acid.

### **Chapter 3: Experiment with piperine and black pepper with the procured Raman spectrometer and the developed one**

In this chapter, the procedure of estimating the piperine in black pepper with the procured Raman spectrometer and the developed one are described. Both the classification and regression models were considered for assessment of the quality of the black pepper seeds. Additionally, it was observed how the pre-processing techniques influence the performance and the robustness of the prediction model.

### **Chapter 4: Development of a portable NIR spectrometer**

The chapter presents the design and development of a portable NIR spectrometer. Furthermore, the chapter also describes the optical components and customized graphical user interface of the developed portable Raman spectrometer. Finally, the chapter shows the measurement methods and calibration of spectral data for the developed instrument

### **Chapter 5: Experiment with andrographolides and *Andrographis paniculate* with the procured NIR spectrometer and the developed one**

This chapter presents the estimation of andrographolides in *Andrographis paniculata* with the standard NIR spectrometer and the developed one. Both the classification and regression models were analysed here. *Andrographis paniculata* samples were classified into three categories – good, medium and bad based on their andrographolide content.

### **Chapter 6: Conclusion and future scope**

The chapter briefly summarizes the overall work on the development of spectrometers and their applications in assessing the quality of the medicinal plants. The summarization elaborates the research work presented in the chapters of the thesis relevant to the research scope and objectives of the thesis. The research questions are answered and potential future research directions of the work are mentioned.

**Reference**

- [1] P. K. Mukherjee, M. Sahu, and B. Suresh, "Indian herbal medicines," *Eastern pharmacist*, vol. 41, no. 490, pp. 21–23, 1998.
- [2] P. K. Mukherjee, "Problems and prospects for good manufacturing practice for herbal drugs in Indian systems of medicine," *Drug information journal: DIJ/Drug Information Association*, vol. 36, no. 3, pp. 635–644, 2002.
- [3] G. Bodeker and C.-K. Ong, *WHO global atlas of traditional, complementary and alternative medicine*, vol. 1. World Health Organization, 2005.
- [4] M. Ekor, "The growing use of herbal medicines: issues relating to adverse reactions and challenges in monitoring safety," *Frontiers in pharmacology*, vol. 4, p. 177, Jan. 2014, doi: 10.3389/fphar.2013.00177.
- [5] A. Hallquist, S. Jansen, and S. Mielke, "Global trade: transportation of turmeric from India to the United States," *Global trade assignment executive summary*, 2010.
- [6] "<https://www.nmpb.nic.in/content/medicinal-plants-fact-sheet>."
- [7] P. K. Mukherjee, "Evaluation of Indian traditional medicine," *Drug Information Journal*, vol. 35, no. 2, pp. 623–632, 2001.
- [8] P. K. Mukherjee, "Exploring botanicals in Indian system of medicine—regulatory perspectives," *Clinical Research and Regulatory Affairs*, vol. 20, no. 3, pp. 249–264, 2003.
- [9] Y.-Z. Shu, "Recent natural products-based drug development: a pharmaceutical industry perspective," *Journal of natural products*, vol. 61, no. 8, pp. 1053–1071, 1998.
- [10] T. Tamizhmani, P. K. Mukherjee, S. Manimaran, and B. Suresh, "Indian herbal drug development—problems and prospects," *Pharma Times*, vol. 34, pp. 13–15, 2003.
- [11] S. H. Deck, C. T. Morrow, P. H. Heinemann, and H. J. Sommer, "Comparison of a neural network and traditional classifier for machine vision inspection of potatoes," *Applied Engineering in Agriculture*, vol. 11, no. 2, pp. 319–326, 1995.
- [12] J. B. Njoroge, K. Ninomiya, N. Kondo, and H. Toita, "Automated fruit grading system using image processing," pp. 1346–1351, 2003, doi: 10.1109/sice.2002.1195388.

- [13] N. Aleixos, J. Blasco, F. Navarrón, and E. Moltó, “Multispectral inspection of citrus in real-time using machine vision and digital signal processors,” *Computers and Electronics in Agriculture*, vol. 33, no. 2, pp. 121–137, 2002, doi: 10.1016/S0168-1699(02)00002-9.
- [14] P. Menguito, “Study on Sorting System for Strawberry Using Machine Vision (Part 2),” *JOURNAL of the JAPANESE SOCIETY of AGRICULTURAL MACHINERY*, vol. 62, no. 2, pp. 101–110, 2000, doi: 10.11357/jsam1937.62.2\_101.
- [15] J. J. Workman, “NIR spectroscopy calibration basics,” *Practical Spectroscopy Series*, vol. 13, p. 247, 1992.
- [16] W. William. Wendlandt and H. G. Hecht, “Reflectance spectroscopy.” Inter science Publishers, New York, 1966. [Online]. Available: <http://books.google.com/books?id=kHhOAQAIAAJ>
- [17] E. L. Simmons, “Diffuse reflectance spectroscopy: a comparison of the theories,” *Applied optics*, vol. 14, no. 6, pp. 1380–1386, 1975.
- [18] P. Kubelka, “New Contributions to the Optics of Intensely Light-Scattering Materials. Part I,” *J. Opt. Soc. Am.*, vol. 38, no. 5, pp. 448–457, May 1948, doi: 10.1364/JOSA.38.000448.
- [19] G. Zaccanti and P. Brusaglioni, “Deviation from the Lambert-Beer law in the transmittance of a light beam through diffusing media: experimental results,” *Journal of Modern Optics*, vol. 35, no. 2, pp. 229–242, 1988.
- [20] M. A. Hanif *et al.*, “Evaluation of the effects of Zinc on the chemical composition and biological activity of basil essential oil by using Raman spectroscopy,” *Industrial Crops and Products*, vol. 96, pp. 91–101, Feb. 2017, doi: 10.1016/j.indcrop.2016.10.058.
- [21] T. Belt, T. Keplinger, T. Hänninen, and L. Rautkari, “Cellular level distributions of Scots pine heartwood and knot heartwood extractives revealed by Raman spectroscopy imaging,” *Industrial Crops and Products*, vol. 108, pp. 327–335, Dec. 2017, doi: 10.1016/j.indcrop.2017.06.056.

- [22] X. Zhang, Q. H. Tan, J. bin Wu, W. Shi, and P. H. Tan, "Review on the Raman spectroscopy of different types of layered materials," *Nanoscale*, vol. 8, no. 12. Royal Society of Chemistry, pp. 6435–6450, Mar. 28, 2016. doi: 10.1039/c5nr07205k.
- [23] K. Kneipp, H. Kneipp, I. Itzkan, R. R. Dasari, and M. S. Feld, "Ultrasensitive Chemical Analysis by Raman Spectroscopy," *Chemical Reviews*, vol. 99, no. 10, pp. 2957–2975, Oct. 1999, doi: 10.1021/cr980133r.
- [24] J. Jehlička and H. G. M. Edwards, "Raman spectroscopy as a tool for the non-destructive identification of organic minerals in the geological record," *Organic Geochemistry*, vol. 39, no. 4. Pergamon, pp. 371–386, Apr. 01, 2008. doi: 10.1016/j.orggeochem.2008.01.005.
- [25] C. Krafft, B. Dietzek, and J. Popp, "Raman and CARS micro spectroscopy of cells and tissues," *Analyst*, vol. 134, no. 6. Royal Society of Chemistry, pp. 1046–1057, Jun. 01, 2009. doi: 10.1039/b822354h.
- [26] I. Nabiev, I. Chourpa, and M. Manfait, "Applications of Raman and surface-enhanced Raman scattering spectroscopy in medicine," *Journal of Raman Spectroscopy*, vol. 25, no. 1. John Wiley & Sons, Ltd, pp. 13–23, Jan. 01, 1994. doi: 10.1002/jrs.1250250104.
- [27] I. Kouadri and H. Satha, "Extraction and characterization of cellulose and cellulose nanofibers from *Citrullus colocynthis* seeds," *Industrial Crops and Products*, vol. 124, no. August, pp. 787–796, 2018, doi: 10.1016/j.indcrop.2018.08.051.
- [28] H. J. Butler, M. R. McAinsh, S. Adams, and F. L. Martin, "Application of vibrational spectroscopy techniques to non-destructively monitor plant health and development," *Analytical Methods*, vol. 7, no. 10, pp. 4059–4070, 2015, doi: 10.1039/c5ay00377f.
- [29] L. F. Maia *et al.*, "Tracking pteridine and flavopteridine in pau-pereira using Raman and SERS spectroscopies," *New Journal of Chemistry*, vol. 43, no. 28, pp. 11200–11208, 2019, doi: 10.1039/c9nj01314h.
- [30] M. Sixt, G. Gudi, H. Schulz, and J. Strube, "In-line Raman spectroscopy and advanced process control for the extraction of anethole and fenchone from fennel (*Foeniculum vulgare* L. MILL.)," *Comptes Rendus Chimie*, vol. 21, no. 2, pp. 97–103, 2018, doi: 10.1016/j.crci.2017.12.004.

- [31] G. Gudi, A. Kräbmer, I. Koudous, J. Strube, and H. Schulz, “Infrared and Raman spectroscopic methods for characterization of *Taxus baccata* L. - Improved taxane isolation by accelerated quality control and process surveillance,” *Talanta*, vol. 143, pp. 42–49, 2015, doi: 10.1016/j.talanta.2015.04.090.
- [32] P. Vargas Jentsch and V. Ciobotă, “Raman spectroscopy as an analytical tool for analysis of vegetable and essential oils,” *Flavour and Fragrance Journal*, vol. 29, no. 5, pp. 287–295, 2014, doi: 10.1002/ffj.3203.
- [33] C. W. Huck, “Selected latest applications of molecular spectroscopy in natural product analysis,” *Phytochemistry Letters*, vol. 20, pp. 491–498, 2017, doi: 10.1016/j.phytol.2016.12.028.
- [34] H. Schulz and M. Baranska, “Identification and quantification of valuable plant substances by IR and Raman spectroscopy,” *Vibrational Spectroscopy*, vol. 43, no. 1, pp. 13–25, 2007, doi: 10.1016/j.vibspec.2006.06.001.
- [35] K. H. Norris and J. D. Rowan, “Automatic detection of blood in eggs,” *Agricultural Engineering*, vol. 43, no. 3, pp. 154–159, 1962.
- [36] D. R. Bittner and K. H. Norris, “Optical properties of selected fruits vs maturity,” *Transactions of the ASAE*, vol. 11, no. 4, pp. 534–536, 1968.
- [37] K. H. NORRIS, “Direct spectrophotometric determination of moisture content of grain and seeds,” in *Proc. of the 1963 International Symposium on Humidity and Moisture*, 1965, vol. 4, p. 19.
- [38] K. H. Norris, “Design and development of a new moisture meter,” *Agric. Eng.*, vol. 45, no. 7, pp. 370–372, 1964.
- [39] J. J. Workman Jr, “Interpretive spectroscopy for near infrared,” *Applied Spectroscopy Reviews*, vol. 31, no. 3, pp. 251–320, 1996.
- [40] D. A. Burns and E. W. Ciurczak, “Commercial NIR instrumentation,” *Handbook of Near-Infrared Analysis (3rd Edition)*. Burns DA, Ciurczak EW (Eds). CRC Press, Boca Raton, FL, USA, pp. 189–205, 2008.
- [41] P. Williams and K. Norris, *Near-infrared technology in the agricultural and food industries*. American Association of Cereal Chemists, Inc., 1987.

- [42] M. Blanco and I. Villarroya, “NIR spectroscopy: a rapid-response analytical tool,” *TrAC Trends in Analytical Chemistry*, vol. 21, no. 4, pp. 240–250, 2002.
- [43] S. J. Choquette, J. C. Travis, C. Zhu, and D. L. Duewer, “Wavenumber Standards for Near-Infrared Spectrometry,” *Handbook of Vibrational Spectroscopy*, 2006.
- [44] J. T. Alander, V. Bochko, B. Martinkauppi, S. Saranwong, and T. Mantere, “A review of optical non-destructive visual and near-infrared methods for food quality and safety,” 2013.
- [45] P. K. S. Rajesh, C. Kumaravelu, A. Gopal, and S. Suganthi, “Studies on identification of medicinal plant variety based on NIR spectroscopy using plant leaves,” in *2013 15th International Conference on Advanced Computing Technologies (ICACT)*, 2013, pp. 1–4.
- [46] K. B. Beć, J. Grabska, and C. W. Huck, “Near-infrared spectroscopy in bio-applications,” *Molecules*, vol. 25, no. 12, p. 2948, 2020.
- [47] P. Wang and Z. Yu, “Species authentication and geographical origin discrimination of herbal medicines by near infrared spectroscopy: A review,” *Journal of Pharmaceutical Analysis*, vol. 5, no. 5, pp. 277–284, 2015.
- [48] B. M. Nicolai *et al.*, “Non-destructive measurement of fruit and vegetable quality by means of NIR spectroscopy: A review,” *Postharvest biology and technology*, vol. 46, no. 2, pp. 99–118, 2007.
- [49] K. B. Walsh, J. Blasco, M. Zude-Sasse, and X. Sun, “Visible-NIR ‘point ‘spectroscopy in postharvest fruit and vegetable assessment: The science behind three decades of commercial use,” *Postharvest Biology and Technology*, vol. 168, p. 111246, 2020.
- [50] L. S. Magwaza, U. L. Opara, H. Nieuwoudt, P. J. R. Cronje, and W. Saeys, “NIR Spectroscopy Applications for Internal and External Quality Analysis of Citrus Fruit — A Review,” *Food Bioprocess Technol* [, pp. 425–444, 2012, doi: 10.1007/s11947-011-0697-1.
- [51] X. Lai *et al.*, “Rapid simultaneous determination of andrographolides in *Andrographis paniculata* by near-infrared spectroscopy,” *Analytical Letters*, vol. 51, no. 17, pp. 2747–2762, 2018.

- [52] M.-Z. Zhu *et al.*, “The quality control of tea by near-infrared reflectance (NIR) spectroscopy and chemometrics,” *Journal of Spectroscopy*, vol. 2019, 2019.
- [53] A. K. Hazarika *et al.*, “Quality assessment of fresh tea leaves by estimating total polyphenols using near infrared spectroscopy,” *Journal of Food Science and Technology*, vol. 55, no. 12, pp. 4867–4876, 2018, doi: 10.1007/s13197-018-3421-6.
- [54] D. Kusumaningrum, H. Lee, S. Lohumi, C. Mo, M. S. Kim, and B. K. Cho, “Non-destructive technique for determining the viability of soybean (*Glycine max*) seeds using FT-NIR spectroscopy,” *Journal of the Science of Food and Agriculture*, vol. 98, no. 5, pp. 1734–1742, 2018, doi: 10.1002/jsfa.8646.
- [55] H. Cen and Y. He, “Theory and application of near infrared reflectance spectroscopy in determination of food quality,” *Trends Food Sci Technol*, vol. 18, pp. 72–83, 2007, doi: 10.1016/j.tifs.2006.09.003.
- [56] A. G. and S. S. P. K. Sahaya Rajesh, C. Kumaravelu, “Studies on identification of medicinal plant variety based on NIR spectroscopy using plant leaves,” in *15th International Conference on Advanced Computing Technologies (ICACT)*, 2013, pp. 1–4.
- [57] T. Y. H. Fu, Q. Shi, L. Wei, L. Xu, X. Guo, O. Hu, W. Lan, S. Xie, “Rapid recognition of geoherbals and authenticity of a Chinese herb by data fusion of near-infrared spectroscopy (NIR) and mid-infrared (MIR) spectroscopy combined with chemometrics,” *J. Spectrosc.*, 2018.
- [58] X. L. Y. Huang, W. Dong, A. Sanaeifar, X. Wang, W. Luo, B. Zhan, X. Liu, R. Li, H. Zhang, “Development of simple identification models for four main catechins and caffeine in fresh green tea leaf based on visible and near-infrared spectroscopy,” *Comput. Electron. Agric.*, 2020.
- [59] C. Su. T. Li, “Authenticity identification and classification of *Rhodiola* species in traditional Tibetan medicine based on Fourier transform near-infrared spectroscopy and chemometrics analysis,” *Spectrochimica Acta A*, vol. 204, pp. 131–140, 2018.
- [60] Z. C. L. Xu, W. Sun, C. Wu, Y. Ma, “Discrimination of *trichosanthis fructus* from different geographical origins using near infrared spectroscopy coupled with chemometric techniques,” *Molecules*, vol. 24, p. 1550, 2019.



- [61] R. M. A. E.-K. D.A. Selim, E. Shawky, “Detection and quantification of active pharmaceutical ingredients as adulterants in *Garcinia cambogia* slimming preparations using NIR spectroscopy combined with chemometrics,” *Rec. Pharm. Biomed. Sci.*, vol. 4, pp. 62–71, 2020.
- [62] D. V. A. Režan, M. Benković, T. Jurina, A. JurinjakTušek, J. GajdošKljusurić, “Application of near infrared spectroscopy for detection of ground medicinal herbs,” *J. Hyg. Eng. Design*, vol. 27, pp. 152–156, 2019.
- [63] Q. S. S. Li, B. Xing, D. Lin, H. Yi, “Rapid detection of saffron (*Crocus sativus* L.) Adulterated with lotus stamens and corn stigmas by near-infrared spectroscopy and chemometrics,” *Ind. Crops Prod.*, vol. 152, 2020.
- [64] W.-C. C. Y.-K. Chuang, S. Chen, Y.M. Lo, I.-C. Yang, Y.-F. Cheng, C.-Y. Wang, C.-Y. Tsai, R.-M. Hsieh, K.-H. Wang, C.-C. Lai, “Quantification of bioactive gentiopicroside in the medicinal plant *Gentiana scabra* Bunge using near infrared spectroscopy,” *J. Food Drug Anal.*, vol. 21, pp. 317–324, 2013.
- [65] J. U. Porep, D. R. Kammerer, and R. Carle, “On-line application of near infrared (NIR) spectroscopy in food production,” *Trends in Food Science and Technology*, vol. 46, no. 2, pp. 211–230, 2015, doi: 10.1016/j.tifs.2015.10.002.
- [66] I. O. Afara *et al.*, “Characterization of connective tissues using near-infrared spectroscopy and imaging,” *Nature Protocols*, vol. 16, no. 2, pp. 1297–1329, 2021, doi: 10.1038/s41596-020-00468-z.
- [67] Å. Rinnan, F. van den Berg, and S. B. Engelsen, “Review of the most common pre-processing techniques for near-infrared spectra,” *TrAC - Trends in Analytical Chemistry*, vol. 28, no. 10, pp. 1201–1222, 2009, doi: 10.1016/j.trac.2009.07.007.
- [68] C. L. Y. Amuah, E. Teye, F. P. Lamptey, K. Nyandey, J. Opoku-Ansah, and P. O. W. S. of the U. of H. N. S. for S. A. and Q. of Q. P. in I. P. Adueming, “Feasibility Study of the Use of Handheld NIR Spectrometer for Simultaneous Authentication and Quantification of Quality Parameters in Intact Pineapple Fruits,” *Journal of Spectroscopy*, vol. 2019, 2019, doi: 10.1155/2019/5975461.
- [69] N. B. Gallagher, “Savitzky–Golay filter for smoothing and differentiation,” *Signal processing*, no. January, pp. 2–6, 2013.

- [70] M. Zareefet *et al.*, “An Overview on the Applications of Typical Non-linear Algorithms Coupled With NIR Spectroscopy in Food Analysis,” *Food Engineering Reviews*, vol. 12, no. 2, pp. 173–190, 2020, doi: 10.1007/s12393-020-09210-7.
- [71] T. Fearn, “A look at some standard pre-treatments for spectra,” *NIR news*, vol. 10, no. 1, p. 10, 1999, doi: 10.1255/nirn.519.
- [72] S. Rezzi, D. E. Axelson, K. Héberger, F. Reniero, C. Mariani, and C. Guillou, “Classification of olive oils using high throughput flow 1H NMR fingerprinting with principal component analysis, linear discriminant analysis and probabilistic neural networks,” *Analytica Chimica Acta*, vol. 552, no. 1–2, pp. 13–24, 2005, doi: 10.1016/j.aca.2005.07.057.
- [73] Y. Xu, S. Zomer, and R. G. Brereton, “Support vector machines: A recent method for classification in chemometrics,” *Critical Reviews in Analytical Chemistry*, vol. 36, no. 3–4, pp. 177–188, 2006, doi: 10.1080/10408340600969486.
- [74] S. Karthika and N. Sairam, “A Naïve Bayesian classifier for educational qualification,” *Indian Journal of Science and Technology*, vol. 8, no. 16, 2015, doi: 10.17485/ijst/2015/v8i16/62055.
- [75] M. Arslan *et al.*, “Rapid Screening of Phenolic Compounds from Wild *Lyciumruthenicum* Murr. Using Portable Near-Infrared (NIR) Spectroscopy Coupled Multivariate Analysis,” *Analytical Letters*, vol. 54, no. 3, pp. 512–526, 2021, doi: 10.1080/00032719.2020.1772807.
- [76] A. K. Hazarika *et al.*, “Quality assessment of fresh tea leaves by estimating total polyphenols using near infrared spectroscopy,” *Journal of Food Science and Technology*, vol. 55, no. 12, pp. 4867–4876, 2018, doi: 10.1007/s13197-018-3421-6.
- [77] A. Demiriz, K. P. Bennett, C. M. Breneman, and M. J. Embrechts, “Support Vector Machine Regression in Chemometrics,” *Computing Science and Statistics: Proceedings of Interface, Volume 33*, 2001.

## **Chapter 2**

# **Development of a portable Raman spectrometer**

## 2.1 Introduction

Chandrasekhara Venkata Raman was an Indian physicist born at Tiruchirappalli in Southern India on 7<sup>th</sup> November 1888. It is believed that the foundation to the discovery of Raman effect was unconsciously laid down during a trip by C. V. Raman to Europe in 1921. While passing the Mediterranean Sea, Raman was fascinated by the deep blue colour of the sea water. As explained by Lord Rayleigh at that time, the blue colour of the sea water was just the reflection of the blue sky which was due to the scattering of sunlight by molecules in the atmosphere. However, Raman was not satisfied with his explanation that the blue colour of the sea water was merely because of the reflection of the blue sky. On board the ship, Raman carried out a few experiments which convinced him that the blue colour of the deep sea was a distinct phenomenon. This event made Raman do series of experiments and theoretical studies on the scattering of light in transparent media of different kinds at the Indian association for the cultivation of science [1]. Raman and Krishnan communicated their findings to Nature on 16<sup>th</sup> February 1928 in a letter entitled “*A new type of secondary radiation*” which got published on 31<sup>st</sup> March 1928. The first detailed demonstration of the discovery was made by Raman on 16<sup>th</sup> March 1928 at South Indian science association in Bangalore [2]. The full text of the lecture was published in the Indian Journal of Physics on 31<sup>st</sup> March 1928 with photographs of the scattered spectrum of Benzene. Raman was awarded the Noble prize for physics and the Hughes medal in the year 1930. The discovery of Raman effect is regarded as one of the best three discoveries in experimental physics of that decade.



## 2.2 Commercially available Raman spectrometer


At the initial stage, the application and development of Raman spectroscopy was very poor for a variety of difficulties. The problems were the use of sunlight as a source, visual observation as detector, most of application in liquid samples and presence of fluoresce effect. However, later the invention of lasers in 1960, these challenges were resolved, and situation altered radically. The use of laser in Raman spectroscopy increased the application of the methodology in different field.

There was always a demand for low-cost solution using Raman spectroscopy. This led to development of portable and low-cost Raman spectrometer. However, most of the Raman systems that are used today are either so large and bulky that it finds place only inside

laboratories or are so expensive that it questions affordability. For instance, take the example of assessment tea quality. Instead of taking the tea leaves for quality testing at a laboratory using conventional methods like HPLC how nice it would be if the test can be done in-situ by just touching a probe over the leaves. Several such commercial devices are already in the market. A small comparison of them is given in Table 2.1. Most of them are above \$30,000. Therefore, to make an affordable device with sufficient accuracy by using minimum number of components is the need of the hour so that it could serve satisfactorily both in industrial sectors and research laboratories. This chapter describes the contribution for this nobler cause.

Table 2. 1 Comparison of different Raman systems available in the market [Price of some items may not have been updated] [3]

Raman hand-held systems	Specifications	Price
<p>NanoRam Handheld RAMAN System, B&amp;W Tek[3]</p> 	<ul style="list-style-type: none"> <li>• <b>Laser Output Power</b>- 300 mW Max Adjustable in 10% Increments</li> <li>• <b>Excitation Wavelength</b>- 785 nm</li> <li>• <b>Output response</b> - 176 <math>cm^{-1}</math> to 2900 <math>cm^{-1}</math></li> <li>• <b>Resolution</b> - 9 <math>cm^{-1}</math> at 912 nm</li> <li>• <b>Detector</b>-Thermo electrically Cooled Linear Charge coupled device</li> <li>• <b>Power supplies</b> - Battery Rechargeable Li-ion, (&lt;4 hours)</li> <li>• <b>Electrical</b> - AC Adaptor: 12V DC, (min. 2A)</li> <li>• <b>Dimensions</b> - 22 x 10 x 5 cm</li> </ul>	\$46,405
<p>Thermo Scientific™ TruScan™ RM Handheld Raman Analyzer[4]</p> 	<ul style="list-style-type: none"> <li>• <b>Laser Output</b> - 250mW <math>\pm</math>25</li> <li>• <b>Laser Excitation Wavelength</b> – 785nm <math>\pm</math> 0.5</li> <li>• <b>Spectral Range</b> - 250 to 2875<math>cm^{-1}</math></li> <li>• <b>Spectral Resolution</b> - 8 to 10.5<math>cm^{-1}</math></li> <li>• <b>External Power Supply</b> - DC Wall</li> </ul>	\$56,780

	<p><i>Adapter, 100-240VAC 50/60Hz</i></p> <ul style="list-style-type: none"> <li>• <b>Dimensions (L x W x H)</b> - 8.2 x 4.2 x 1.7 in.</li> <li>• <b>Weight</b> - 0.9kg</li> </ul>	
<p>Raman Systems Portable-PinPointer™[5]</p> 	<ul style="list-style-type: none"> <li>• <b>Laser</b> - 785 nm</li> <li>• <b>Excitation Power</b> - 5-300 mW</li> <li>• <b>Output Range</b> - 200 - 3000 <math>cm^{-1}</math></li> <li>• <b>Resolution</b> - 12 <math>cm^{-1}</math></li> <li>• <b>External input</b> - Rechargeable battery, less than 4 hrs./charge</li> <li>• <b>Size</b> - 8.5" x 4.3" x 2.5"</li> <li>• <b>Weight</b> - 3 lbs.</li> </ul>	\$26,912
<p>Optosky ATR6500 4<sup>th</sup> Gen Handheld Raman Analyzer [6]</p> 	<ul style="list-style-type: none"> <li>• <b>Operating System</b> - Android</li> <li>• <b>Excitation Wavelength</b> - 785 <math>\pm</math> 0.5nm</li> <li>• <b>Wavenumber Range</b> - 200-4000 <math>cm^{-1}</math></li> <li>• <b>Resolution</b> - 10 <math>cm^{-1}</math></li> <li>• <b>Touch Screen</b> - 5.5", 1920x1080, c</li> <li>• <b>Weight</b> - 450g</li> <li>• <b>Size</b> - 6.7"x3.1"x1.2"</li> <li>• <b>Interface</b> - WIFI, USB Type-C, Bluetooth, GSM</li> <li>• <b>Battery</b> - 4–6-hour continuous operation</li> </ul>	\$19,800

MetrohmMira M-1[5]



- **Size (H) - 39.0mm**
- **Excitation- Basic Class 1**
- **Excitation -less than or equal 100 mW**
- **Excitation)- 785nm**
- **Length (mm) - 131**
- **Width (mm) - 85**
- **Optical Resolution (cm<sup>-1</sup>) - 16-18**
- **Output response (cm<sup>-1</sup>) - 400-2300**
- **Output presentation - Touchscreen**

> \$17,500  
(basic) –  
\$32,000  
(advanced)

### 2.3 Development of the portable Raman spectrometer

Here, we describe the design and development of a portable Raman spectrometer with the off-the-shelf components. For development of the prototype Raman spectrometer, the configuration is determined which uses lesser number of components to keep the procurement cost of the parts to a minimum without compromising much on the performance. The design of the spectrometer can be primarily divided into three parts — 1) Laser power supply, 2) Optical assembly and 3) Detector. In the following section, these three categories have been discussed in detail. Finally, the prototype was developed as a standalone instrument for quality estimation of marker molecule of a plant.

### 2.3.1 Laser Power supply

#### 2.3.1.1 Working principle of the Laser power supply

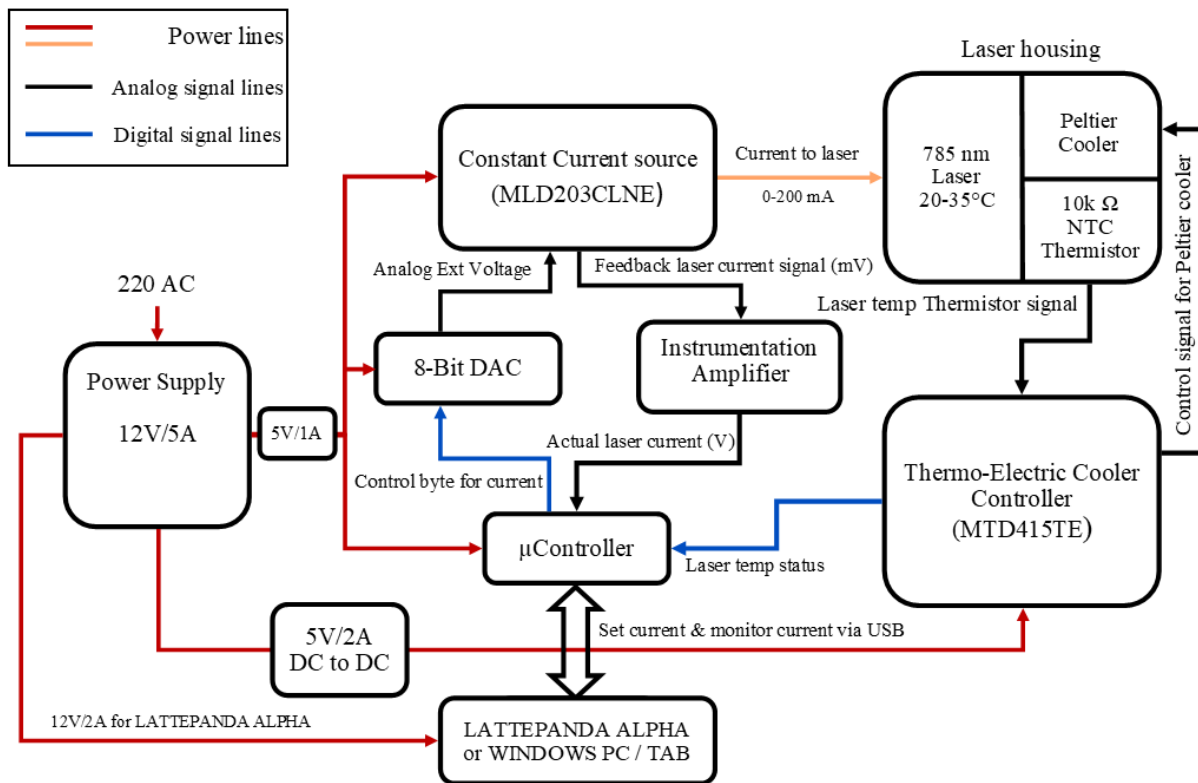


Figure 2. 1 Block diagram of the laser power supply

The Laser power supply facilitates the user to control and monitor the laser current along with maintaining the laser temperature. The block diagram of the laser power supply is shown in figure 2.1. The Hub of the laser power supply is an 8-bit microcontroller which coordinates with all the components.

The microcontroller receives a set-point laser current value from the user and an external control voltage proportional to the set-point current value is sent to the laser current driver. The laser current driver then generates the laser current proportional to the external control voltage and supplies it to the laser diode. Hence, the laser is powered with a constant current set by the user. The constant current laser driver then provides a differential voltage proportional to the current flowing through the laser which is amplified and read by the 10-bit ADC of the microcontroller. This enables the user to monitor the current flowing through the laser in real time after fixing the set-point laser current value.







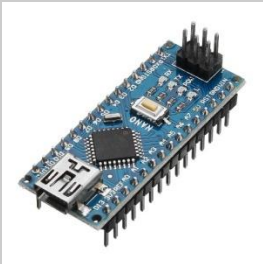
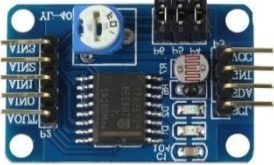

The temperature of the laser is monitored and maintained by the Thermo Electric Cooler (TEC) controller. The TEC controller is programmed with the temperature value set by the user which acts as the set-point. The controller senses the temperature of the laser by measuring the resistance of the 10K $\Omega$  NTC thermistor placed inside the laser packaging. TEC controller now tries to maintain the set-point temperature value by controlling the current flowing through the Peltier cooler placed inside the laser housing. An allowable temperature window is also set in the TEC controller. The TEC controller sends a digital signal to the microcontroller whenever the temperature of the laser falls out of this window.

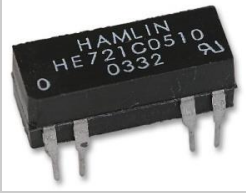
### 2.3.1.2 Components of the laser power supply

The laser power supply is mainly designed to provide constant current to the laser diode. In Raman spectroscopy, a single-wavelength (785 nm) laser is used to excite the sample. In addition to the constant current that flows through the laser, the temperature of the laser also needs to be controlled. The laser power supply is designed to perform all the functionalities mentioned above. The components of the laser power supply are shown in brief in the table 2.2.

Table 2. 2 The components used for the laser power supply

Sl No.	Component Name	Part/ Model No.	Description	Maker
1	Power Supply 	LM7805 and DC to DC converter (JSM1012S05) from	12v, 5A	STMicroelectronics and XR Power
2	Constant current module 	MLD203CLNE	250 mA Precision Constant Current Laser Driver	Thorlabs Inc., USA
3	Laser	I0785S50100B	785 nm single frequency with integral TEC	Innovative Photonic

			Power: 60 mW Working voltage: 2 V Current: 150 mA at sample	Solutions, USA
4	TEC Controller Module  	MTD415TE	3 W, 1 A	Thorlabs Inc., USA
5	Micro-controller  	ATmega328/P	32Kbytes of flash memory and 2Kbytes of SRAM	Atmel®
6	DAC  	PCF8591	8-bit A/D & D/A converter	NXP Semiconduct ors
7	<b>Instrumentation Amplifier</b>  	AD620 module	40 ppm maximum nonlinearity	Analog Devices

8	<b>Reed Relay</b> 	HE721C0500	short the Power_SW pins of the Lattepanada Delta 432	Littelfuse

### 2.3.1.3 Design and calibration of the electronic circuitry

The laser diode and the electronic circuitry were first tested on a bread board. The temperature of the laser is electronically controlled by checking the resistance of the thermistor with the help of a Peltier cooler placed in the laser housing. The temperature of the laser is kept at 30°C. The TEC controller is programmed, and oscillation test was performed using the MTD series software provided by the manufacturer before placing it inside the circuit. The values of P share, I share, and D share were determined in the oscillation test. At first, there was a significant deviation of the measured laser current from the calculated laser current. Figure 2.2 shows that the deviation occurred more in the lower values of laser current. This is because of the nonlinear variations in the output voltage of the DAC. The cubic spline interpolation method was implemented to obtain a function that can describe the variation in the output of the DAC with its control byte. Better results have been achieved and the deviation of the measured laser current value from the calculated value has reduced with a RMSE of 2.509.

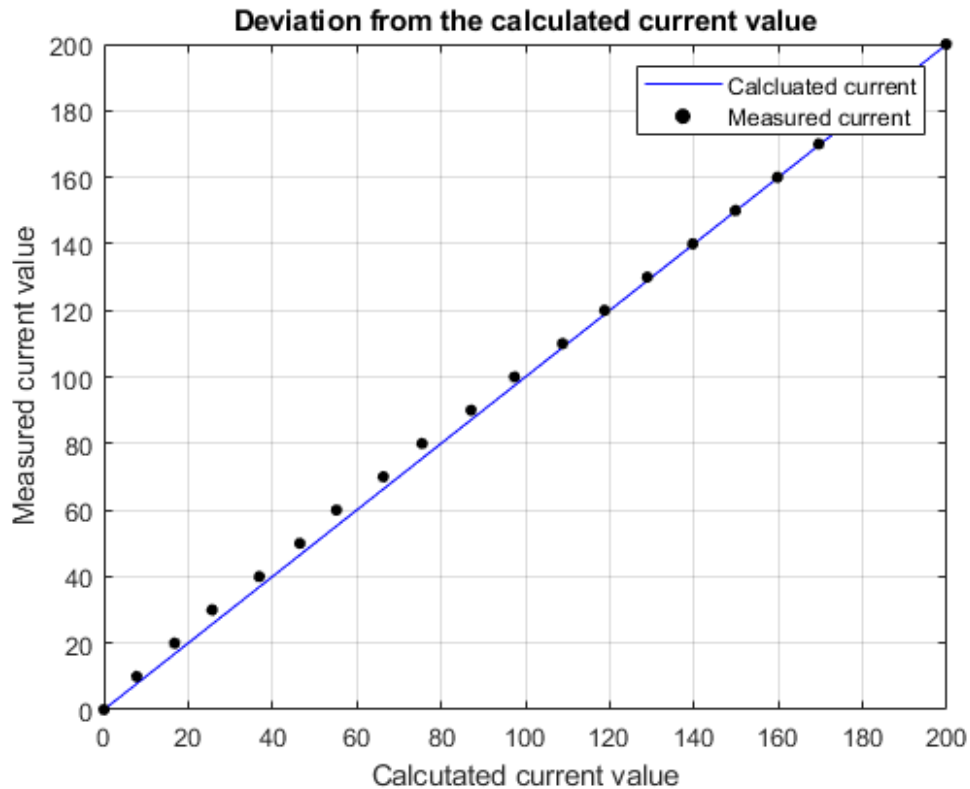


Figure 2. 2 Measured laser current versus calculated current

As the electronic circuitry for the laser power supply was to be placed inside the Raman spectrometer setup, the dimensions of the circuit were very crucial. In addition to that, the heat dissipation of the circuit was also a concern as it could have an effect on the readings of the detector. To overcome both these issues, the circuit was divided into two parts and was put one above the other in a stacked manner. This type of design could fit inside the spectrometer enclosure and also provided ventilation among the components. The design was transformed into two PCBs which were stacked on top of the other with a gap of 3 cm in between them. Before creating the circuits, a 3D model was developed to determine the volume and compactness of the design so that it can be easily incorporated inside the Raman setup. Figure 2.3 shows the 3D models of the two circuits that have been developed for the laser power supply. Only the PCBs and other important components are shown in the 3D model (without wiring). Figure 2.4 and figure 2.5 show the 3D models of the final arrangement of the laser power supply. The development of the final prototype are shown in figures 2.6 and 2.7.

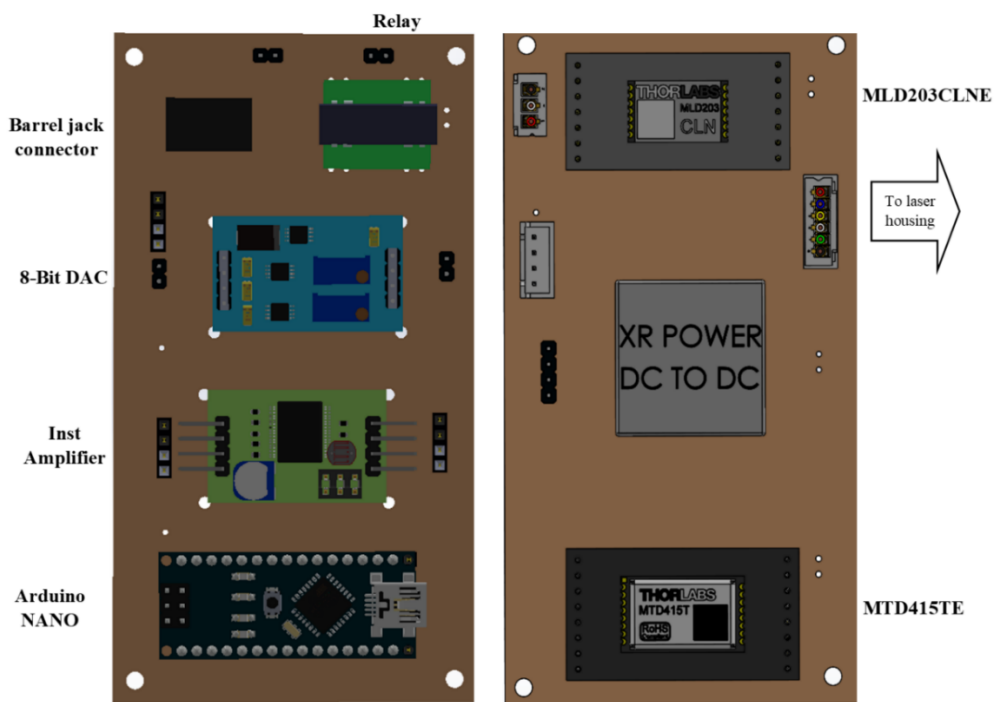


Figure 2. 3 Three-dimensional model of the Laser power supply circuit. (top view)

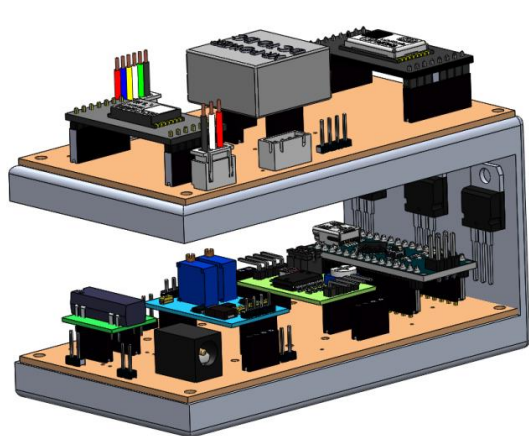


Figure 2. 4 3D model of the complete laser power supply with housing (View-1).

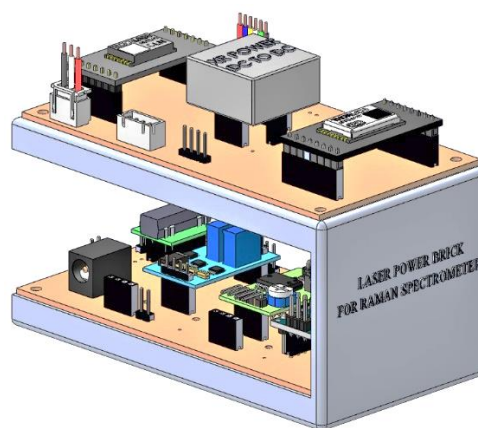


Figure 2. 5 3D model of the complete laser power supply with housing (View-2).

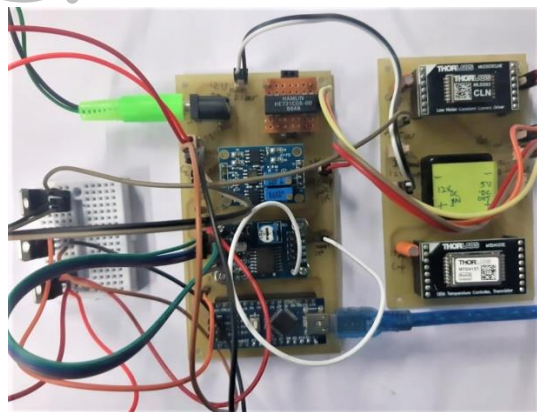


Figure 2. 6 Prototype of proposed laser power supply circuit.

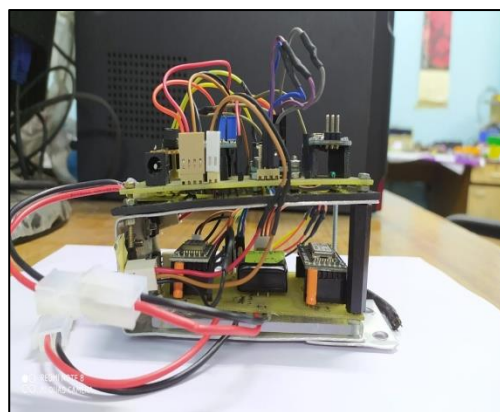


Figure 2. 7 Photograph of Laser power supply of a Raman Spectrometer

#### 2.3.1.4 Developing the graphical user interface for the Laser power supply

The laser current and temperature are controlled and monitored using a graphical user interface created using Visual Studio. It is a simple .NET Framework application written in Visual Basic which can perform serial communication with onboard microcontroller. The laser power supply gets connected to PC or tablet via USB. The current can be set from 0 – 180 mA by entering the current value in the editable text field of the UI. After the current is set, the actual current flowing through the laser is shown in the UI which updates the display every one second. The temperature of the laser is monitored as shown in the UI by sensing the status signal coming from the TEC controller. The status signal is a digital signal which stays high as long as the laser is under the defined temperature window. The GUI is shown in figure 2.8. A .NET Framework DLL with all the functions needed to control the laser power supply is also created so that the functions can be called from different applications or GUIs. This helps in integrating the control of laser power supply directly to different applications written in different platforms.

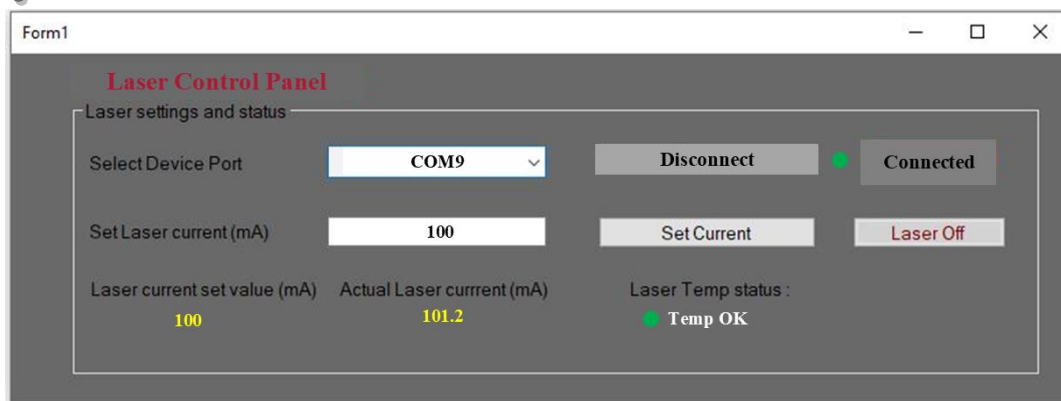


Figure 2. 8 PC-based GUI for the laser power supply.

### 2.3.2 Optical Assembly

The optical assembly as a whole act as a waveguide for the monochromatic laser and the scattered Raman rays to reach the sample and the detector respectively. In this design, the detector is also a part of the optical assembly. The assembly provides isolation of the radiation from external noises and interferences. It consists of optical components to reflect, bend and filter radiations so that only the useful part of the radiation is retained and is guided to the sample and the detector.

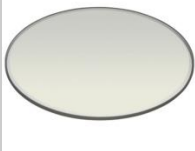


#### 2.3.2.1 Components of the Optical Assembly

The Optical Assembly is an opto-mechanical system of different mechanical and optical components. It is an enclosed compartment consisting of necessary optical parts for irradiating the sample, collecting the scattered Raman radiation and focussing the collected radiation on the detector. Numerous components have been used to develop the optical assembly. However, for the sake of simplicity, only the important components have been explained here (table 2.3).

Table 2. 3. List of components used to develop a portable Raman Spectrometer

Sl No.	Component Name	Part/ Model No.	Description	Maker
1.	Power supply module for Laser	Designed with MLD203CLNE & MTD415TE	Current range: 0mA to 180mA	Customized design with the components from Thorlabs Inc.
2	Dichroic Mirror 	DMLP805R	25 mm x 36 mm Longpass Dichroic Mirror, 805 nm Cut-On	Thorlabs Inc., USA
3	Off-Axis Parabolic Mirror 1 (OAP-1) 	MPD129-P01	Ø1" 90° Off-Axis Parabolic Mirror, Prot. Silver, RFL = 2"	Thorlabs Inc., USA
4	Off-Axis Parabolic Mirror 2 (OAP-2)	MPD149-P01	Ø1" 90° Off-Axis Parabolic Mirror, Prot. Silver, RFL = 4"	Thorlabs Inc., USA
5	Long-pass edge filter	BLP01-785R-25	Transmission: 812-1200 nm Edge Wavelength: 805nm	Semrock Inc., USA



				
6	Notch filter 	NF785-33	Ø25 mm Notch Filter, CWL = 785 nm, FWHM = 33 nm	Thorlabs Inc., USA
7	Detector 	TF C13054MA	Spectral response range: 790 to 920 nm	HAMAMAT SU Photonics UK Limited, UK

### 2.3.2.2 Designing of the Optical Assembly

The optical assembly of the Raman Spectrometer is designed keeping in mind about its size, weight, and ease in usability. Portability is one of the primary concerns of this design. Therefore, before building the optical assembly, its design was analysed using SOLIDWORKS 3D CAD. Efforts have been put to keep the form factor of the design as small and compact as possible without compromising on its performance. The complete setup rests on a 6" x 6" x 3/8" Mini-Series Aluminium Breadboard from Thorlabs, Inc. The components have been placed in a way that every component fits inside the breadboard properly. The two off-axis parabolic mirrors are placed at two consecutive vertices of the square breadboard. The dichroic mirror housing is placed in between the two off-axis parabolic mirrors and is mechanically and optically connected using lens tube (SM1M10). The off-axis parabolic mirror having reflected focal length of 2" is placed at the sample holder side and the mirror having reflected focal length of 4" is placed at the detector side. The laser housing is attached to the dichroic mirror housing and the laser diode faces the dichroic mirror at an angle of 45°. The parabolic mirror housing provides  $\pm 4^\circ$  kinematic pitch and yaw adjustment to focus the collimated laser on to the sample and detector's slit.

The sample holder is created at our laboratory using 6 mm acrylic sheets and it sits on the breadboard about 1.5" apart from the off-axis parabolic mirror. The notch filter and broadband precision window are mounted inside a lens tube and the lens tube is placed in between the dichroic mirror housing and the off-axis parabolic mirror of the detector side. The detector is placed at exactly 4" away from the off-axis parabolic mirror. The height of the detector is matched with the optical axis of the parabolic mirror to ensure that the beam is focused exactly on the entrance slit of the detector. This is done by placing an acrylic support at the base of the detector. All the components are rigidly fixed at their positions because a slight displacement of any of the components can affect the optical beam path and prevent it from focusing on the sample and the detector. The design of the optical assembly is shown in figure 2.9 and figure 2.10. The photograph of the optical assembly is shown in figure 2.11.

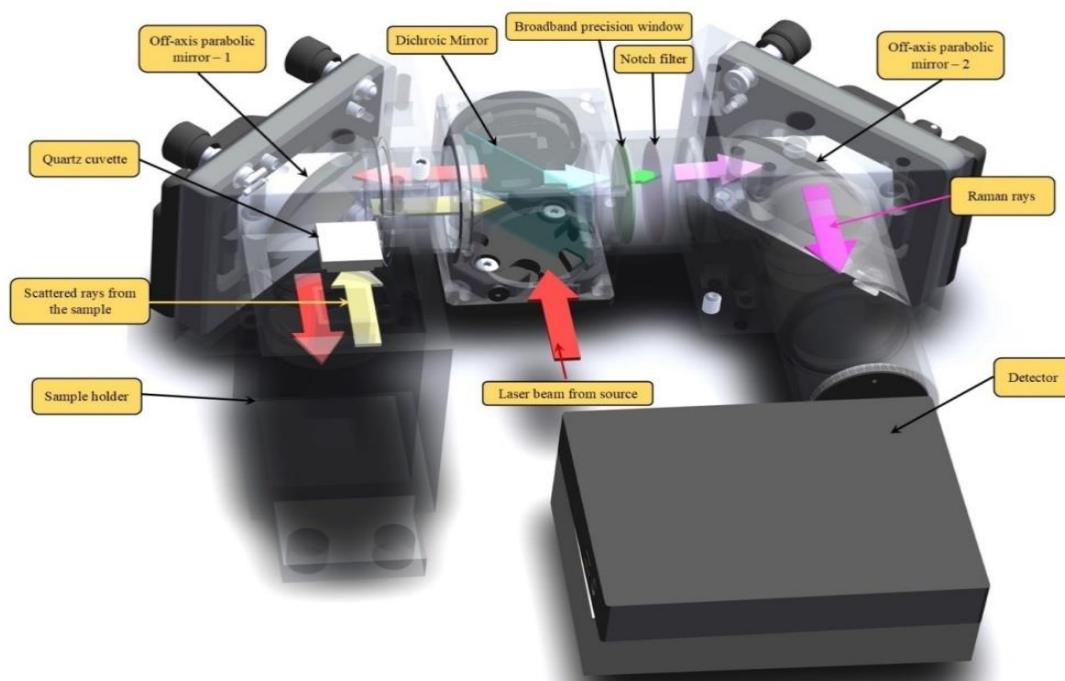


Figure 2. 9 Optical assembly of the Raman spectrometer with all its components. The beam path is shown with colored arrows. (Laser not shown)

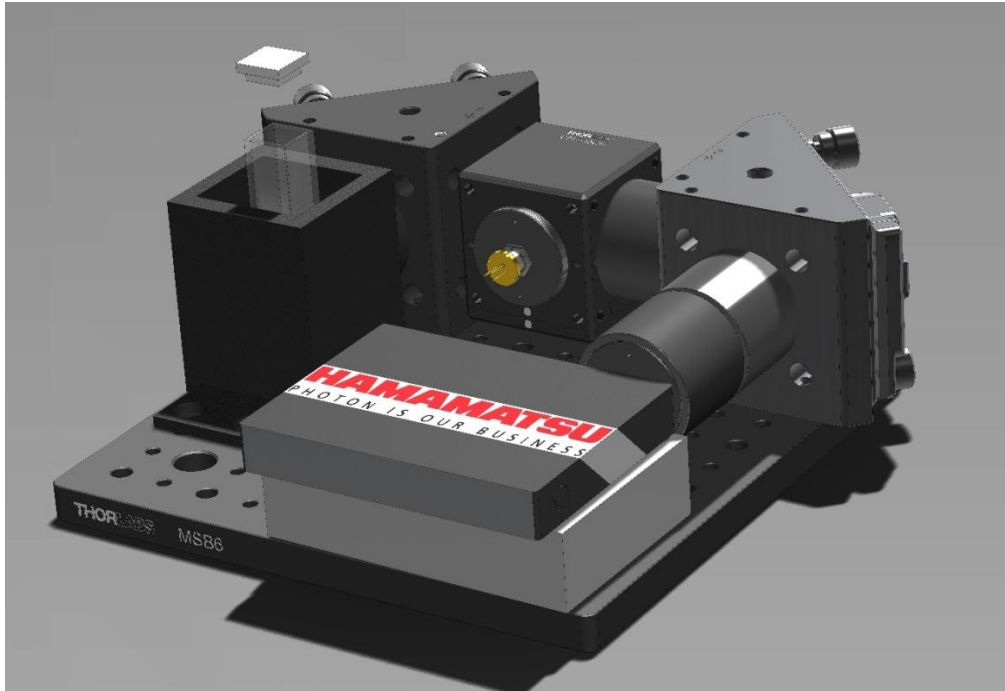


Figure 2. 10 3D model of the proposed optical assembly

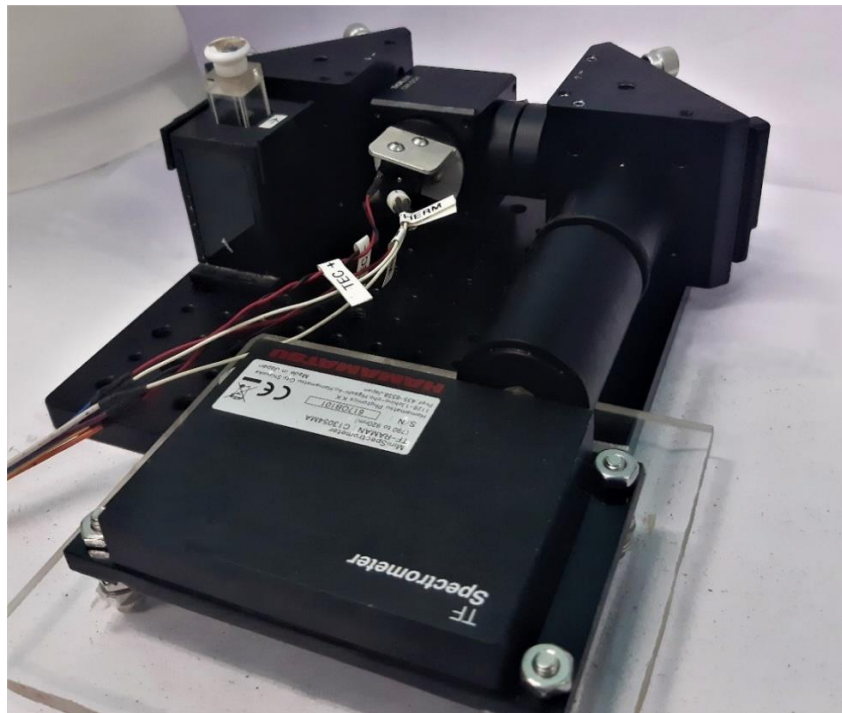


Figure 2. 11 Photograph of the Optical setup.

### 2.3.3 Detector

The scattered radiation from the optical head goes via the optic fiber to the detector containing the necessary optical components and the high-sensitivity CMOS image sensor.

The detector consists of a slit of dimension 10 x 400  $\mu\text{m}$ , a collimating lens, a transmission grating, a focusing lens and a CMOS image sensor of 512 pixels as shown in Figure 2.12. The detector has a spectral resolution (FWHM) of 0.4 nm. The interface electronics has a 16-bit ADC and integrate from as low as 11  $\mu\text{s}$  to 100ms. It supports USB to facilitate connection with a PC and draws only a typical of 220 mA current.

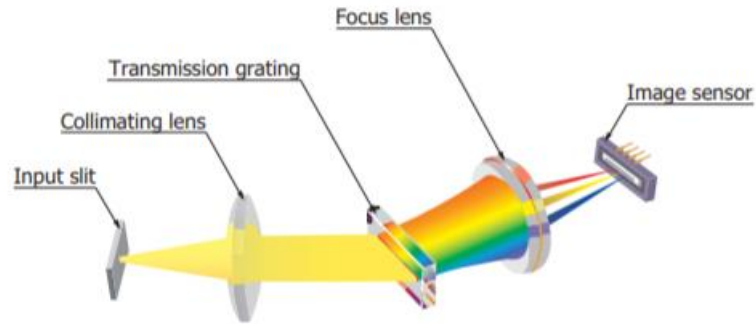


Figure2. 12 Optical component layout of the detector

The data acquired at each pixel corresponds to each wavelength of the spectrum and is A/D converted in proportion to the light intensity. When saving this data with the evaluation software of Hamamatsu Photonics, Japan, the horizontal axis can be specified as pixels or wavelength. The following quantic equation (provided by the manufacturer) can be used to calculate which pixel corresponds to the wavelength axis.

$$\text{wavelength (nm)} = a_0 + a_1 \cdot \text{pix} + a_2 \text{pix}^2 + a_3 \text{pix}^3 + a_4 \text{pix}^4 + a_5 \text{pix}^5 \quad (6)$$

, where *pix* is any pixel value of the image sensor. The coefficients are as follows (provided by Hamamatsu Photonics, Japan):

- $a_0 = 778.6461498$
- $a_1 = 0.3585042305$
- $a_2 = -0.0001745020601$
- $a_3 = 1.85457711 \times 10^{-7}$
- $a_4 = -3.284555756 \times 10^{-10}$
- $a_5 = 2.567910792 \times 10^{-13}$

### 2.3.4 Working principle of the Optical Assembly

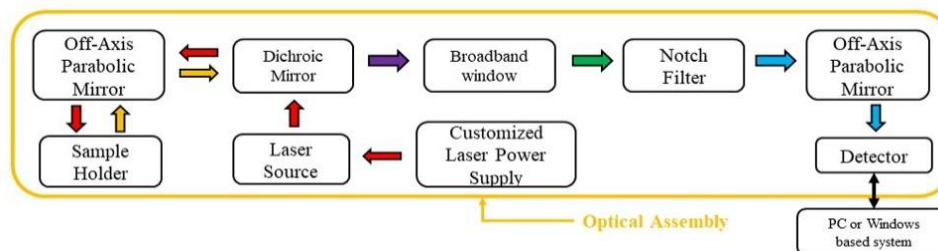


Figure 2. 13 Block diagram of the optical head.

Figure 2.13 shows the overall workflow of the optical assembly. The functionality of the optical assembly can be described in a sequential manner. The 785 nm monochromatic laser travels through the optical assembly and gets directed towards the sample. The path of the laser is changed by a Dichroic mirror and Off-axis parabolic mirrors placed at appropriate locations inside the optical assembly. The Dichroic mirror has a cut-on wavelength of 805 nm, so it reflects the 785 nm monochromatic laser coming from the laser source towards the off-axis parabolic mirror OAP-1. The off-axis parabolic mirror then focuses the laser beam onto the sample. The radiation interacts with the sample and gets scattered in all directions. The back scattered rays comprising of the Rayleigh and Raman signals are collimated and reflected towards the dichroic mirror. The strong Rayleigh signal which is of 785 nm wavelength gets suppressed at the dichroic mirror and the weak Raman signals which have wavelengths greater than 805 nm are made to pass through it. There is a broadband precision window (Long-pass edge filter, part no: BLP01-785R-25) with transmission range of 650 – 1050 nm placed after the dichroic mirror for eliminating the radiations outside the transmission range. Optical Notch filter (part no: NF785-33) with

centre stop-band wavelength of  $785 \pm 2\text{nm}$  is used to further suppress the Rayleigh signal. The filtered signal which now primarily consists of Raman scattered rays is then focused on the detector's slit using another off-axis parabolic mirror OAP-2. On entering the detector's (part no: TF C13054MA) slit, the optical information is collimated and dispersed into a spectrum by the collimating lens and the transmission grating, respectively. The spectrum is then linearly focused by a focusing lens onto a CMOS linear image sensor which converts light at each pixel into an electrical signal. The electrical signal is then A/D converted by the 16-bit ADC and the information is saved and displayed on a PC or windows device. The 3D model of photograph of the optical head is shown in figure 2.14 and 2.15 respectively. The 3D model and the photograph of the prototype Raman spectrometer is shown in figure 2.16 and figure 2.17 respectively. The important specification of the developed Raman spectrometer is given in table 2.4.

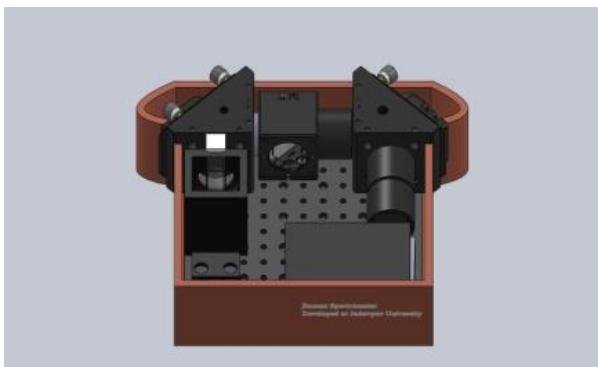


Figure 2. 14 3D model of the optical head of portable Raman spectrometer

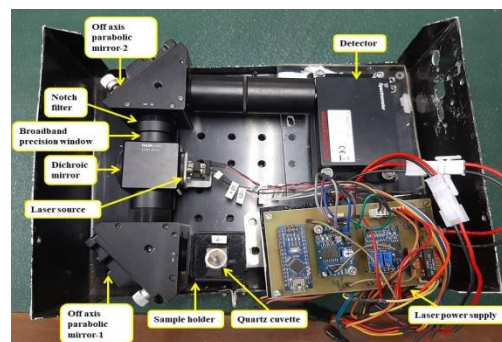


Figure 2. 15 Inside Photograph of the prototype Raman spectrometer with its associated components

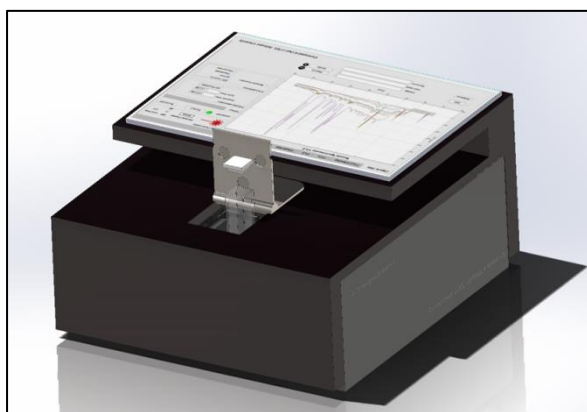


Figure 2. 16 3D model of the portable Raman spectrometer



Figure 2. 17 Photograph of the developed prototype portable Raman spectrometer

Table 2. 4 Important specifications for the developed portable Raman spectrometer

Parameter	Specification
Weight	1.8 kg
Dimension(W×D×H)	(28×20.5×15.2 )cm
Spectral Range	(80 – 1870) $\text{cm}^{-1}$
Spectral Resolution	0.4 nm
Light Source	Laser(785nm)
Detector	High-sensitivity CMOS linear image sensor
Data Export Formats	.csv,.txt
Operating Temperature	5 °C – 50 °C
Method of Measurement	Diffuse Reflection Transmission

### 2.3.5 Developing Graphical User Interfaces in Visual Studio and MATLAB App Designer for the Raman spectrometer

The Mini-Raman spectrometer detector C13054MA from Hamamatsu Photonics KK comes with an evaluation software - SpecEvaluationUSB2. The software lets us easily perform basic spectrometer operations like capturing data, converting the image sensor pixel numbers to wavelengths, showing the data graphically, storing the data etc.

The evaluation software SpecEvaluationUSB2 provides simple and basic features for spectroscopic measurements. It is neither configurable nor efficient for Raman analysis. Though it may be useful for capturing raw spectral data for initial analysis, it is not suitable in the long run where analysis becomes complex. Moreover, the software lacks features like



pre-processing and regression analysis etc for which the raw spectral data from this software need to be transferred to other statistical analysis software. The GUI provided by Hamamatsu Photonics, Japan is shown in figure 2.18.

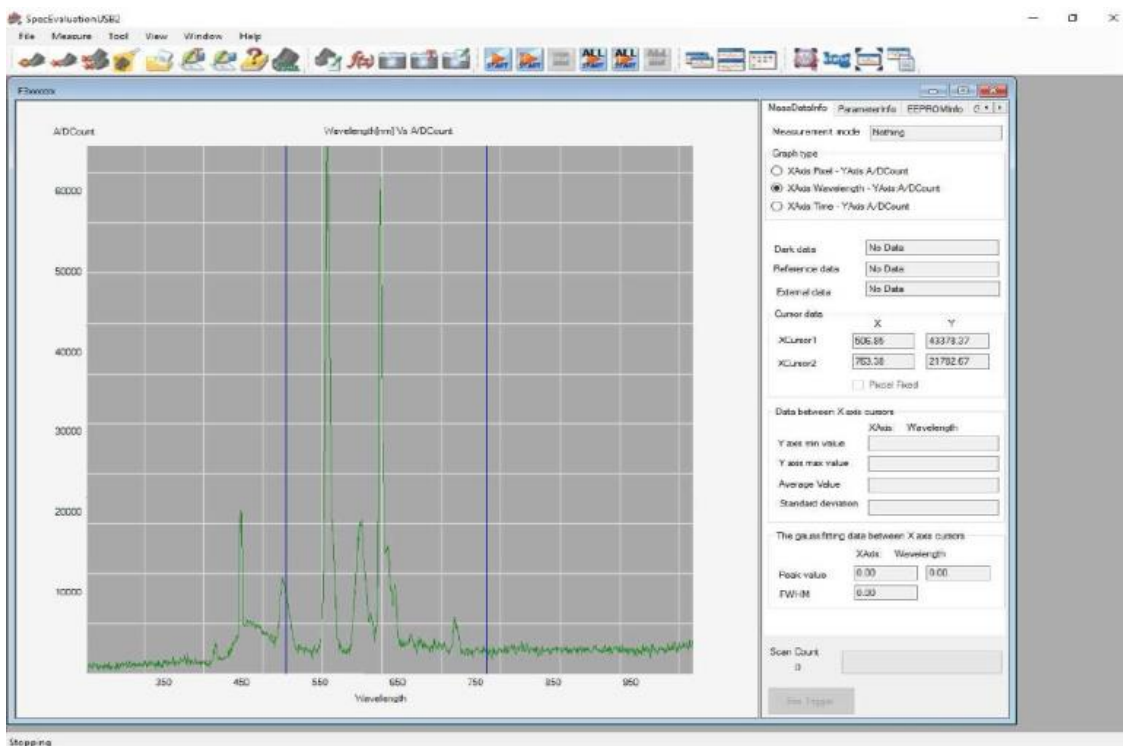


Figure 2. 18 GUI of the SpecEvaluationUSB2 software from Hamamtsu Photonic

### 2.3.5.1 Need of customized GUI for Hamamatsu Raman spectrometer

The SpecEvaluationUSB2 software lets the user to set measurement conditions and take basic measurements. The software lets the user to capture the data, graphically visualize the data and save it for further analysis. It also lets the user perform basic arithmetic operations like dark data subtraction, Gaussian fitting function etc. But for research purpose this software is not ideal. It has the underlying limitations:

- It does not provide pre-processing techniques like SNV, MSC etc, smoothing and derivative techniques.
- It does not provide machine learning techniques for development of classification and regression models.
- It does not provide statistical and chemometric techniques.



- It does not provide the tool to instantly predict the concentration of biomarkers in unknown sample.

Thus, this software can be used for only acquiring data from the detector. After that separate software like MATLAB, Python, R etc has to be used to analyze the data for predicting concentration of biomarkers in the unknown sample. This process becomes time taking and cumbersome.

### 2.3.5.2 Designing the GUI

MATLAB provides a method “NET.addAssembly()” for loading private .NET assemblies into MATLAB. This method was used to load the Hamamatsu DLL into MATLAB environment. The loading of the DLL was successful, and all the function contained in the DLL were visible and could be called from MATLAB. However, all the functions did not execute successfully. Some of the most important functions like USB2\_getImageData returned error. This is probably because these DLL functions were supposed to be called from a .NET Framework application as suggested by the manufacturer. A probable explanation to this problem is that the data structure used in the Hamamatsu DLL were not being handled or understood by MATLAB [7]. At this moment, developing the GUI in MATLAB seemed impossible since the Hamamatsu DLL is a compiled (.dll) file which cannot be configured or decompiled. Many approaches were tried and out of them, the concept of “Wrapper DLL” offered a solution to this problem.

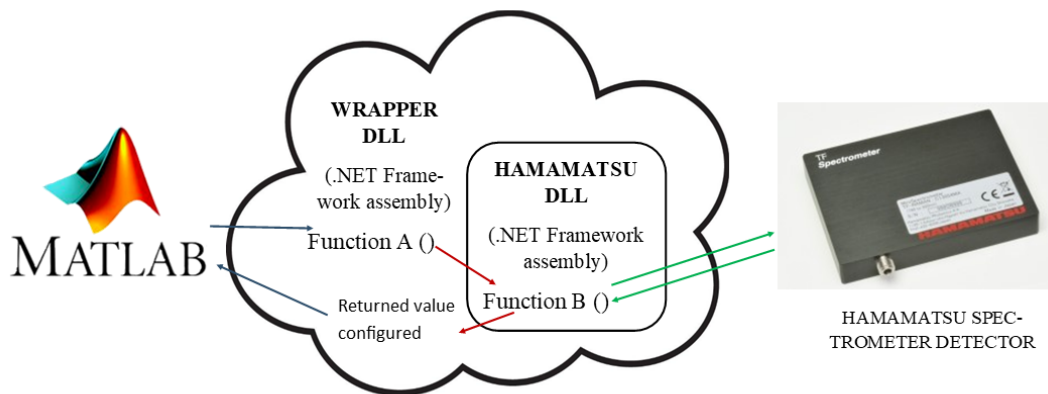


Figure2. 19 Illustration of the concept of wrapper DLL to be used along with the original DLL.

As the name would suggest, the Wrapper DLL is a DLL that is created to wrap the original DLL[8]. It forms a compatibility layer between the original DLL and the new application that is calling it. Since, the structure of the original DLL cannot be modified according to the new application, these modifications can be done in the wrapper DLL. A Wrapper DLL is created in the same platform as that of the original DLL. If the original DLL was intended to be called from a .NET Framework application, then the Wrapper DLL needs to be created as a .NET Framework library. The steps or processes involved in calling the original DLL via Wrapper DLL are:

1. The Wrapper DLL is created, and functions have been written which calls the functions of the original DLL.
2. The new application calls a function defined in the Wrapper DLL.
3. This function from the Wrapper DLL makes a call to the function in the original DLL.
4. The original DLL executes the function and returns the result to the Wrapper DLL.
5. The Wrapper DLL modifies the structure of the result according to the new application and sends it to the new application.

The Wrapper DLL (Hamamatsu wrapper) for the Hamamatsu DLL was created

as .NET Framework Library. Some of the functions of the Hamamatsu DLL were grouped and made as a single function in the Hamamatsu wrapper. For example: To set the data capture parameters of the spectrometer, 6 functions of the Hamamatsu DLL need to be called. Calling of these 6 functions is grouped into a single function in the Hamamatsu wrapper and calling this single function in Hamamatsu wrapper calls the 6 functions of the Hamamatsu DLL. The Hamamatsu wrapper successfully communicated and controlled the Hamamatsu spectrometer detector.

### 2.3.5.3 Modules of the GUI

The software has been developed on MATLAB App Designer, with an appropriate graphical user interface (GUI) (figure 2.20) for operation of the machine.

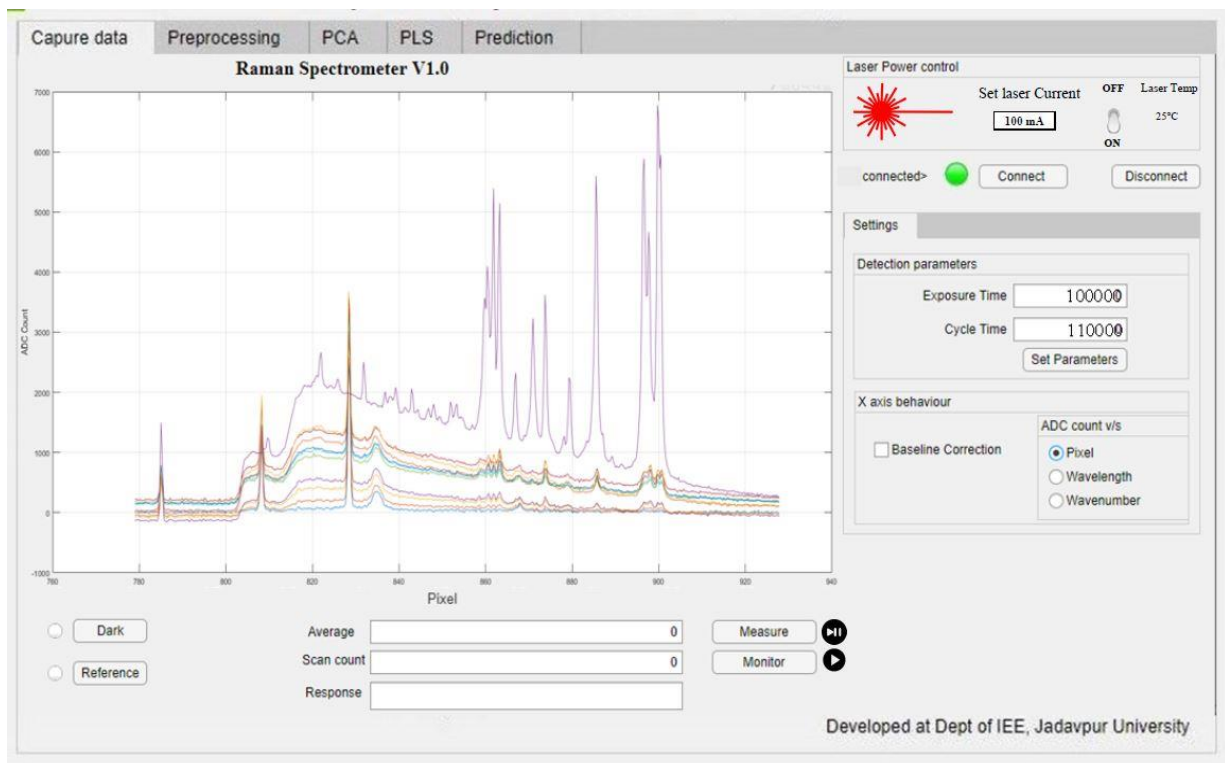


Figure 2. 20 GUI developed for the Raman spectrometer using MATLAB App designer.

The graphical user interface has the below mentioned properties:

- 1) Laser power control unit—It is used to control the laser source.

- 2) Categorization control unit —It is used for governing the constraint for a particular application.
- 3) Capture data module—This module is used for taking care of the spectral data acquisition from the sample for continuous monitoring.
- 4) Graphical representation—It represents the real-time data of a sample.
- 5) Preprocessing module- Here, spectral data acquisition and background noise elimination that occur due to random error and random spikes [9] are carried out. In addition, captured spectral data can be pre-processed using minmax normalization, detrend, mean centering, standard normal variate (SNV), extended multiplicative scatter correction (EMSC), 1<sup>st</sup> derivatives and 2<sup>nd</sup> derivatives [10];
- 6) Classification module-Initial assessment of the capture data can be performed for classification of the spectral data in this module;
- 7) Regression module –Regression analysis can be performed to develop the prediction model to estimate the marker molecule piperine of the test sample;
- 8) Data archival module— It keeps the data for further processing.
- 9) Prediction module- Using the regression coefficients of the prediction model and the spectral data from the spectrometer, the prediction of piperine in an unknown sample can be done instantly. The prediction tab of the GUI is shown in figure 2.21.

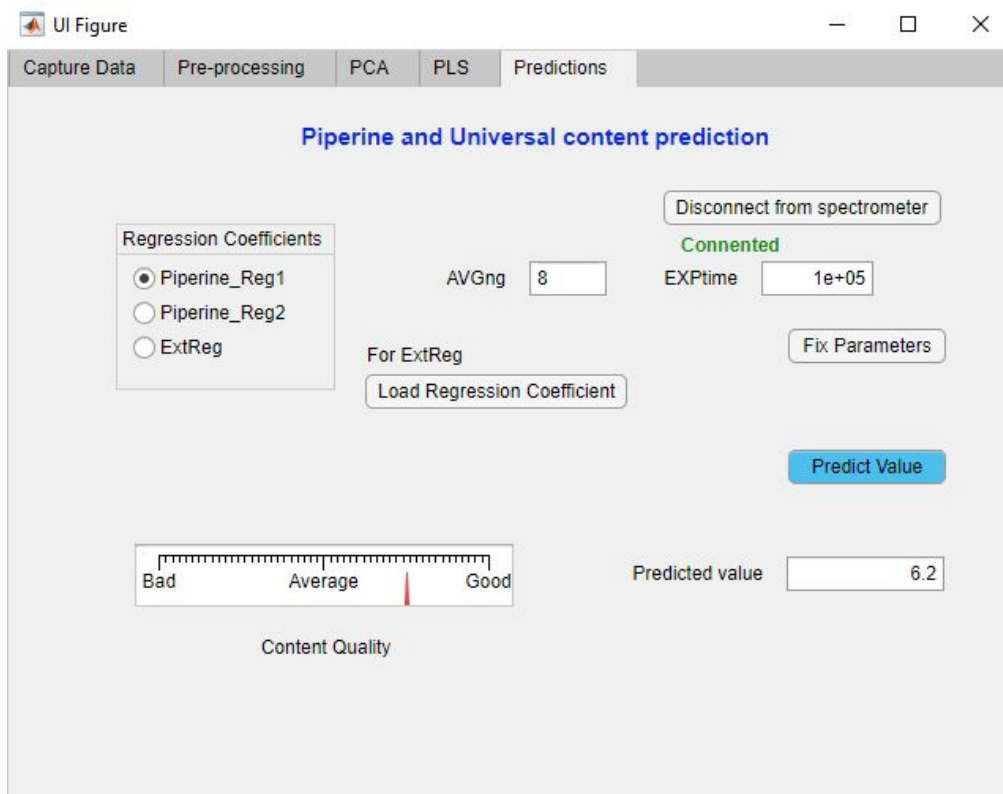


Figure 2. 21 Standalone GUI for Piperine content estimation using Raman spectroscopy.

## 2.4 Result and discussions for verification and validation of the developed instrument

The developed Raman spectrometer was used to take spectra of few standard compounds to validate its accuracy and performance. Raman active compounds such as Benzene, Chloroform, Glacial Acetic acid and Piperine were used for this purpose. 32 Raman spectra of each of the compounds were taken and averaged. The exposure time was set for 100 milliseconds. Most of the photo detectors exhibit dark spectrum which is a spectrum obtained when no light is falling on the detector. The dark spectrum can be caused due to many reasons like thermal excitation of carriers (dark current), ambient light conditions etc. The optical signal from a sample falling on the detector gets superimposed with the dark spectrum which brings noises and baseline shifts in the raw spectrum of the sample. Subtracting the dark spectrum from the raw spectrum of the sample produces better interpretable spectrum with reduction of the unwanted and useless signals in the spectrum. The dark spectrum subtraction was performed for all the above-mentioned standard compounds. The performance of the spectrometer was evaluated based on the comparison of the spectral data

produced by it with the spectral data of already accepted and published works of authors in the same field. The results are discussed in the subsequent sub-sections.

### 2.4.1 Benzene

The Raman spectrum of Benzene has been observed by many researchers since the discovery of Raman scattering. Wood observed more than 15 peaks of Benzene up to 3164  $\text{cm}^{-1}$ . However, the configuration of the developed Raman spectrometer provides Raman shifts up to 2000  $\text{cm}^{-1}$ . Hence the peaks of benzene occurring above 2000  $\text{cm}^{-1}$  are not considered in this analysis. The Raman shifts of Benzene observed by Wood [11], Krasser[12], Zhang [13] and NIST[14] are given in table 2.5.

Table 2. 5 Comparison of Raman shift ( $\text{cm}^{-1}$ ) of Benzene in the developed spectrometer with other reports

Sl. No.	*NIST [16]	R.W. Wood [11]	W. Krasser [12]	X. Zhang [13]	Developed Spectrometer
1	605.6	606	606	606	<b>606</b>
2	NA	849	850	NA	<b>NA</b>
3	848.9	992	992	992	<b>992</b>
4	991.6	1178	1178	1177	<b>1178</b>
5	1178	1584	1585	1586	<b>1586</b>
6	1584.6	1603	1605	NA	<b>1608</b>

\*NIST= National Institute of Standards and Technology, United States Department of Commerce

The Raman spectrum of Benzene obtained by our developed Raman spectrometer is shown in figure 2.22. The most prominent peak of Benzene could be seen at 992  $\text{cm}^{-1}$  which is also present in all the mentioned literatures. This peak corresponds to the breathing vibration of the Benzene ring. The peaks of Benzene at 606  $\text{cm}^{-1}$  and 1178  $\text{cm}^{-1}$  are also prominently visible in the spectrum and are supported by the literatures. These peaks correspond to the CCC deformation and CH shear vibration. The peaks observed at 1586  $\text{cm}^{-1}$  and 1608  $\text{cm}^{-1}$

have slight variations in the shifts, but the variations are very little and not more than  $5\text{ cm}^{-1}$ . It can be also seen that the peak at  $849\text{ cm}^{-1}$  or  $850\text{ cm}^{-1}$  given in the first two literatures are not present in the observed spectrum of Benzene by the instrument.

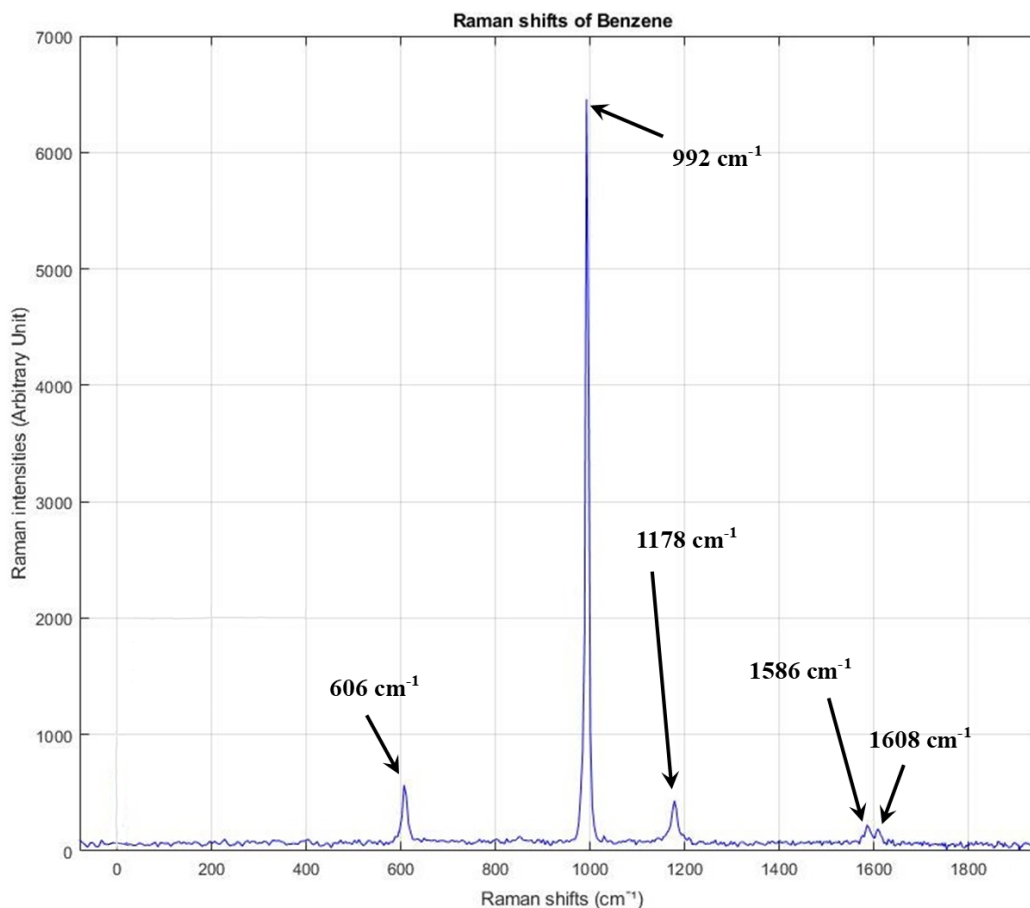


Figure 2. 22 Raman spectra of Benzene obtained from the developed Raman spectrometer

### 2.4.2 Chloroform

The Raman shifts of Chloroform obtained by Bhagavantam and Venkateswaran [9], Dabadghao [10], Langer and Meggers [11], and Rao [12] along with the peaks observed by our instrument are given in table 2.6.

Table 2. 6 Comparison of Raman shift ( $\text{cm}^{-1}$ ) of Chloroform in the developed spectrometer with other reports

Sl No	NIST [18]	Bhagavanta m and Venkateswa ran [9]	Dabadgh ao [10]	Langer and Megge rs [11]	Viswesw ara Rao [12]	Developed Spectrome ter
1	261	261	262	261	259	NA
2	363	367	366	367	367	<b>367</b>
3	672	669	667	668	664	<b>666</b>
4	760	762	762	760	757	<b>757</b>
5	1217	1218	1213	1215	1215	<b>1216</b>

It can be observed from the table that there are five fundamental vibrations of Chloroform below  $2000 \text{ cm}^{-1}$  without considering the overtones and combination tones. The Raman spectrum of Chloroform obtained using the developed Raman spectrometer is shown in the figure 2.23. The figure 3.2.15 shows that the strongest Raman peak of Chloroform has occurred at  $666 \text{ cm}^{-1}$ . This agrees with the data given in the table where the third peak of Chloroform occurs at around  $664 - 669 \text{ cm}^{-1}$  in all the literatures. According to the table, the second peak of Chloroform occurs at around  $366 - 367 \text{ cm}^{-1}$  which is also detected by the instrument at  $367 \text{ cm}^{-1}$  as shown in the figure 3.2.15. Similarly, the fourth and fifth peak of Chloroform shown in the figure 3.2.15 are also in accordance with the peaks given in the literatures. However, the first peak of Chloroform which occurs at around  $259 - 262 \text{ cm}^{-1}$  as per the table is missing in the spectrum obtained by the developed instrument.



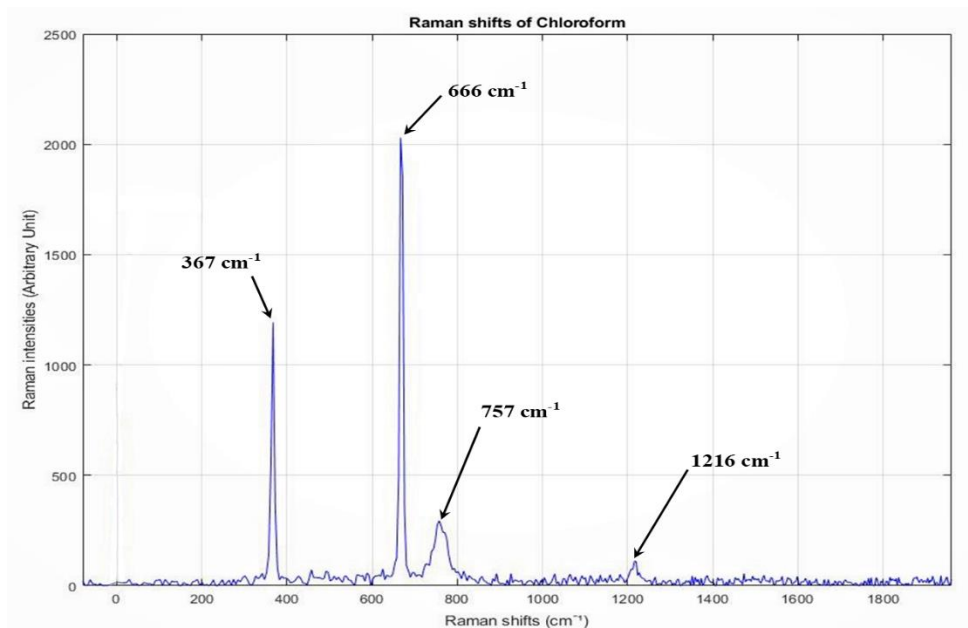


Figure 2. 23 Raman spectra of Chloroform obtained from the developed Raman spectrometer

### 2.4.3 Glacial acetic acid

There are not many literatures found related to the Raman spectrum of Glacial acetic acid that could be used for the comparison. However, Fu Wan [13] has shown in his paper a method to analyse dissolved Acetic acid in transformer oil where he has discussed about the Raman spectrum of pure Acetic acid that has been used here for comparison. The Raman shifts of Acetic acid observed by Fu Wan along with our observations are given in table 2.7.

Table 2. 7 Comparison of Raman shift (cm<sup>-1</sup>) of Glacial acetic acid in the developed spectrometer with other reports

SL No	Fu Wan [13]	Developed Spectrometer
1	446	447
2	603	606
3	621	620
4	893	896

5	1014	1004
6	1280	1290
7	1366	1355
8	1428	1429
9	1664	1684
10	1758	NA

It can be seen from the table that the first four Raman shifts of Acetic acid obtained from the developed spectrometer has greatly matched the shifts observed by Fu Wan with a deviation of no more than  $3\text{ cm}^{-1}$ . However, the subsequent shifts have shown little variation of about  $10\text{ cm}^{-1}$ . It can be also seen in the figure 2.24 that the last 6 peaks are less prominent than the first four. There can be many reasons for such phenomenon like contamination of the sample, accumulation of dust on the optical components or poor calibration of the instrument etc.

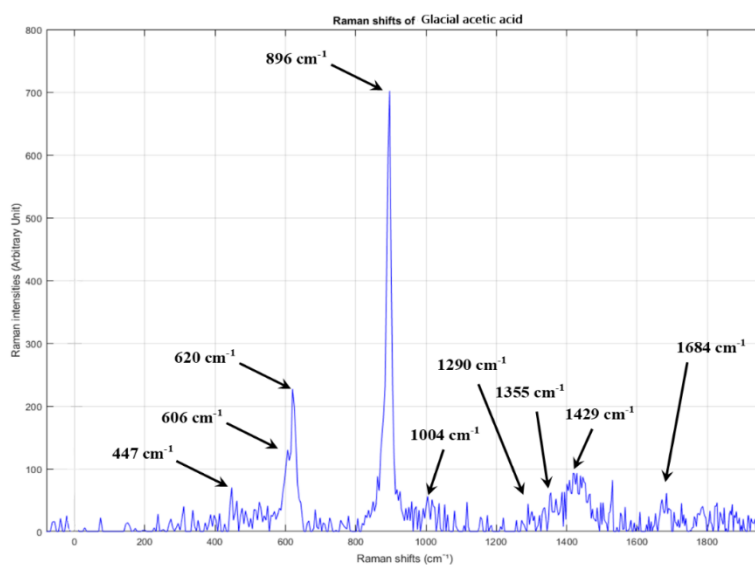


Figure 2. 24 Raman spectra of Glacial acetic acid obtained from the developed Raman spectrometer.

### 2.4.4 Piperine

Piperine is one of the major chemical markers in *Piper nigrum* L (Black pepper). It shows a very prominent Raman spectrum for which it can be used here for comparison. Dry powdered form of Piperine was used to obtain the Raman Spectrum and the major shifts are listed in the table 2.25 along with the Raman shifts of Piperine observed by Schulz [14].

Table 2. 8 Comparison of Raman shift ( $\text{cm}^{-1}$ ) of piperine in the developed spectrometer with other reports

SL No	Schulz	Developed Spectrometer
1	NA	1116
2	NA	1136
3	1153	1155
4	NA	1205
5	1256	1257
6	1295	1294
7	NA	1369
8	1448	1446
9	1584	1586
10	1600	1599
11	1625	1624

The Raman spectrum of piperine obtained from the developed spectrometer is shown in figure 2.25. The spectrum of piperine was very much affected with baseline shift and hence the spectrum has been processed with baseline removal [15]. It can be understood from the table that all the shifts that have been observed by the literature

(Schulz) are also identified by the developed spectrometer. Furthermore, three more shifts have also been seen in the spectrum obtained by the spectrometer which are absent in the literature data. The reason for this is not known, perhaps the quality of Piperine used as a sample may have caused this since the sample of piperine was 99 % pure.

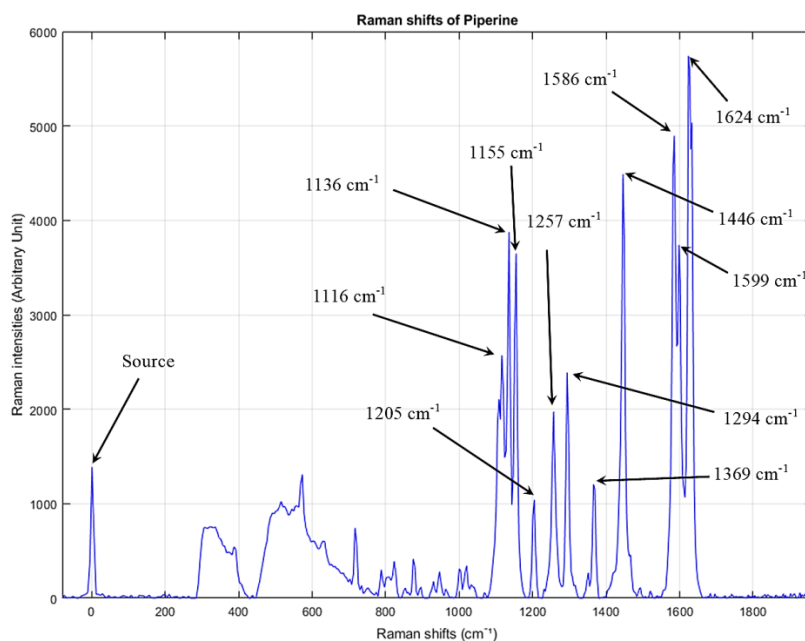


Figure 2. 25 Raman spectra of piperine obtained from the developed Raman spectrometer

## 2.5 Conclusion

The chapter illustrated the development of a Raman spectrometer. It includes design and assembling of the required hardware and design and development of the custom GUI. The spectrometer has been developed by assembling off-the-shelf components. The software was designed for real time prediction of marker molecule concentration in a sample and provision for the selection of analysis techniques was also kept. The calibration of the developed Raman spectrometer was successfully done using benzene, chloroform, and glacial acetic acids. This concluded that the developed Raman spectrometer could be employed for quality assessment purposes in both industrial and research sectors for quality assessment of different samples. Also, in terms of increased portability and reasonably reliable quality performance, the developed Raman spectrometer is cost-effective and commercially viable with respect to various other spectrometers available in the market.

**Reference**

- [1] R. S. Krishnan and R. K. Shankar, "Raman Effect: History of the Discovery," pp. 1–8, 1981.
- [2] R. Singh, "C. V. Raman and the Discovery of the Raman Effect \*," vol. 4, pp. 399–420, 2002.
- [3] "NanoRam Handheld RAMAN System, B&W amp; Tek | VWR." <https://us.vwr.com/store/product/13244534/nanoram-handheld-raman-system-b-w-tek> (accessed May 14, 2019).
- [4] "TruScan™ RM Handheld Raman Analyzer." <https://www.thermofisher.com/order/catalog/product/TRUSCANRM> (accessed May 14, 2019).
- [5] "Welcome to Raman systems - Pin Pointer." <http://www.ramansystems.com/english/pinpointer.htm> (accessed May 14, 2019).
- [6] "The 4th Generation 785nm Handheld Raman Analyzer (450g) - Optosky." <https://optosky.com/raman-analyzer.html> (accessed May 15, 2019).
- [7] "What is a Wrapper DLL and When Do I Need One? - National Instruments." <https://knowledge.ni.com/KnowledgeArticleDetails?id=kA00Z000000PA8QSAW&l=en-IN> (accessed Jul. 02, 2020).
- [8] A. K. Ghosh, M. Schmid, and F. Hill, "Wrapping windows NT software for robustness," *Proceedings - Annual International Conference on Fault-Tolerant Computing*, pp. 344–347, 1999, doi: 10.1109/ftcs.1999.781070.
- [9] M. Gnyba, J. Smulko, A. Kwiatkowski, and P. Wierzba, "Portable Raman spectrometer - Design rules and applications," *Bulletin of the Polish Academy of Sciences: Technical Sciences*, vol. 59, no. 3, pp. 325–330, 2011, doi: 10.2478/v10175-011-0040-z.
- [10] A. Biancolillo and F. Marini, "Chemometric Methods for Spectroscopy-Based Pharmaceutical Analysis," *Frontiers in Chemistry*, vol. 6, p. 576, 2018, doi: 10.3389/fchem.2018.00576.
- [11] R. W. Wood, "Raman Spectra of Benzene and Diphenyl," *Phys. Rev.*, vol. 36, no. 9, pp. 1431–1434, Nov. 1930, doi: 10.1103/PhysRev.36.1431.
- [12] W. Krasser, H. Ervens, A. Fadini, and A. J. Renouprez, "Raman scattering of benzene and deuterated benzene chemisorbed on silica-supported nickel," *Journal of Raman Spectroscopy*, vol. 9, no. 2, pp. 80–84, 1980, doi: <https://doi.org/10.1002/jrs.1250090205>.
- [13] X. Zhang, Q. Zhou, Y. Huang, Z. Li, and Z. Zhang, "Contrastive Analysis of the Raman Spectra of Polychlorinated Benzene: Hexachlorobenzene and Benzene," *Sensors*, vol. 11, no. 12, pp. 11510–11515, 2011, doi: 10.3390/s111211510.

- [14] T. Shimanouchi, "Tables of Molecular Vibrational Frequencies Consolidated Volume I," *National Bureau of Standards*, 1972. <https://webbook.nist.gov/cgi/cbook.cgi?ID=C67663&Mask=800>
- [15] S. Bhagavantam, S and Venkateswaran, "The Raman spectra of some organic halogen compounds," *Proceedings of the Royal Society of London. Series A, Containing Papers of a Mathematical and Physical Character*, vol. 127, pp. 360–373, 1930.
- [16] W. Dabaghao, "Raman Spectra under High Dispersion," *Indian Journal of Physics*, 1930.
- [17] S. Venkateswaran, "Light scattering in liquids [4]," *Nature*, vol. 128, no. 3238, pp. 870–871, 1931, doi: 10.1038/128870b0.
- [18] M. V. Rao, "Overtone and combination lines in the Raman spectrum of chloroform," *Proceedings of the Indian Academy of Sciences - Section A*, vol. 24, no. 6, pp. 510–513, 1946, doi: 10.1007/BF03176923.
- [19] F. Wan, L. Du, W. Chen, P. Wang, J. Wang, and H. Shi, "A novel method to directly analyze dissolved acetic acid in transformer oil without extraction using raman spectroscopy," *Energies*, vol. 10, no. 7, 2017, doi: 10.3390/en10070967.
- [20] "Keywords: NIR-FT-Raman, piperine, quality, piper nigrum, chemometrics," *New York*, pp. 409–410.
- [21] A.-R. Ayad, "Raman Spectrum Baseline Removal - File Exchange - MATLAB Central." 2020. Accessed: Feb. 22, 2020. [Online]. Available: <https://in.mathworks.com/matlabcentral/fileexchange/69649-raman-spectrum-baseline-removal>.

## **Chapter 3**

# **Quality assessment of black pepper with the procured and developed Raman spectrometers**

### 3.1 Introduction

*Piper nigrum* L. (family- Piperaceae) commonly known as “black pepper” is used as a popular seasoning to add flavor to food and also used in different systems of traditional medicine all over the world like Ayurveda and Unani from India, traditional Chinese medicine and Kampo and many more. Piperine is the major constituent alkaloid imparting flavour and taste [1], [2]. Piperine has shown various pharmacological properties like anti-inflammatory [3], antitumor [1], anticancer [3], anti-bacterial, antioxidant [4], anti-apoptotic [5], antidepressant [2], antifungal [6], analgesic, and anti-pyretic [7] activities. The commercial importance of black pepper makes its quality control very important and hence the estimation of piperine, the marker molecule.

Traditional medicine quality control is a key and necessary part of ensuring therapeutic efficacy, safety, and justification of their usage in healthcare [8]. Chemical profiling of the product is crucial in order to assess the quality of drugs. The plant materials are generally obtained from wild sources and thus maintaining the consistency in quality is a great challenge [9]. Further, due to variation in environmental conditions, cultivation, and storage methods, these plant products vary in physical appearance as well as in chemical constituents. Thus, the plant extracts and final products made directly from crude plant material show substantial difference in quality and therapeutic effects [10]. Raman spectroscopy has proven to be a useful technique for chemical analysis and is being widely used for quantitative estimation of principle constituents in various chemical compounds [11]. Quantitative estimation of a (Raman active) compound in a sample requires various steps like spectral data collection, pre-processing, and prediction modelling etc. Usually, the spectral data collection process is achieved using the software provided by the manufacturer of the spectrometer. The spectral data are then transferred to a data analysis software where they are pre-treated and analysed using appropriate pre-processing and regression techniques [12]. In most experiments, the total number of samples are divided in two parts, i.e., calibration part and prediction part. The calibration part is used to develop the model and the prediction part is needed for testing the accuracy of the prediction model. Finally, the prediction model is evaluated based on correlation factor ( $R^2$ ), accuracy, root mean square error of cross-validation (RMSECV) and root mean square error of prediction (RMSEP).



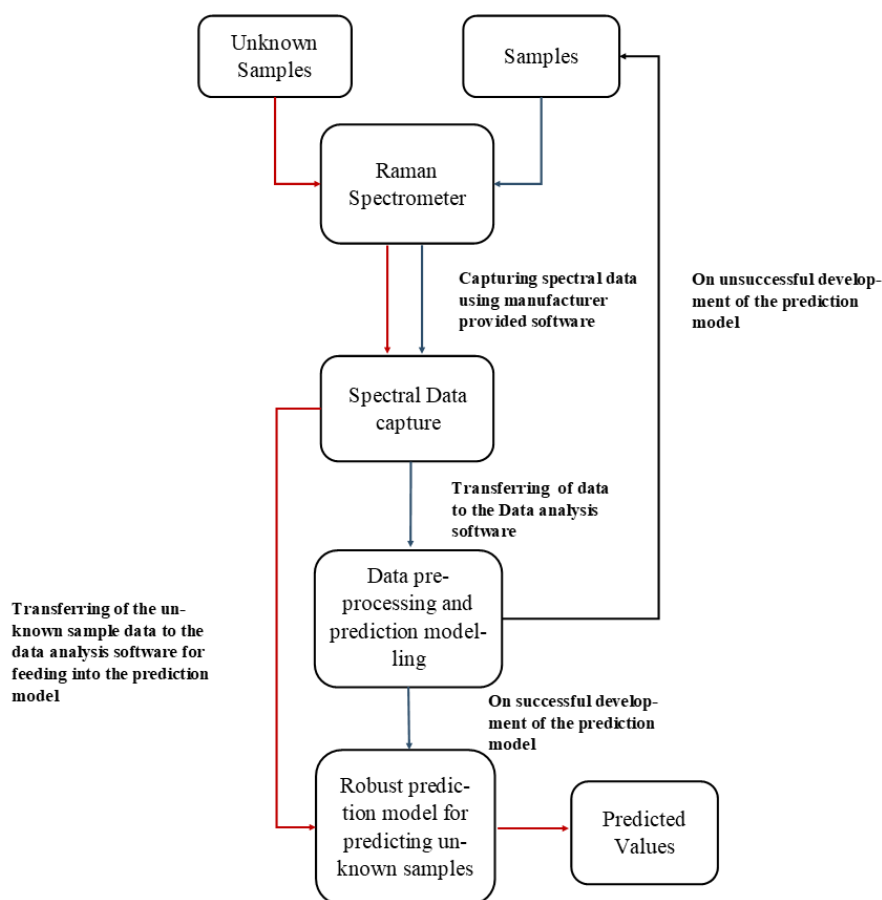


Figure 3. 1 Block diagram of regression modeling for chemical analysis using Raman spectroscopy.

Predicting the concentration of the target compound in an unknown sample usually involves matrix multiplication of the regression coefficients with the explanatory variable from the spectral data of the unknown sample whose target compound concentration must be estimated:

$$Y = \beta_1 X + \beta_2 X + \beta_3 X + \dots \beta_P X \quad (6)$$

$$= [\beta_1 \ \beta_2 \ \beta_3 \ \dots \ \beta_P] \begin{bmatrix} X_1 \\ X_2 \\ X_3 \\ \cdot \\ \cdot \\ X_P \end{bmatrix}$$

Here,  $Y$  is the purpose variable or the predicted value,  $\beta$  are the regression coefficients and  $X$  are the pre-processed radiation intensities at different wavelengths of the Raman signal of an unknown sample.

Conventionally or during experimental phase, the spectral data of the unknown sample are acquired. The data are then transferred to the data analysis software where they get pre-treated and multiplied with the regression coefficients to show the predicted values of the target compound of the unknown sample. The entire process is shown in figure 3.1.

In this chapter, two experiments were conducted. First experiment was the feasibility study of using commercially available Raman spectroscope for quantification of black pepper. Second experiment was conducted for qualitative estimation of black pepper using our developed portable Raman spectrometer. Finally, a comparison study on performance between the commercially available Raman instrument and our developed portable Raman spectrometer is described.

### **3.2 Experiment I: Feasibility study of using commercially available Raman spectroscopy for quantification of black pepper**

In this study, the feasibility of using Raman spectra for estimating piperine in black pepper samples was investigated. Study on the computation of vibrational spectra of piperine molecule was carried out using Density functional theory (DFT) with the Gaussian 03W software package. The Raman shift peaks obtained from the theoretical study was verified with twenty (20) samples of black pepper and an IDRamamicro Microscope (Ocean Optics, Inc., Florida, USA). The spectra were collected from the samples of piper nigrum and then subjected to several data preprocessing and analyzing techniques. While the principal component analysis (PCA) and linear discriminant analysis (LDA) were used for assessing the discrimination capability of the scheme, partial least square regression (PLSR) was used for quantification of piperine in black pepper. Very effective prediction accuracy for the set of five test samples of the method was observed, which confirms the efficacy of the proposed method.

### 3.2.1 Material and methods

#### 3.2.1.1 Chemical and reagent

Piperine standard used (> 95 % HPLC) was from Sigma Aldrich. Methanol (HPLC grade), glacial acetic acid (HPLC grade), petroleum ether and ethyl acetate (analytical grade) and all other solvents (AR grade) were procured from Merck, India. A Milli-Q water purification system (Bedford, MA, USA) along with 0.22 µm Millipak Express filter and Eyela (Tokyo, Japan) rotary vacuum evaporator were used. For filtration of the mobile phase and the sample solution, Membrane filters (0.45 µm pore) (Millipore) and syringe filters (NYL 0.45 µm) were used respectively. Quantitative estimation was performed with LC Solutions software programs using the external standard calibration method.

#### 3.2.1.2 Plant Material

The dried fruit of *piper nigrum* was collected from local market in Kolkata, West Bengal, India. Plant materials were identified and validated by Dr. S. Rajan, Former Field botanist, the medicinal plant collection unit, Ooty, Tamil Nādu, Govt. of India. The voucher specimens of 20 samples (specimen no. SNPS/JU/2018/12-31) were kept at SNPS, Jadavpur University, Kolkata, India for future reference. The measurement statistics about the piperine concentration in the black pepper samples is shown in Table 3.1.

Table 3. 1 Statistics about piperine content in the measured black pepper samples used for calibration and prediction sets.

Sample sets	Number. of samples	Minimum (mg/g)	Maximum (mg/g)	Mean (mg/g)	Median (mg/g)	Standard Deviation (mg/g)
Total samples	20	0.92	3.95	2.45	2.5	0.191
Calibration set	15	0.92	3.95	2.45	2.5	0.193

Prediction set	5	0.95	3.86	2.05	2.0	0.18
----------------	---	------	------	------	-----	------

### 3.2.1.3 Extraction

Samples of *Piper.nigrum* fruits were pulverized by using a mechanical grinder to make a moderately coarse powder. Methanol extracts were made from the powdered samples (50 g) using rotary shaker at 150 rpm. The extraction process was triplicated. The extract was filtered and dried by vacuum evaporation using a rotary evaporator at 50 °C. The dried extract (10 mg) was dissolved in methanol and filtered through 0.22 µm membranes to get the stock solution (10 mg/mL). The stock solution was diluted to get 1 mg/mL sample concentration for High performance liquid chromatography (HPLC).

### 3.2.1.4 High performance liquid chromatography (HPLC) fingerprints

A Reverse Phase High Performance Liquid Chromatography (RP-HPLC) system (Waters, USA) was used in this study consisted of a LC-30AD pump, UV/Vis detector equipped with 3 Lines degasser (Volume 400 µL) and a rheodyne 7725i injector having 20 µL loop. An isocratic RP-HPLC method was developed with the mobile phase of piperine as Methanol: Water (2% acetic acid) - 70:30 v/v. Using 1 percent (v/v) glacial acetic acid, the pH of solvent B (water) was held at 2.8. The mobile phase was filtered using a Millipore membrane filter with a pore size of 0.45 µm, followed by sonication to degas the solvent. A C18 column (5µm particle size, 250 4.6") was used to separate the samples. The temperature of the column was reserved at 25°C and given input volume was 20 µL. The total run time was set at ten minutes. For maximum absorption of the compound, the flow rate and  $\lambda_{\max}$  were chosen at 1.0 ml/min and 230 nm respectively.

### 3.2.1.5 Method validation

For the validation of the RP-HPLC technique, the International Conference on Harmonization (ICH Q2(R1) Guideline was used to determine linearity, specificity, accuracy and precision, limit of quantification, and limit of detection. The retention time of standard and test samples were compared to calculate the method specificity. In order to determine the sensitivity, the Limit of Detection (LOD) and Limit of Quantification (LOQ) were calculated based on the

equation:  $LOD = 3.3 \sigma/S$  and  $LOQ = 10 \sigma/S$  respectively, where  $\sigma$  is the standard deviation and  $S$  is the slope of the calibration curve. Standard addition technique was used for obtaining the accuracy and expressed in terms of % relative standard deviation (% RSD). The samples were spiked with three different amounts of standard compounds in triplicate.

### 3.2.1.6 Raman spectral data collection

An ID Raman micro Microscope (Ocean Optics, Inc., Florida, USA) was used to collect the Raman spectra. The spectrophotometer was equipped with a laser of 785nm, and the optical power was 100mW (40mW at sample) with 40X microscopic objective for  $>2 \mu\text{m}$  spot size. A CCD detector with thermo-electric cooler was used to reduce the effect of temperature variation. The spectral range of the grating was  $200\text{-}3200\text{cm}^{-1}$  and the resolution was set to  $8 \text{cm}^{-1}$ . Each spectrum was saved as the average of 16 scans with an exposure time of 0.1 s. The instrument was controlled by OceanView Program software. Black pepper samples were crushed into fine powder using Mixer grinder (Model No: HL7600/04, Philips). 25 mg of finely crushed powder was taken for sample preparation using Electronic weighing balance (SI No. 6680, Wensar). The piper nigrum fruit powder samples were dissolved in chloroform to get samples (25 mg/ml) while reading the spectra. Here, the crushed black pepper powder was thoroughly mixed with a stock solution of chloroform by Digital Ultrasonic Cleaner (Model No: LMUC-3, Labman scientific Instrument), and spinix-vortex shaker (SI no: 18/01541, Tarsons). The mixture was then filtered sample by sample using Syringe filter (part no: 5191-5911, Agilent Technologies). The sample container was thoroughly cleaned with chloroform each time a new sample was introduced for data collection. A constant room temperature of  $22^\circ \text{C}$  and a constant laser current of 151.1mA were maintained. Before taking any reading, a background spectrum was taken and eight replicates spectra of each sample were collected.

Gaussian 03W software package was used for molecular geometry optimization and vibrational spectra computation of piperine (FRISCH and J., 2004). It uses the Density functional theory (DFT) method with B3LYP hybrid exchange–correlation function [13], [14].

## 3.2.2 Results and discussion

### 3.2.2.1 The Piperine Molecule and Its Assignment of Raman Peaks

Piperine (molecular formula:  $C_{17}H_{19}NO_3$ ), containing N-acylpiperidine which is piperidine replaced by a (1E, 3E)-1-(1,3-benzodioxol-5-yl)-5-oxopenta-1,3-dien-5-yl set at the nitrogen atom, is mainly composed of C-N, C=O, C=C, C-O, and C-H groups. Figure 3.2 and Figure 3.3 show the molecular structure of 2D Ball and Stick Model and B3LYP/6-31G (d) optimized geometry of piperine molecule respectively.

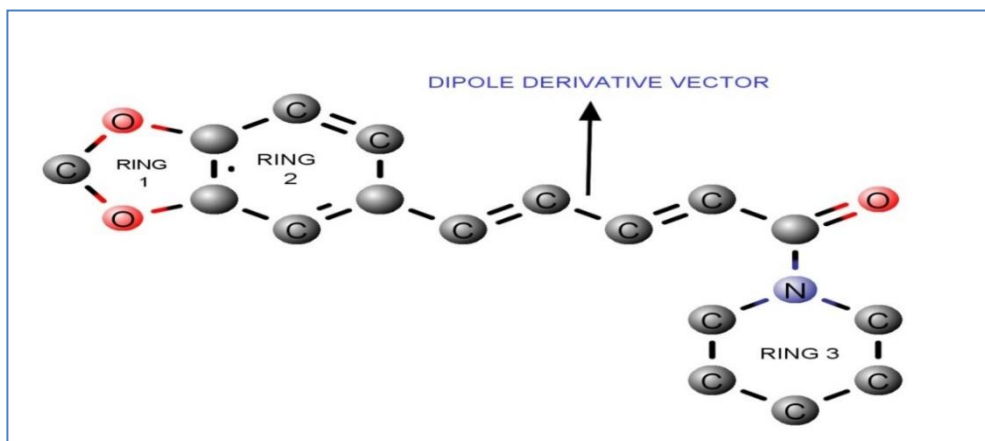


Figure 3. 2 Two-dimensional Ball and Stick Model of Piperine

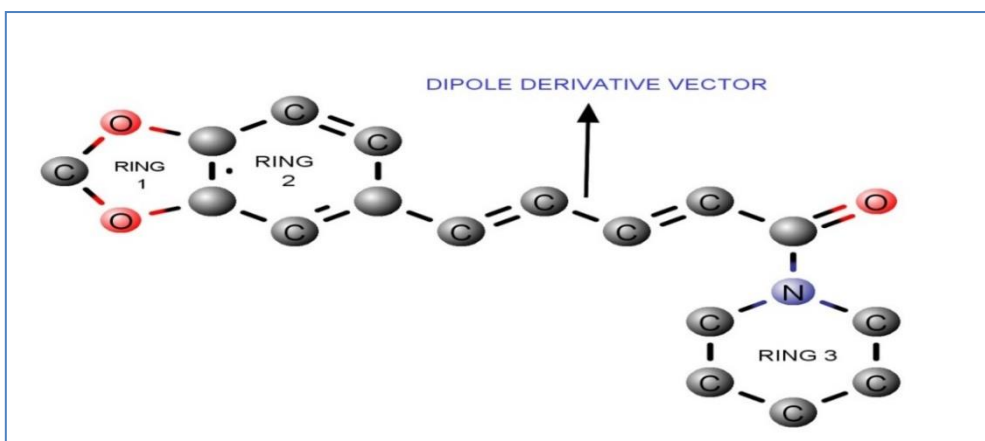


Figure 3. 3 B3LYP/6-31G(d) optimized geometry of Piperine molecule.

The probabilistic assignment by DFT of Raman peaks of piperine and that given by estimated Raman spectrum have been listed in Table 3.2. As can be seen in Table 3.2, DFT-calculated Raman peaks are well correlated (within  $\pm 2\text{cm}^{-1}$ ) with the experimentally detected Raman peaks of piperine. A few Raman peaks by DFT differed significantly from the peaks obtained experimentally, but their peak intensities are small and thus can be neglected.

Table 3.2 Experimental and theoretical vibrational Raman data of piperine with the proposed assignments.

<b>Exp.</b>	<b>Theoretical</b>	<b>Vibrational</b>
<b>Wave number</b>	<b>Wave number</b>	<b>Assignment</b>
<b>189.29</b>	191.69	B(C-H) Ring 1, 2 + B(C-H) + B(C-H) Ring 3
<b>216.08</b>	216.52	B(C-H) + B(C-H) Ring 3
<b>232.04</b>	231.68	B(C-H) Ring 1,2 +B(C-H) + B(C-H) + B(C-H) Ring 3
<b>279.44</b>	278.74	S(C=C) + B(C-H) + B(C-H) Ring 3 + B(C-H) Ring 3 + B(C-H) Ring 2
<b>544.58</b>	545.42	B(C-H) Ring 2 + B(C-H)
<b>606.21</b>	607.8	B(C-H) Ring2 + B(C-H)
<b>629.57</b>	630.32	B(C-H) + S(C-C)
<b>666.58</b>	664.69	S(C-H) Ring 2 +S(C-H)
<b>680.34</b>	681.4	B(C-H) Ring2 +B(C-H) Ring 3
<b>743.69</b>	744.94	B(C-H) Ring 3
<b>788.11</b>	789.06	B(C-H) + S(C-C) + S(C-N) + B(C-H) Ring 3 + S(C-C) Ring 3
<b>792.52</b>	793.52	S(C-H) Ring3 + B(C-H) Ring 3 + B(C-H) + S(C-C) + B(C-H) Ring 2 + S(C-O) Ring 1
<b>840.52</b>	838.62	B(C-H) Ring 1 + S(C-O) Ring 1 + B (C-H) Ring 2 + S(C=C) Ring 2 + B(C-H) + B(C-H) Ring 3
<b>853.48</b>	852.32	S(C-N) + B(C-H) Ring 3+S (C-C) Ring 3
<b>874.93</b>	875.57	B(C-H) + S(C-C)

<b>900.46</b>	901.81	B(C-H) Ring 2 + S(C=C) Ring 2 + B(C-H) + S(C-C) + B(C-H) Ring 3 + S(C-C) Ring 3
<b>942.51</b>	944.29	B(C-H) Ring 2 + B(C-H) + S(C-C) + S(C=O) + S(C-N)
<b>983.92</b>	983.84	B(C-H) Ring 2 + B(C-H) + S(C-C) + S(C=O)
<b>1036.82</b>	1035.1	B(C-H) Ring 2 + S(C-C) + B(C-H)
<b>1060.9</b>	1060.03	B(C-H) Ring 3 + S(C-C) Ring 3 + S(C-N) Ring 3
<b>1096.61</b>	1096.63	B(C-H) Ring 2 + B(C-H)
<b>1100.54</b>	1098.59	B(C-H) Ring 2 + S(C-O) Ring 1+ B(C-H) Ring 1
<b>1131.84</b>	1133.93	B(C-H) Ring 1, 2+ S (C-O) Ring 1 + S(C=C) Ring 2
<b>1147.34</b>	1147.38	S(C-N) Ring 3 + B(C-H) Ring 3 + S(C-H) Ring 3
<b>1197.11</b>	1196.41	B(C-H) Ring 1, 2 + B(C-H) + S (C-C)
<b>1204.68</b>	1203.98	B(C-H) Ring 1 + B(C-H)
<b>1264.46</b>	1264.19	S(C-O) Ring 1+B(C-H) Ring2 + S(C=C) Ring2
<b>1268.15</b>	1269.71	S(C-N) Ring 3+B(C-H) Ring 3
<b>1279.18</b>	1279.69	B(C-H) +S(C=O)
<b>1308.38</b>	1307.21	B(C-H) +S(C-N) +S(C-N) Ring 3+B(C-H) Ring 3
<b>1330.05</b>	1329.69	B(C-H) +S(C=C)
<b>1347.96</b>	1346.56	B(C-H) Ring 3 + S(C-C) Ring 3
<b>1376.35</b>	1375.55	B(C-H) Ring 3 + S(C-C) Ring 3 +S(C-N) Ring 3
<b>1383.4</b>	1382.72	S(C-O) Ring 1+ B(C-H) Ring 1
<b>1407.9</b>	1407.58	B(C-H) Ring 2+S(C=C) Ring 2
<b>1479.94</b>	1480.7	B(C-H) Ring 3
<b>1614.54</b>	1614.51	S(C-O) Ring 1+B(C-H) Ring 1+S(C=C) Ring



		2+B(C-H) Ring 2
<b>1627.26</b>	1627.32	B(C-H) +S(C-C) +S(C=O) +B(C-H) Ring2
<b>1639.91</b>	1641.2	B(C-H) +S(C-C) +S(C=O)

Abbreviations: S- stretching, B- bending, Rings 1–3 as shown in the Fig. 1.

### 3.2.2.2 Data pre-processing

The baseline drift in the spectrum caused by fluorescence was minimized using the fifth order polynomial algorithm [15]. Figure 3.4 shows the average Raman spectra of the data after fluorescent background subtraction and baseline correction, which provides better indication of the differences between the samples. The spectra are then pre-treated by Savitzky-Golay smoothing (S-G)[16] and standard normal variation (SNV)[17] techniques.

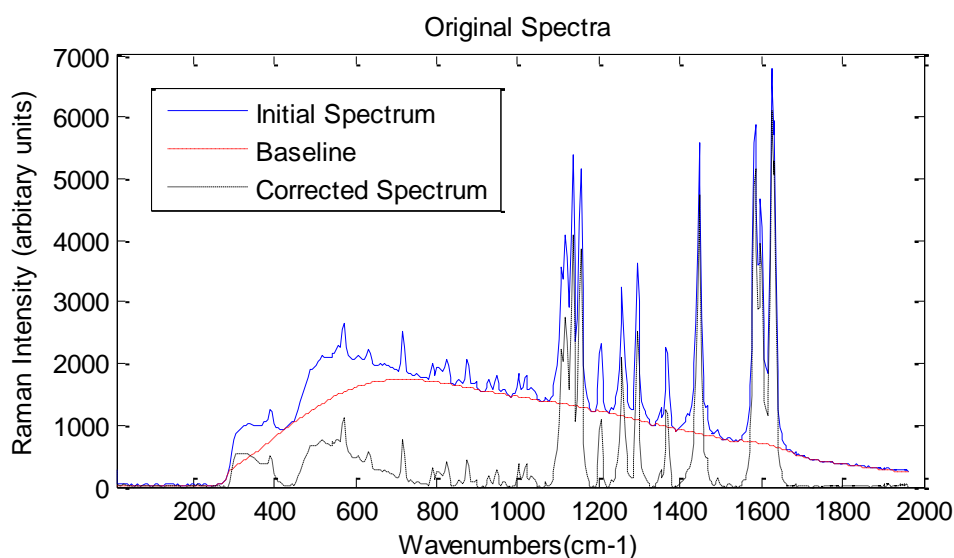


Figure 3. 4 The raw and baseline corrected Raman spectra of black pepper.

### 3.2.2.3 Qualitative analysis using PCA and LDA

Exploratory data analysis on 20 samples of black pepper fruit has been performed using Principal Component Analysis (PCA) and Linear Discriminant Analysis (LDA) after baseline correction to distinguish different clusters in the Raman spectra,

In this study, the vibrational characterisation of alkaloids found from black pepper samples from various collecting sites, as well as exploratory analysis using principle component analysis, are combined. Principle component analysis was tested using Raman shift data from

twenty different geographical locations that were subjected to varied treatments, could discriminate the occurrence of different alkaloid contents. The PCA scores plot with the first two principle components have been shown in Figure 3.5. Here, PC1 represents 90.44% and PC2 represents 3.17%. Thus, the ability to visualise grouping patterns as per sample type has been made accessible.

In this work we also used a supervised statistical approach, LDA, in an attempt to identify black pepper samples based on their Raman spectra. Figure 3.6 depicted the scores plot of the first two LDA vectors for all the black pepper samples investigated. Clearly visible, the black pepper is clustered together, but a closer look at the black pepper cluster reveals that each of these black peppers form a distinct group.

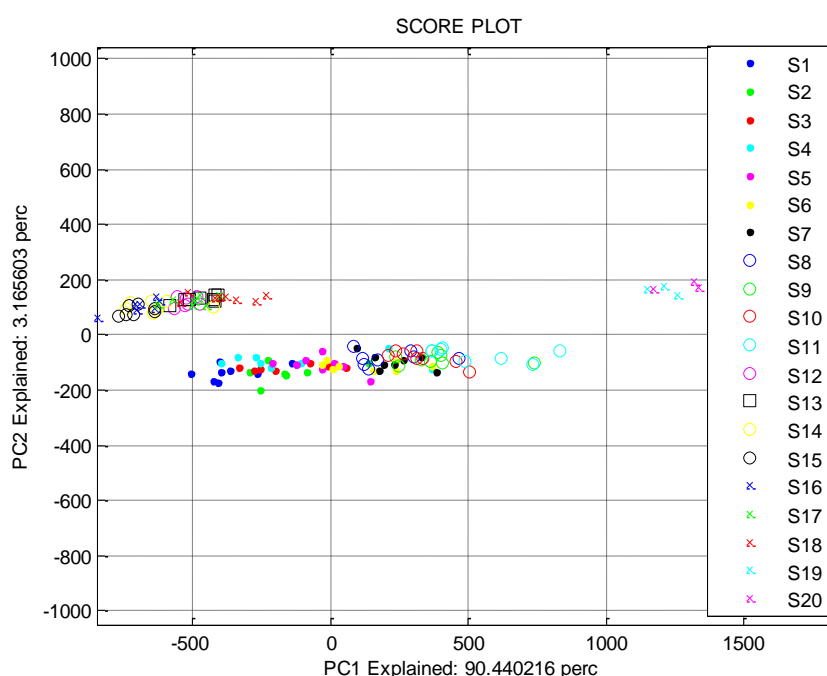


Figure 3. 5 PCA plot with first two PC.

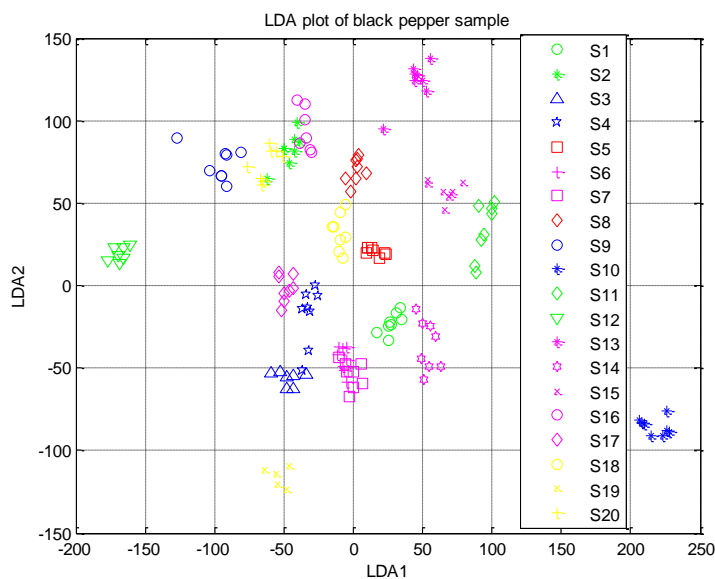


Figure 3. 6LDA plot with first two components.

#### 3.2.2.4 Quantitative analysis using PLSR

The calibration model of partial least square regression technique was built using pre-processed data of black pepper. The sample set was divided into two groups, among which 15 samples were considered for calibration and 5 for validation.

SNV was chosen as the final pre-processing method for the calibration model due to its better accuracy. By calculating the RMSEC of calibration, the number of components of partial least square regression was optimised. Here, an optimal value of 5 components was selected as the x-variance is 91.23% and y-variance is 97.55%. with the first 5 components and correlation coefficient ( $R^2$ ) root mean square error of calibration were obtained as 0.97 and 0.11 respectively. The RMSE vs. no of components plot is shown in figure 3.7.

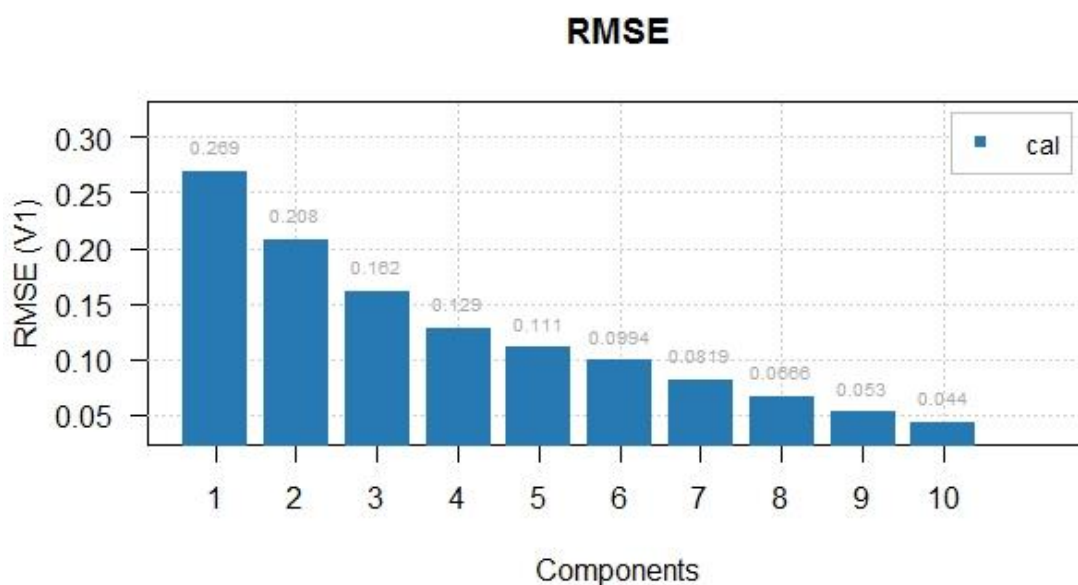


Figure 3. 7 RMSE comparison of calibration results for 15 samples obtained SNV for component number 1 to 10

It was found that the average accuracy of prediction with the five samples of the prediction set was 92.03%. RMSEP of five samples was likewise found to be adequately low, at 0.13, and  $R^2$  was 0.93, indicating a high correlation between the calibration and prediction models.

It was also observed that the root mean square error of prediction (RMSEP) of 5 samples was sufficiently low i.e., 0.13 and correlation coefficient ( $R^2$ ) was 0.93 which exhibits good correlation between training and testing set. The maximum standard deviation of the predicted value was  $\pm 0.44$  and minimum was  $\pm 0.16$ . In this context it may be mentioned that the average RPD value of the test set was 3.9.

Residual prediction deviation values below 1.5 are regarded unusable, those between 1.5 and 2.0 are adequate for rough prediction, those between 2.0 and 2.5 are suitable for quantitative predictions, and those between 2.5 and 3.0 are called good and outstanding prediction models, according to Mouazen et al. [18].

Partial least square scatter diagrams of calibration set and prediction set with SNV pre-processing method are shown in Figure 3.8, and the prediction result of 5 samples has been provided in Table 3.3.

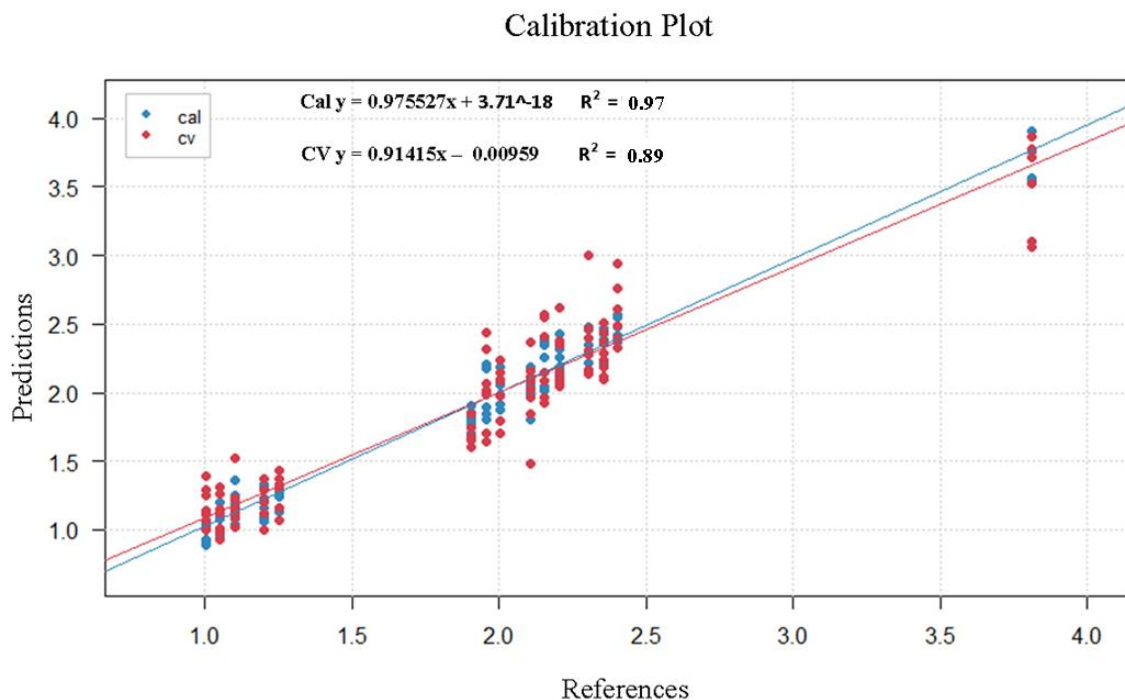


Figure 3. 8 Scatter diagram of calibration set by PLS using preprocessing of SNV.

Table 3. 3 Test result of five black pepper samples

Reference Piperine value (% w/w)	Predicted Piperine Value (% w/w)	Deviation on prediction	% of Accuracy	Average Accuracy	RMSEP	R <sup>2</sup>	RPD
2.05	1.97	±0.28	95.76				
2.25	2.24	±0.21	99.46				
0.95	1.11	±0.18	83.15	92.03	0.13	0.93	3.9
1.15	1.03	±0.16	89.38				
3.86	3.57	±0.44	92.42				

The best prediction parameters of piperine in black pepper were obtained as  $R_p^2 = 0.93$ ,  $RMSEP = 0.13$  mg/ml,  $RPD = 3.9$  (Table 2). It can be observed that the prediction results of PLS model were satisfactory; revealing that piperine in black pepper could be quantitatively

determined by Raman Spectroscopy. The scatter plot of the prediction model is shown in figure 3.9.

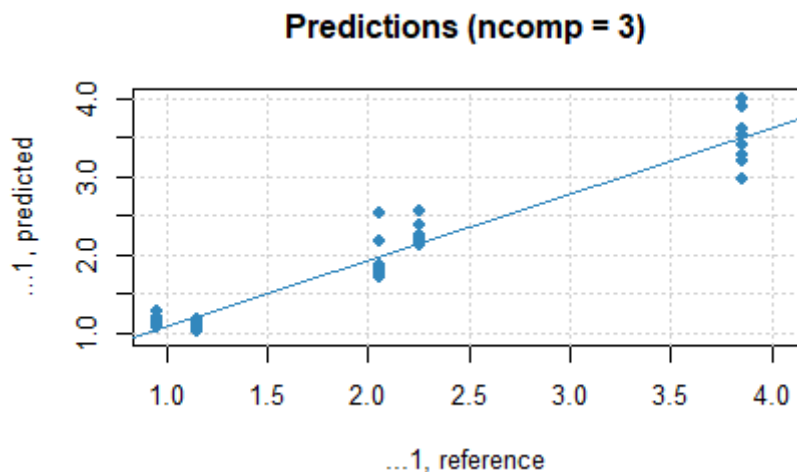


Figure 3.9 Scatter diagram of prediction set by PLS using preprocessing of SNV

### 3.3 Experiment II: Qualitative estimation of black pepper using our developed portable Raman spectrometer

#### 3.3.1 Black pepper samples

Total 25 samples were considered in this study. 20 samples were considered for the calibration set and 5 samples were considered in the prediction set. The measurement statistics about the piperine concentration in the black pepper samples is shown in table 3.4.

Table 3.4 Statistics about piperine content in the measured black pepper samples used for calibration and prediction sets.

Sample sets	Number. of samples	Minimum (mg/g)	Maximum (mg/g)	Mean (mg/g)	Median (mg/g)	Standard Deviation (mg/g)
Total samples	25	2.2	6.5	4.5	4.52	0.191
Calibration set	20	2.2	6.5	4.5	4.52	0.193

Prediction set	5	2.21	6.10	4.24	4.22	0.18
----------------	---	------	------	------	------	------

### 3.3.2 Result and discussion

Figure 3.10 shows the scatter plot of regression of SVM estimates versus HPLC estimates for 20 calibration samples. The samples were distributed closely around the regression line, with RMSEC,  $R^2$ , and RPD value of 0.99, 0.15 and 8.08 respectively.

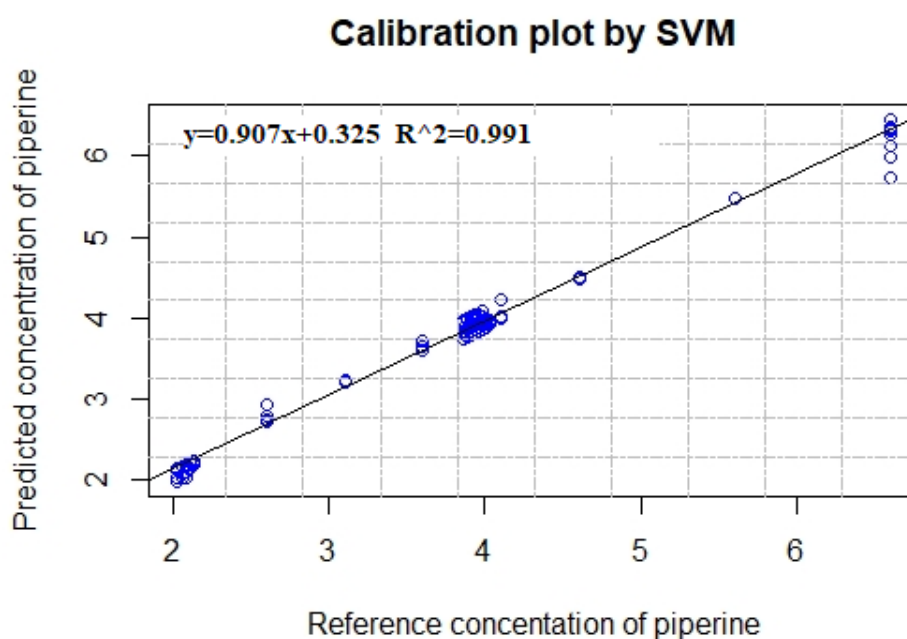


Figure 3.10 Scatter plot of actual versus measured piperine values for the calibration set.

The established SVM model with SNV preprocessing showed excellent performance with high coefficient of determination for the test set ( $R^2_p$ ) = 0.98, RMSEP = 0.33 mg/mL and RPD = 4.52 (Table 3.5).

Table 3.5 Test results for the five black pepper samples

Reference piperine concentration	Predicted piperine concentration	Deviation on prediction	Percentage of accuracy	Average accuracy (%)	$R^2$	RMSEP	RPD

(% w/w)	ation (% w/w)						
2.165	2.21	$\pm 0.055$	97.45	95.83	0.98	0.33	4.52
3.81	3.89	$\pm 0.079$	97.93				
4.06	4.02	$\pm 0.042$	98.97				
5.10	4.91	$\pm 0.190$	96.28				
6.10	5.40	$\pm 0.701$	88.52				

The paired 't' value was 1.81, and the corresponding 'p' value as 0.07 for SNV preprocessed data showing, adequate accuracy of estimation of piperine by our spectrometer. Figure 3.11 shows the scatter plot of regression of SVM estimates versus HPLC estimates for 5 prediction samples. The samples were distributed closely around the regression line, with RMSEC,  $R^2$ , and RPD value of 0.946, 0.543 and 2.06 respectively. Here, RPD was above 2 for both calibration and validation sample set which depicted a good model [19]–[21].

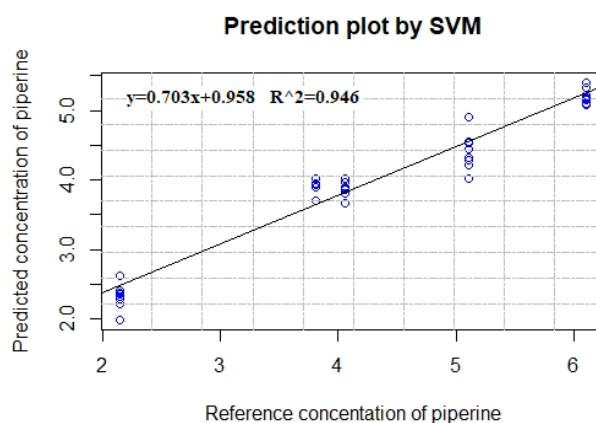


Figure 3.11 Scatter plot of actual versus measured piperine values for the prediction set.

### 3.4 Comparison study between commercially available spectrometer and our developed spectrometer

From table 3.6, it can be noted that the correlation coefficient ( $R^2$ ) and RPD values were better for predicting the TF values with the developed Raman spectrometer compare to our



previous study. Here, RMSEP is less, but average accuracy is better for developed spectrometer with respect to commercially available spectrometer.

Table 3. 6 Comparison of evaluation performance between our low-cost spectrometer and the spectrometer used by Sing et al. referred above

Type of spectrometer	Average accuracy (%)	R <sup>2</sup>	RMSEP	RPD
Developed spectrometer	95.8	0.98	0.33	4.52
Spectrometer used by Sing et al. 2021[22]	92.03	0.93	0.13	3.9

In the comparison given in the above table 3.6, the regression technique used in the developed spectrometer was SVM-R while in previous study[22] it was Partial least square regression (PLS-R) and the sample sets used in the two studies were also different.

### 3.5 Conclusion

In this chapter, we observe that there is a good linear correlation between DFT prediction and Raman peak intensity of pure piperine concentration. Also, 1097–1627 cm<sup>-1</sup> Raman shift for piperine in black pepper was analyzed and the best result was obtained using PLS model when the raw spectra were pre-treated by standard normal variation (SNV). The content of piperine in the HPLC analysis and Raman spectroscopy study showed a linear relationship, which reflects the content uniformity of piperine in the sample under study. The chapter also demonstrated the feasibility of deploying a portable Raman spectrometer for the quality assessment black pepper samples. The developed Raman spectrometer has successfully predicted the concentration of piperine in black pepper berries. The actual concentration as obtained by HPLC technique was further compared with the result obtained from the ID Raman micro spectrometer and the developed Raman spectrometer. High correlation >0.9 was evident between them. This concluded that the developed Raman spectrometer could be employed in both industrial and research sectors for quality assessment of different samples. Also, in terms of increased portability and reasonably reliable quality performance, the developed Raman spectrometer is cost-effective and commercially viable with respect to various other spectrometers available in the market.

### References

- [1] V. M. A. S. Grinevicius, K. S. Andrade, F. Ourique, G. A. Micke, S. R. S. Ferreira, and R. C. Pedrosa, “Antitumor activity of conventional and supercritical extracts from *Piper nigrum* L. cultivar Bragantina through cell cycle arrest and apoptosis induction,” *Journal of Supercritical Fluids*, vol. 128, pp. 94–101, Oct. 2017, doi: 10.1016/j.supflu.2017.05.009.
- [2] S. Li, C. Wang, W. Li, K. Koike, T. Nikaido, and M. W. Wang, “Antidepressant-like effects of piperine and its derivative, antiepilepsirine,” *Journal of Asian Natural Products Research*, vol. 9, no. 5, pp. 421–430, 2007, doi: 10.1080/10286020500384302.
- [3] F. Tasleem, I. Azhar, S. N. Ali, S. Perveen, and Z. A. Mahmood, “Analgesic and anti-inflammatory activities of *Piper nigrum* L.,” *Asian Pacific Journal of Tropical Medicine*, vol. 7, no. S1, pp. S461–S468, Sep. 2014, doi: 10.1016/S1995-7645(14)60275-3.
- [4] Z. Zarai, E. Boujelbene, N. Ben Salem, Y. Gargouri, and A. Sayari, “Antioxidant and antimicrobial activities of various solvent extracts, piperine and piperic acid from *Piper nigrum*,” *LWT - Food Science and Technology*, vol. 50, no. 2, pp. 634–641, Mar. 2013, doi: 10.1016/j.lwt.2012.07.036.
- [5] N. Pathak and S. Khandelwal, “Cytoprotective and immunomodulating properties of piperine on murine splenocytes: An in vitro study,” *European Journal of*

- Pharmacology*, vol. 576, no. 1–3, pp. 160–170, Dec. 2007, doi: 10.1016/j.ejphar.2007.07.033.
- [6] U. Arslan, K. Ilhan, and O. A. Karabulut, “Antifungal activity of aqueous extracts of spices against bean rust (*Uromyces appendiculatus*).,” *Allelopathy Journal*, vol. 24, no. 1, pp. 207–213, Jul. 2009.
- [7] V. S. Parmar *et al.*, “Phytochemistry of the genus Piper,” *Phytochemistry*, vol. 46, no. 4, pp. 597–673, Oct. 1997, doi: 10.1016/S0031-9422(97)00328-2.
- [8] P. K. Mukherjee, S. Bahadur, R. K. Harwansh, S. Biswas, and S. Banerjee, “Paradigm shift in natural product research: traditional medicine inspired approaches,” *Phytochemistry Reviews*, vol. 16, no. 5, pp. 803–826, Oct. 2017, doi: 10.1007/s11101-016-9489-6.
- [9] P. K. Mukherjee, S. Bahadur, S. K. Chaudhary, A. Kar, and K. Mukherjee, “Quality Related Safety Issue-Evidence-Based Validation of Herbal Medicine Farm to Pharma,” in *Evidence-Based Validation of Herbal Medicine*, Elsevier Inc., 2015, pp. 1–28. doi: 10.1016/B978-0-12-800874-4.00001-5.
- [10] P. K. Mukherjee, “Chapter 17 - Plant Metabolomics and Quality Evaluation of Herbal Drugs,” in *Quality Control and Evaluation of Herbal Drugs*, P. K. Mukherjee, Ed. Elsevier, 2019, pp. 629–653. doi: <https://doi.org/10.1016/B978-0-12-813374-3.00017-X>.
- [11] Q. Yang, L. Zhang, L. Wang, and H. Xiao, “MultiDA: Chemometric software for multivariate data analysis based on Matlab,” *Chemometrics and Intelligent Laboratory Systems*, vol. 116, pp. 1–8, 2012, doi: 10.1016/j.chemolab.2012.03.019.
- [12] A. Biancolillo and F. Marini, “Chemometric Methods for Spectroscopy-Based Pharmaceutical Analysis,” *Frontiers in Chemistry*, vol. 6, p. 576, 2018, doi: 10.3389/fchem.2018.00576.
- [13] A. D. Becke, “Density-functional exchange-energy approximation with correct asymptotic behavior,” *Physical Review A*, vol. 38, no. 6, pp. 3098–3100, Sep. 1988, doi: 10.1103/PhysRevA.38.3098.
- [14] Y. De Liu, Y. X. Zhang, H. Y. Wang, and B. Ye, “Detection of pesticides on navel orange skin by surface-enhanced Raman spectroscopy coupled with Ag

- nanostructures,” *International Journal of Agricultural and Biological Engineering*, vol. 9, no. 2, pp. 179–185, 2016, doi: 10.3965/j.ijabe.20160902.1960.
- [15] A.-R. Ayad, “Raman Spectrum Baseline Removal - File Exchange - MATLAB Central.” 2020. Accessed: Feb. 22, 2020. [Online]. Available: <https://in.mathworks.com/matlabcentral/fileexchange/69649-raman-spectrum-baseline-removal>
- [16] G. Vivó-Truyols and P. J. Schoenmakers, “Automatic selection of optimal Savitzky-Golay smoothing,” *Analytical Chemistry*, vol. 78, no. 13, pp. 4598–4608, Jul. 2006, doi: 10.1021/ac0600196.
- [17] T. Fearn, C. Riccioli, A. Garrido-Varo, and J. E. Guerrero-Ginel, “On the geometry of SNV and MSC,” *Chemometrics and Intelligent Laboratory Systems*, vol. 96, no. 1, pp. 22–26, Mar. 2009, doi: 10.1016/j.chemolab.2008.11.006.
- [18] K. Williams, P.; Norris, *Near-infrared technology in the agricultural and food industries*. American Association of Cereal Chemists, Inc., 1987.
- [19] N. Panigrahi, C. S. Bhol, and B. S. Das, “Rapid assessment of black tea quality using diffuse reflectance spectroscopy,” *Journal of Food Engineering*, vol. 190, pp. 101–108, 2016, doi: 10.1016/j.jfoodeng.2016.06.020.
- [20] C.-W. Chang, A. L. David, J. M. Maurice, and R. H. Charles, “Analyses of Soil Properties,” *Soil Science Society of America Journal*, pp. 480–490, 2001.
- [21] G. Ren *et al.*, “Quantitative analysis and geographical traceability of black tea using Fourier transform near-infrared spectroscopy (FT-NIRS),” *Food Research International*, vol. 53, no. 2, pp. 822–826, 2013, doi: 10.1016/j.foodres.2012.10.032.
- [22] D. Sing *et al.*, “Rapid estimation of piperine in black pepper: Exploration of Raman spectroscopy,” *Phytochemical Analysis*, 2021.

## **CHAPTER 4**

# **Development of a portable NIR spectrometer**

## 4.1 Introduction

The phenomenon of NIR spectroscopy was discovered by Herschel in eighteenth centuries. Using a series of thermometers with darkened bulbs, he discovered dispersion of electromagnetic waves beyond the visual region of the spectrum. He used a large glass prism for dispersing sunlight onto three thermometers having carbon-blackened bulbs for finding out the effect of every colour due to dispersion of white sunlight in increasing the temperature of the materials which were targeted to them. He observed that the heating effect became apparent towards the red end of the spectrum. But beyond it, there was no visible light, and the temperature exhibit the highest value. He mentioned to this discovery as “radiant heat” and the “thermometrical spectrum.” Specifically, this form of energy was considered different from light by him. He used blackened bulb thermometers and glass prisms which were transparent to short wave NIR radiation and his achievement was reported by referring to the region found beyond the red as “calorific rays” [1]. The region was later named infrared, according to the Greek prefix “infra” which means “below”.

Abney and Festing in 1881, was the first to record infrared spectrum of organic liquids. The spectra were recorded in the range of 1 to 1.2  $\mu\text{m}$ . They recognised atomic grouping as well as the relevance of the hydrogen bond in the near infrared spectrum as a result of their investigation [2]. This work was very significant as it represented the first NIR interpretations along with measurements. Coblenz provided a new tool to the chemists, by which some structural information about compounds could be obtained [3].


In 1912, the first quantitative NIR measurement, the determination of atmospheric moisture was done by F. E. Fowle [4] at the Mount Wilson observatory, followed by Ellis and Bath in 1938, who estimated the water content in gelatin [5]. In the early 1940s, fuels were analyzed by Barchewitz [6] and Barr and the spectra of some vegetable oils was published by Harp. However, major developments in NIR spectroscopy occurred after 1960. Karl Norris, an agricultural engineer of USDA (United States Department of Agriculture) in 1960's employed NIR spectroscopy in quality assessment of agricultural product and succeeded in doing so. Statistical methods were applied by him to develop calibration model using NIR data. His unique idea and the digital evolution in the 1960's and 70's paved the way for practical applications of NIR spectroscopy. He is regarded as the “father” of modern near-infrared spectroscopic analysis. His efforts were crucial in the invention of NIR methodology,





which can be used to assess a wide range of food and grain quality attributes in an easy, accurate, fast, and low-cost solution [7].

## 4.2 Commercially available NIR spectrometers

The commercially available NIR spectrometers have a tread-off between price and portability. The starting range spectrometers with moderate price have good sensitivity and can be used for qualitative and quantitative analysis, but they are very bulky and therefore not suitable for in-situ analysis. The spectrometers having high resolution, high signal to noise ratio and high portability are very expensive. So, the current need is of a NIR spectrometer with good resolution, good signal to noise ratio, which can be employed for in-situ analysis at an affordable cost. The different commercially available NIR spectrometers are listed in table 4.1.

Table 4. 1 Comparison of different NIR systems available in the market.

NIR spectrometer	Specifications	Price (approx.)
Thermo Scientific Antaris II FT-NIR Analyzers[8] 	<ul style="list-style-type: none"> <li>• Wavelength range: 833–2630 nm.</li> <li>• Resolution: 4 cm<sup>-1</sup> at 1250 nm; 2 cm<sup>-1</sup> at 1250 nm.</li> <li>• Source: Halogen source.</li> <li>• Detector: InGaAs.</li> <li>• Dimensions (W x D x H):40.6 cm × 68.5 cm × 33 cm</li> <li>• Weight 47.7 kg.</li> <li>• Operating Temperature Range 15–35 °C.</li> <li>• Power Requirements 90–264 VAC.</li> </ul>	\$55,000
Bruker Optics Tango FT-NIR[9]	<ul style="list-style-type: none"> <li>• Wavelength range: 870–2,500nm.</li> <li>• Resolution (nm): 0.6.</li> <li>• FT-NIR.</li> <li>• Simple and rapid.</li> <li>• Strong and simple components.</li> <li>• Data exchange via network.</li> </ul>	Rs. 30 lakhs

		
<p>FossNIRS™ DA1650[10]</p> 	<ul style="list-style-type: none"> <li>• Wavelength range: 1100 - 1650 nm.</li> <li>• Resolution (nm): 0.5.</li> <li>• Experimental methods: Reflectance or Transflectance</li> <li>• Detector: 256-pixel InGaAs diode array.</li> <li>• BW: 10.44 ±0.5 nm.</li> <li>• Absorbance range: Up to 2 AU.</li> <li>• Experimental time: &lt;1 min.</li> <li>• Accuracy: &lt;0.5 nm.</li> <li>• Wavelength precision: &lt;0.05 nm</li> <li>• Size (W x D x H): 230 x 530 x 280 mm.</li> <li>• Weight: 16 kg.</li> </ul>	<p>Rs. 17 lakhs</p>
<p>B&amp;W Tek Sol 1.7[11]</p> 	<ul style="list-style-type: none"> <li>• Wavelength range: 900 nm – 1700 nm.</li> <li>• Resolution (nm): 0.35.</li> <li>• Detector: InGaAs array.</li> <li>• 512 pixels.</li> <li>• 5VDC power supply.</li> <li>• Built-in 16-bit digitizer.</li> <li>• USB 2.0 plug-and-play compatible.</li> </ul>	<p>Rs. 19.31 lakhs</p>
<p>StellarNet DWARF-STAR[12]</p> 	<ul style="list-style-type: none"> <li>• Wavelength range: 900 nm – 1700 nm.</li> <li>• Resolving resolution (nm): 2.5.</li> <li>• Dynamic range: 4000:1 with 5 decades.</li> <li>• Signal to noise: 4000:1 with TEC cooling.</li> <li>• Dimensions (W x D x H): 5”x3”x2”.</li> <li>• InGaAs PDA Detector: 512 pixels.</li> <li>• Interface: USB-2.</li> <li>• Detector Integration time: 1 millisecond to</li> </ul>	<p>\$14,125</p>



	30 secs. <ul style="list-style-type: none"><li>• Digitizer: 16 bit @ 2.5 MHz rates.</li></ul>	
--	---	--

### 4.3 Development of low-cost portable NIR spectrometer using off-the-shelf optical components and detector

In this thesis work, an attempt was made for the development of NIR spectrometer with off-the-shelf components in our laboratory. The cost and size of the spectrometer were optimized to a great extent. The developed NIR spectrometer could be employed for estimation of the content of marker molecules in different organic compounds by employing different chemometric methods. NIR spectrometers can be designed with various configurations as discussed in Chapter 1. In this project, NIR spectrometer is designed in diffused reflectance mode by assembling off-the-shelf components. The number of components has been kept optimum to achieve cost-effectiveness without compromising on its performance. The design of the spectrometer is discussed in detail in this chapter.

#### 4.3.1 Optical Assembly of NIR spectrometer

The optical assembly acts as a waveguide for the light source to reach the sample and altered light from the sample to reach the detector. Filters and lenses eliminate the effect of external noises and interference in this optical assembly.

##### 4.3.1.1 Components of optical assembly

The optical assembly consists of different mechanical and optical components. It is accommodated with components for irradiating the sample, collecting the diffused reflected rays from the sample and focussing it on to the detector. The different components associated with the optical assembly are shown in table 4.2.

Table 4. 2 List of components used to develop a portable NIR Spectrometer

SI No.	Component Name	Part No.	Description	Maker
1	Quartz Tungsten-Halogen Lamp 	QTH10	Quartz Tungsten-Halogen Lamp, 8-32 Tap	Thorlabs Inc., USA
2	Focussing mirror 	CM508-100-M01	Ø2" Gold-Coated Concave Mirror, f = 100.0 mm	Thorlabs Inc., USA
3	Gold Turning Prism Mirror 	CCM5-M01	16 mm Prism Mirror, 8-32 Tap	Thorlabs Inc., USA
4	Aspheric lens 	C280TMD-C	Focusing length = 18.40 mm, Numerical Aperture = 0.15, AR: 1050-1700 nm	Thorlabs Inc., USA
5	Detector 	TFC14486GA	Spectral response range: 790 to 920 nm	HAMAMATSU Photonics UK Limited, UK

### 4.3.2 Designing of the Optical Assembly

The conventional NIR spectrometers available in the market are either too bulky or the sophisticated ones are too expensive. In order to optimise the size and ensuring its greater portability, a 3D modelling software has been used for designing the various opto-mechanical components of this spectrometer as shown in figure 4.1. The design has been made as compact as possible without involving any compromise in its performance.

The setup rests on a 6" x 6" x 3/8" Mini-Series Aluminium Breadboard from Thorlabs, Inc. The lamp is positioned at a certain height from the breadboard base with the help of lamp mount parts from Thorlabs Inc. The concave mirror is mounted at the breadboard base, just below the lamp. The mirror is slightly tilted with respect to the base in order to focus the light from the mirror onto the sample. The sample holder is also positioned at a certain height from breadboard base with the help of sample mount. The prism mirror is placed just below the sample holder for capturing the diffused reflected light from the sample. It is followed by aspheric lens in between the prism mirror and the detector slit. All the components are rigidly fixed at the base of the breadboard. The actual setup of the optical assembly of the NIR spectrometer is shown in figure 4.2 and figure 4.3.

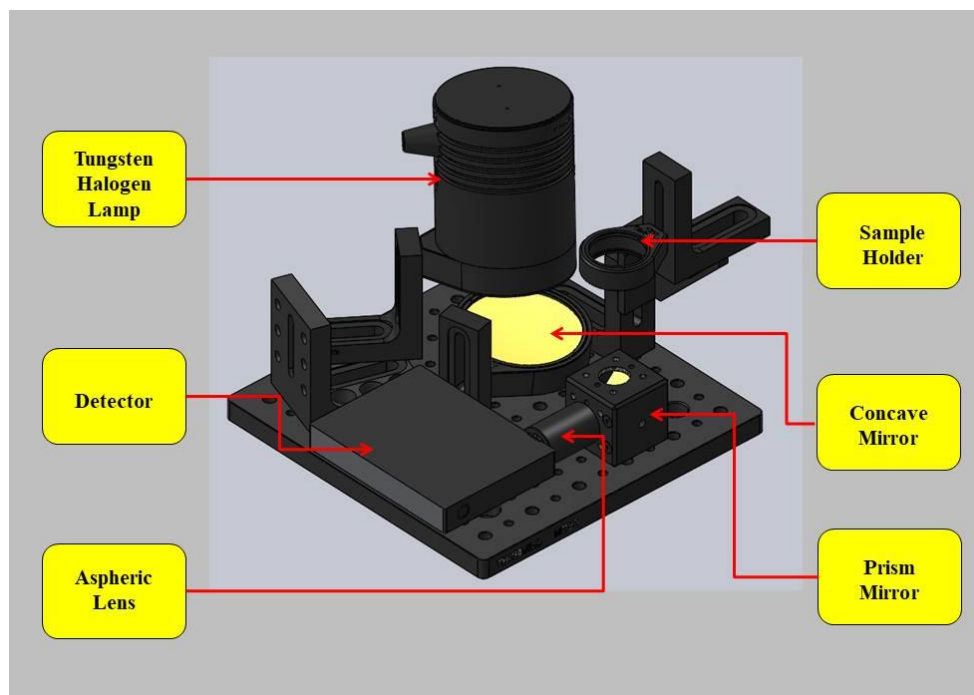


Figure 4. 13D model of the proposed optical assembly of the NIR spectrometer.

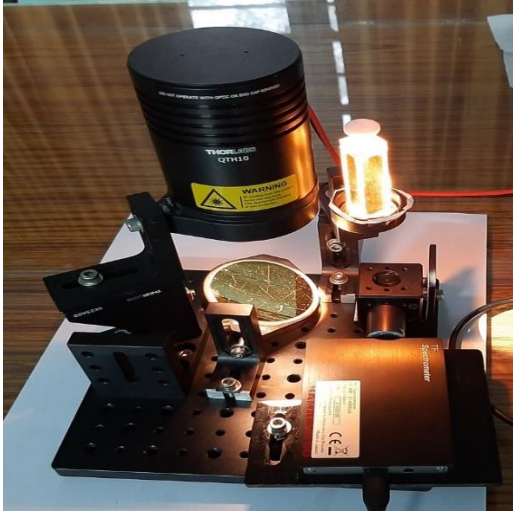


Figure 4. 2 Developed prototype of the Optical assembly of the NIR Spectrometer.

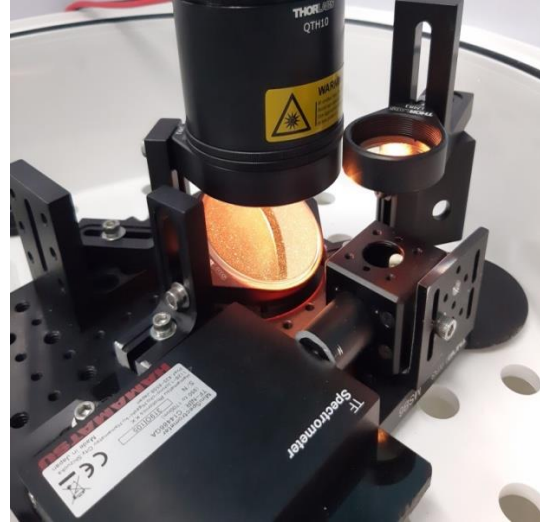


Figure 4. 3 Closer view of the arrangement of optical components in the developed NIR spectrometer.

#### 4.3.3 Working principle of the optical assembly of NIR spectrometer

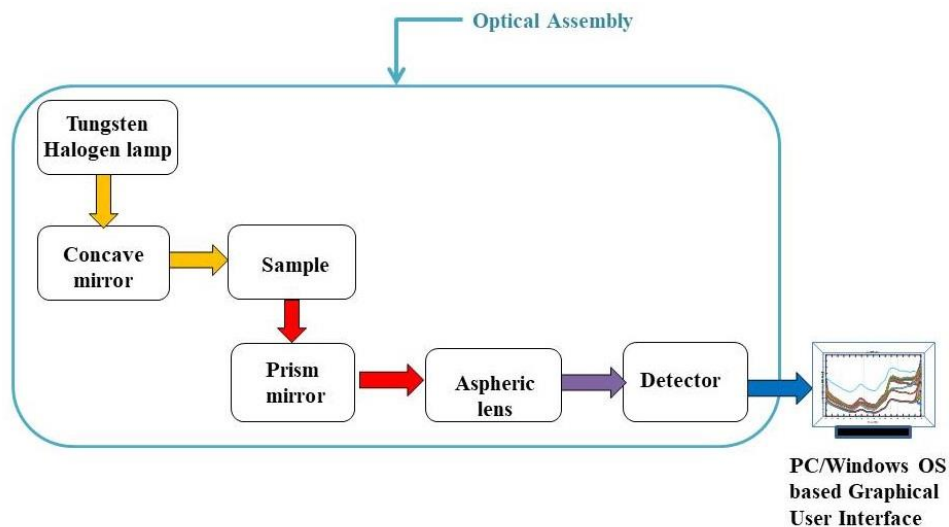


Figure 4. 4 Block diagram of the optical assembly of developed NIR spectrometer.

The overall flow-diagram of the optical assembly is shown in figure 4.4. The working principle of the optical assembly is described below: -

- **Tungsten halogen lamp**-Halogen source is commonly used to irradiate samples in NIR spectroscopy as it provides very stable output. In this setup, tungsten halogen

lamp is positioned at top and broadband emission of wavelength range (400 to 2200 nm) from the lamp is incident on a gold coated concave mirror just below it.

- **Concave mirror**-It is gold coated and facilitates light collection, imaging, and focusing the light onto the sample. From the concave mirror, the light gets reflected and is directed onto the sample.
- **Sample**-The light interacts with the sample and the diffused reflected light from it is directed towards the prism mirror.
- **Prism mirror**-The prism mirror is placed just below the sample holder. The reflected beam from prism mirror exits at an angle of  $90^\circ$  after striking it and is directed to the aspheric lens.
- **Aspheric lens**-It helps in focussing /collimating light without introduction of any spherical aberration. From the aspheric lens, the light gets directed to the slit of the detector.
- **Detector**-The light after entering through the detector slit passes through a series of optical components present in it. The collimating lens prevents spreading of the light at certain angle and directs it onto the transmission grating. The transmission grating disperses the light on the basis of the wavelength. The focussing mirror forms an image of the dispersed light onto the pixels of InGaAs image sensor. The image sensor converts this optical information into electrical signal. The electrical signal generated is then A/D converted with the help of the 16-bit ADC present in the electronic circuitry of the detector [13].
- **PC**-The optical information from the sample is viewed in the form of a spectrum with the help of a PC/Microsoft windows-based device.

#### 4.4 Development of customized GUI for the NIR spectrometer

SpecEvaluationUSB2 is a free software package from Hamamatsu Photonics supplied along with the detector TF-NIR (C14486GA). The Hamamatsu detector supports USB interface for communication with the PC. The basic spectrometer operations like acquisition of data, graphical representation of the data in real time, saving the data for later use are easily performed by the evaluation software. The software lets the user set the values of different parameters which are essential for acquiring the spectrum. Some of them are listed in table 4.3 [14]:-

Table 4. 3 Measurement parameters to be set for acquiring spectral data from Hamamatsu NIR spectrometer.

Serial no.	Parameter	Specified range of values	Property
1	Exposure time	11 $\mu$ s to 100000 $\mu$ s	The duration for which the pixels of the image sensor gets exposed to the radiation.
2	Average count	Within 255 times	Number of scan profiles are averaged and displayed as one profile.
3	Repeat count	Within 5000 times	Number of saved data.
4	Cycle time	Automatic setting	

So, there was a need for developing customized software which can implement multiple functionalities in the same platform. The software should be capable enough for employing both data capture and spectral data analysis functions. This enables rapid prediction in a convenient manner. There would be no need to transfer the data to separate software for analysis. All the works can be achieved in a single window.

The Microsoft Windows application software cannot directly access USB host controller. So, the software interacts with the DLL file to call the necessary functions. The DLL file in turn interacts with the USB host controller via the USB driver. Thus, the NIR spectrometer detector is controlled [13]. The workflow of communication between the application software and the detector is shown in figure 4.5.



Figure 4. 5 Block diagram illustrating communication between SpecEvaluationUSB2 software and detector.

The wrapper DLL assembly file as already explained in Chapter 2 was loaded into the MATLAB environment by using the `NET.addAssembly()` function[15]. The wrapper DLL contains the HSSUSB2A.dll embedded in it. The layout of the GUI created using MATLAB App Designer is shown in figure 4.6.

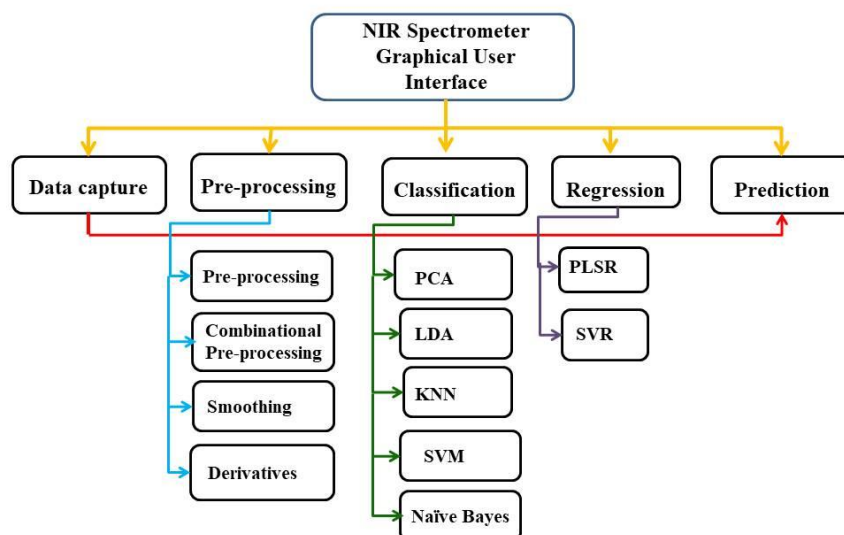


Figure 4.6 Layout of the GUI created using MATLAB App Designer.

The spectrum of the sample is digitally processed using a Microsoft Windows based application or graphical user interface (GUI) (figure 4.7), developed specifically for NIR spectroscopy. The customized GUI facilitates multiple functionalities in a single platform starting from data capture to real time prediction of marker molecule concentration in a test sample. Data communication between the commercially available detector (HAMAMATSU Photonics UK Limited, UK) and the customized GUI was established by creating and using wrapper DLLs.





Figure 4.7 GUI developed for the NIR spectrometer using MATLAB App designer. Here the data capture tab is shown.

The functional modules present in the customized GUI are as follows:

- 1) Data capture module—For taking care of the spectral data acquisition from the sample, viewing variety of plots and saving data for later use.

The different types of data captured are: -

- **Dark data**-It is captured by keeping a black surface on the sample holder without switching on the spectrometer light source. A black surface absorbs all the light from the lamp and ideally reflects no light. It is basically the measure of the noise which needs to be subtracted from the measured data.
- **Reference data**- It is the data with the highest intensity of light. It is captured after switching on the spectrometer light source by keeping a white calibration reference on the sample holder. Generally, the white surface absorbs no light and reflects all the amount of light. So, the absorbance is the maximum for reference data.
- **Result data**-It is the data recorded by keeping the sample on the sample holder.

The saved data had added columns like (Result-Dark data), (Result-Reference data) and absorbance unlike the SpecEvaluationUSB2 software. The absorbance values corresponding to each wavelength could also be calculated in the custom GUI by employing the following formulae [16]:



$$\text{Absorbance} = \log_{10}((\text{Referencedata} - \text{Darkdata})/(\text{Resultdata} - \text{Darkdata}))$$

- 2) Pre-processing module- Here, spectral data acquisition and background noise elimination that occur due to random error and random spikes[18] are carried out. Also, error caused due to variation in light scattering effects due to non-uniform particle sizes is eliminated. Various pre-processing techniques like minmax normalization, detrend, mean centring, standard normal variate (SNV), extended multiplicative scatter correction (EMSC), 1st derivatives and 2nd derivatives[19]and smoothing are incorporated in this module.
- 3) Classification module-Initial assessment of the capture data can be performed for classification of the spectral data in this module.
- 4) Regression module – Regression analysis can be performed to develop the prediction model to estimate the marker molecule andrographolide of the test sample.
- 5) Data archival module— This module is responsible for storing the data for further processing.
- 6) Prediction module- Using the regression coefficients of the prediction model and the spectral data from the spectrometer, the prediction of andrographolide in an unknown sample can be done instantly. The prediction tab of the GUI is shown in figure 4.8.

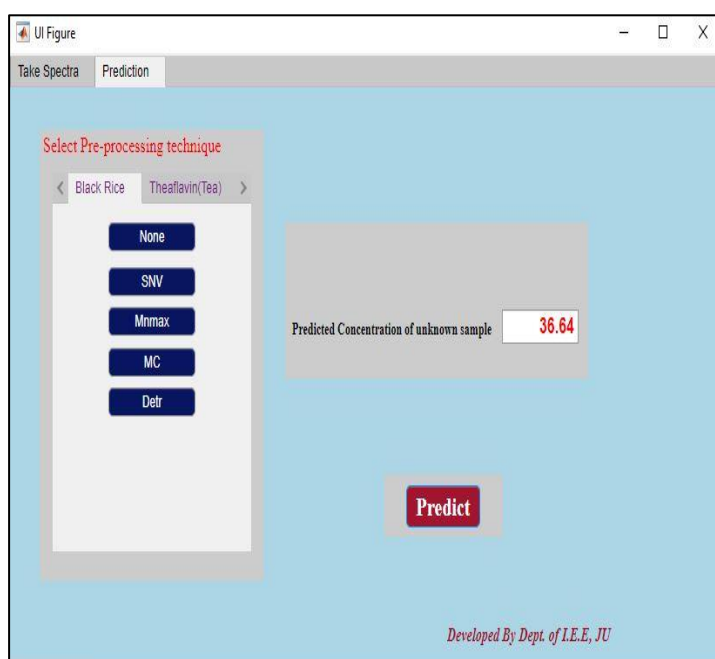


Figure 4.8 Prediction tab of developed GUI for NIR spectroscopy

The prediction tab serves the functionality of real-time prediction of the unknown concentration of the marker molecule present in a sample. The prediction tab utilizes the spectral data captured from the data capture tab for the unknown sample (test data). Matrix multiplication is being performed with the training model regression coefficients as illustrated by the following equation: -

$$Y = \beta_1 X + \beta_2 X + \beta_3 X + \dots \beta_p X \quad (7)$$

$$= [\beta_1 \ \beta_2 \ \beta_3 \ \dots \ \beta_p] \begin{bmatrix} X_1 \\ X_2 \\ X_3 \\ \cdot \\ \cdot \\ \cdot \\ X_p \end{bmatrix}$$

- Y -predicted concentration
- $\beta$  - regression coefficients
- X -pre-processed NIR absorbance data at different wavelengths for the unknown sample.

The unknown concentration of the sample is obtained upon this matrix multiplication. PLS regression algorithm has been used for developing the prediction model in this tab. The general flowchart of this process can be shown in figure 4.9.

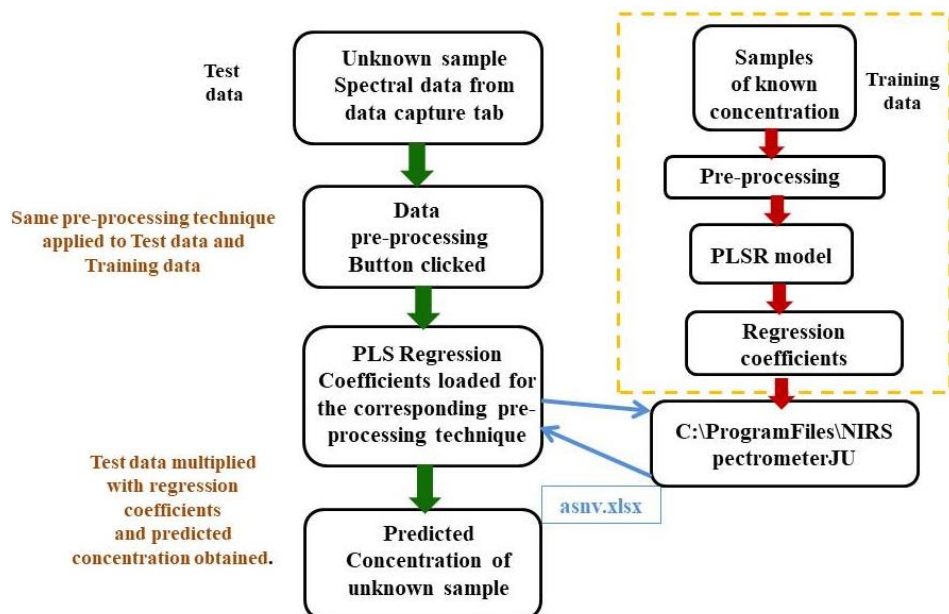


Figure 4.9 Flow diagram of the process involved in real-time prediction of

the concentration of sample through custom GUI of NIR spectrometer.

#### 4.5 NIR spectrometer to work as a standalone instrument

A PC/Windows based device is used in conjunction with the spectrometer for acquiring the NIR spectral data from the detector. But this makes the system a little bulky. To make the system truly stand-alone with increased portability a miniature sized PC is required.

LattePanda Delta 432, is a miniature, sized single board PC that comes along with a 7'' touch display panel was found to appropriate in this situation. It controls the spectrometer in the same way a PC/windows-based device would. The LattePanda delta and touch screen is shown in figure 4.10 and figure 4.11 respectively.



Figure 4.10 Latte panda delta 432 single board PC (left).

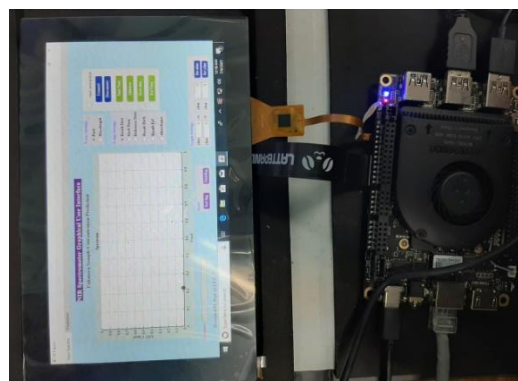


Figure 4.11 Touch display connected to single board PC (right).

The specifications of the Latte Panda Delta 432 are as follows [18]:-

- i. Central processing unit: Intel eight generation.
- ii. Core: from 1.1 to 2.4 giga hertz Quad-Core.
- iii. Storage: 4GB+32GB.
- iv. Display: HDMI Output.
- v. OS Support: Windows 10 Pro Linux Ubuntu.

Not only the spectral data can be captured, viewed and saved for later use, but it can also be analysed in this single board PC. Further real-time prediction of the concentration of the

marker molecule in sample is possible. The custom GUI application can be successfully operated in any PC with or without MATLAB by installing MATLAB Runtime in it. Thus, this instrument serves the purpose of in-situ analysis.

The complete setup of the NIR spectrometer has been housed in an aluminium enclosure to protect it from dust and moisture. The enclosure has been painted black on the outer and the inner surface to avoid the stray reflection of the light. Also, this setup avoids entry of ambient light in the optical assembly, so that the same operating conditions are maintained while taking any measurement. The dimensions of the enclosure are kept as small as possible to increase the portability of the instrument. In order to make the design as compact as possible the design of the enclosure is analysed in 3D software, Solidworks before actual implementation. The dimensions of the enclosure were decided to be (26cm×23cm×12cm). The touch display panel with dimensions (180 mm ×110 mm × 5 mm) was kept in a slanted manner in the front side of the enclosure. The overall, internal and top view of the NIR spectrometer with the enclosure is shown in figure 4.12 and figure 4.13 respectively. The actual prototype of the developed system is shown in figure 4.15 and figure 4.16 respectively. The display screen is fixed in a slanted manner on the enclosure. The three-dimensional model of the prototype with display is shown in figure 4.14. The actual prototype of the NIR spectrometer with the touch display is shown in 4.17.

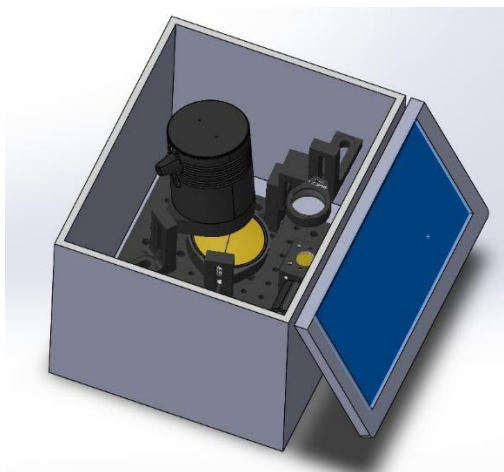


Figure 4.12 Internal arrangement of the proposed NIR spectrometer setup inside the enclosure.

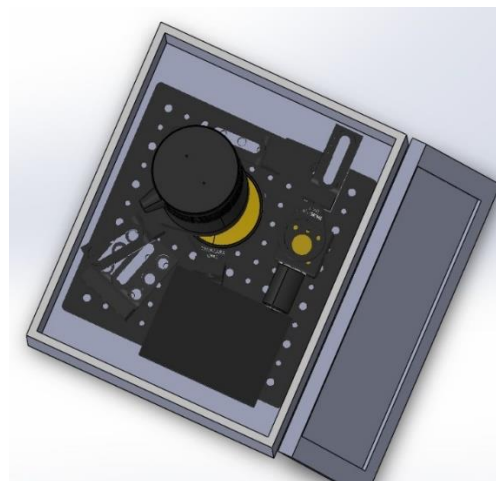


Figure 4.13 Top view of the proposed NIR spectrometer setup inside the enclosure.

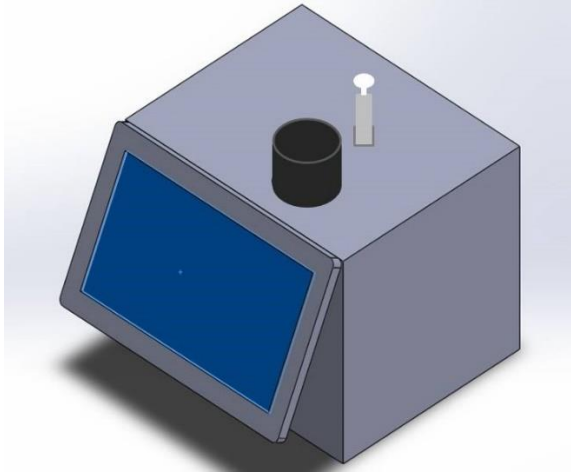


Figure 4.14 3D model of the NIR spectrometer proposed setup with the enclosure and the touch display



Figure 4.15 Top view of the actual prototype of the NIR spectrometer setup inside the enclosure

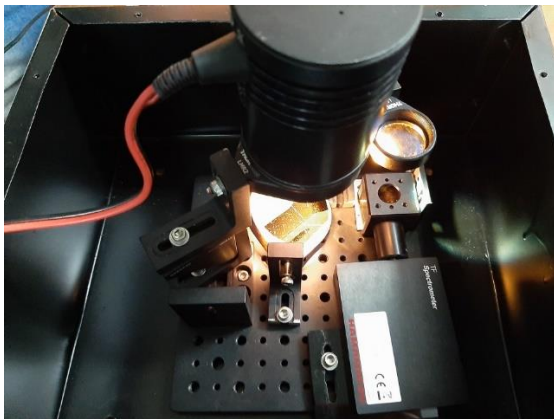


Figure 4.16 Internal arrangement of the actual prototype of the developed NIR spectrometer setup inside the enclosure.

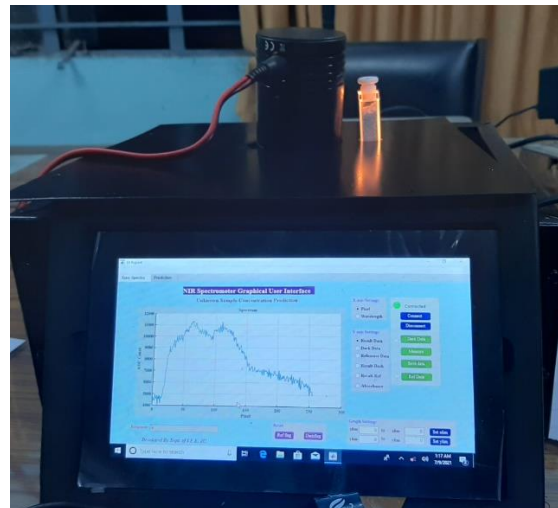


Figure 4.17 Actual prototype of the developed NIR spectrometer with the enclosure and graphical user interface.

Table 4.4 summarises the most essential instrumental and operational characteristics of this portable near infrared spectrometer.

Table 4. 4 Instrumental and operational key performance attributes of developed portable NIR spectrometer

Parameter	Specification
Weight	1.5 kg
Dimension(W×D×H)	(28×20.5×15.2 )cm
Spectral Range	950nm-1700nm
Spectral Resolution	2.92nm
Light Source	Quartz Tungsten-Halogen Light Source(400nm to 2200 nm)
Detector	High-sensitivity InGaAs linear image sensor
Data Export Formats	.csv,.txt
Operating Temperature	5 °C – 50 °C
Method of Measurement	Diffused Reflection
Measuring time	Approximately 2.0 s

#### 4.6 Conclusion

This chapter presents the design and development of a portable NIR spectrometer featuring low cost. The design of the optical assembly for the NIR spectrometer using off-the-shelf opto-mechanical components has been discussed in detail in the chapter. The optical assembly acted as a waveguide for tungsten halogen light source to reach the sample. The external interferences and noises are removed by using lasers, filters etc. Then the desired information from the sample is transmitted to the detector. The number of optical components was kept as minimal as possible without compromising on the instrument performance. The detector from Hamamatsu Photonics consisting of a linear InGaAs image sensor was used in the optical assembly. This instrument works in principle of diffused reflectance mode for acquiring the spectral data from the samples used in the experiment. The detected signal in the NIR detector is converted to the corresponding ADC count. This ADC count is then transmitted to the PC by using an USB interface.

The SpecEvaluationUSB2 software is evaluation software provided with the Hamamatsu NIR detector. It is used for capturing the spectral data, viewing and saving it. Here, customized GUIs dedicated to the NIR spectrometer has been developed using Visual Studio and MATLAB App Designer. The GUI communicates with the NIR detector using DLL libraries. Finally, the GUI was developed using MATLAB App Designer utilizing the concept of Wrapper DLL. Several pre-processing methods, classification and regression techniques

could be implemented in a single platform in the custom GUI. The NIR spectrometer has also been made stand-alone by incorporating a miniature sized single board PC with a 7” touch display panel to the spectrometer and a customized enclosure was fabricated. The chapter demonstrates the feasibility of the implementation of a NIR system that combines many favourable qualities – low cost, ease of construction, operation that can give satisfactory results. Though there are several limitations, and lots of room for improvement since the developed system is still a prototype with good accuracy. This shows that that the system has potential and once perfected, it may serve as a great tool not only in industrial sectors but also in the research labs.

**References**

- [1] C. B. Worth, "Experiments on the Refrangibility of the Invisible Rays of the Sun," vol. 2, no. 1, pp. 6–9, 1950.
- [2] W. Abney and E.R.Festing, "On the Influence of the Atomic Grouping in the Molecules of Organic Bodies on their Absorption in the Infra-red Region of spectrum," *Philos. Trans. R. Soc*, vol. 172, pp. 887–918, 1881.
- [3] W. W. Coblenz, "Investigations of Infrared Spectra Part 1," *Publication No. 35, Carnegie Institute of Washington*, 1905.
- [4] F. E. Fowle, "No Title," *Astophys. J.*, vol. 35, pp. 149–162, 1912.
- [5] J. W. E. and J. Bath, "Modifications in the Near Infra-Red Absorption Spectra of Protein and of Light and Heavy Water Molecules When Water is Bound to Gelatin," *J. Chem. Phys.*, vol. 6, no. 723, 1938.
- [6] P. Barchewitz, "No Title," *J. Chem. Phys.*, vol. 45, no. 40, 1943.
- [7] K. H. Norris, "Cereal Foods World," vol. 31, no. 578, 1986.
- [8] A. I. I. F. Analyzers, "Thermo Scientific Antaris II System Specifications".
- [9] "TANGO CREATES VALUES. Straight forward analyses without delays.," *Analysis*.
- [10] RISO, "FOSS NIRS DA1650," *Riso*, vol. 62, no. 733, pp. 71–3, 1989.
- [11] B&W Tek, "Sol 1.7." <https://bwtek.com/products/sol-1-7/> (accessed Jun. 26, 2021).
- [12] J. Petruzzi, "StellarNet DWARF-STAR," *Analytical Chemistry*, vol. 46, no. 14, p. 1255A, 1974, doi: 10.1021/ac60350a758.
- [13] H. Photonics, "Mini-spectrometers," pp. 1–34.
- [14] H. Photonics, "Usb2.0 mini-spectrometer software instruction manual," pp. 0–74, 2018.
- [15] Mathworks, "Load a Global .NET Assembly." [https://in.mathworks.com/help/matlab/matlab\\_external/load-a-global-net-assembly.html](https://in.mathworks.com/help/matlab/matlab_external/load-a-global-net-assembly.html) (accessed May 14, 2021).



- [16] L. E. Agelet and C. R. Hurburgh, “A tutorial on near infrared spectroscopy and its calibration,” *Critical Reviews in Analytical Chemistry*, vol. 40, no. 4, pp. 246–260, 2010, doi: 10.1080/10408347.2010.515468.
- [17] I. O. Afara *et al.*, “Characterization of connective tissues using near-infrared spectroscopy and imaging,” *Nature Protocols*, vol. 16, no. 2, pp. 1297–1329, 2021, doi: 10.1038/s41596-020-00468-z.
- [18] “Latte Panda Delta 432.” <https://www.lattepanda.com/products/lattepanda-delta-432.html> (accessed Jun. 08, 2021).

## **Chapter 5**

**Quality assessment of *Andrographis paniculata* with the procured and developed NIR spectrometers**

### 5.1 Introduction

*Andrographis paniculata* (Burm. F) Nees, popularly acknowledged as the “king of bitters,” is an herbaceous herb in the family Acanthaceae. This plant is commonly used in China, India, Thailand, and Malaysia to cure sore throats, flu, and upper respiratory tract infections[1]. Its main constituents are the group of diterpenoids designated as andrographolides. Andrographolides have a extensive properties of therapeutic activities, such as anti-inflammatory [2], antibacterial, antitumor, antidiabetic, antimalarial, and hepatoprotective [3], [4], [1]. Clinical research shows that *Andrographis paniculata* can effectively cure viral respiratory infections [6].

The genotype and agroecology of *Andrographis paniculata* determine the nature and quantity of the active molecules like andrographolides and hence the pharmacological activities (Jayakumar et. al. 2013). It is important to estimate the most important active molecules, the andrographolides and classify *Andrographis paniculata* plants with respect to this group of marker molecule. Traditional classifications based on visual inspection of the morphological traits do not consider the active molecules at all. Thus, estimations of active molecules for pharmacognosy, physicochemical studies are mainly based on chemical methods such as HPLC, (HPTLC), LC-MS/MS [7]. These techniques are time-consuming, complicated, labour-intensive, and expensive; moreover, they produce considerable quantities of wastes [8]. Any field level quality control system should be able to handle a large number of samples fast, at a relatively low cost and reasonably dependable accuracy and precision.

Use of NIR Spectra for detection and estimation of specific chemical constituents has proved its worth in diverse fields of application. Its advantages are low cost, speed and simplicity of detection, need for minimal sample preparation and even non-destructive use of samples, feasibility of use at the field level and the feasibility of mechanizing the detection/estimation system for large number of samples. NIR spectroscopy uses liquid and solid samples without any pretreatment. Even when sample extracts are used, NIR spectroscopy obviates the use of further costly chemicals, equipment and time that are required in standard techniques like HPLC. NIR spectroscopy has been successfully used in several areas, like, in the tea leaf quality assessment [9], in food safety assessment [9], [10]; [11] environmental chemistry, microfluidics, biomolecules [13], cancer diagnostic agents, and forensic science [14] as well as explosive detection.

In this chapter, the feasibility of using NIR spectra for estimating andrographolides in *Andrographis paniculata* plant samples and grading the samples based on the estimates was investigated. The performance of NIR spectrum-based technique was examined both in samples of dry powdered leaves and methanol extracts of leaves. Methanol extracts were required for estimation through HPLC, the gold standard [15]. If NIR spectrum can estimate andrographolides with reasonable accuracy compared to HPLC, that itself will be a big advantage in saving cost, time, and make mechanization of large scale estimates feasible.

In this chapter, two experiments were conducted. First experiment was the feasibility study of using commercially available NIR spectroscopy for quantification of *Andrographis paniculata*. Second experiment was conducted for qualitative estimation of *Andrographis paniculata* using our developed portable NIR spectrometer. Finally, a comparison study on performance between the commercially available NIR instrument and the developed portable NIR spectrometer is described.

## **5.2 Experiment I: Feasibility study of using commercially available NIR spectroscopy for quantification of *Andrographis paniculata***

In this experiment, the objective was to grade the *Andrographis paniculata* samples based on the content of andrographolides (IP2014). As only a small portion of the spectra responds to the andrographolides, a low-cost portable spectrometer with customized range can be employed for simple gradation of the samples without the need for highly accurate estimation, and is likely to be used as a ready-to-apply tool by the traders for breeding and improvement of cultivars for obtaining higher drug yield [16].

### **5.2.1 Material and Methods**

#### **5.2.1.1 Plant Material**

Plant material (leaves) of *Andrographis paniculata* was collected from West Medinipur, East Medinipur, Purulia, South 24 Parganas, Hooghly, and Kolkata district of West Bengal, India. Plant material were identified and authenticated by Dr. S. Rajan, ex-field botanist, the medicinal plant collection unit, Tamilnadu, India. The voucher specimens of 18 samples

(specimen no. SNPS/JU/2018/12-29) were retained at SNPS, Jadavpur University, Kolkata, India for forthcoming reference.

Based on the content of andrographolides, *Andrographis paniculata* samples were graded into 3 categories: good quality, medium quality and poor quality. Plants having high andrographolides content (>2.50 %) [17] were considered to be of good quality and placed in grade I; those with <1%, the non-acceptable level according to the Indian Pharmacopeia (IP2014), were placed in grade III. The intermediate types (>=2.5% and <=1%) were placed in grade II.

### 5.2.1.2 Chemical Analysis

#### 5.2.1.2.1 Chemicals and reagents

Andrographolides standard (> 95 % HPLC) was obtained from Sigma Aldrich. Methanol (HPLC grade), glacial acetic acid (HPLC grade), petroleum ether and ethyl acetate (analytical grade) and all other solvents (AR grade) were procured from Merck, India. Quantitative estimation was performed with Empowers software using the external standard calibration method.

#### 5.2.1.2.2 Extraction

The air-dried (at room temperature) samples of 18 plants were powdered to a moderately coarse texture (180 - 355 $\mu$ m) by a mechanical grinder. Methanolic extracts were made from the powdered samples (50 g in 80 mL of methanol) using rotary shaker at 150 rpm for 10mins. Each sample was extracted thrice. The extracts were filtered and dried by vacuum evaporation using a rotary evaporator at 50°C and high pressure. The dried extract (10 mg) was dissolved in methanol and filtered through 0.22  $\mu$ m membranes to get the stock solution (10 mg/mL). The stock solution was diluted to get 1 mg/mL sample concentration for HPLC.

#### 5.2.1.2.3 High performance liquid chromatography (HPLC) Analysis

The Reverse Phase HPLC (RP-HPLC) system (Waters, USA) equipped with a rheodyne 7725i injector having 20  $\mu$ L loop, 3 Lines degasser (Volume 400  $\mu$ L), LC-30AD pump, C18 column (5 $\mu$ m particle size, 250  $\times$  4.6") UV/Vis detector was used for the analysis. The method developed was isocratic with the mobile phase of Methanol: Water (1% acetic acid) - 60:40 v/v/v. A Milli-Q academic water purification system (Bedford, MA, USA) equipped with 0.22  $\mu$ m Millipak express filter. The pH of the solvent B was adjusted at 2.4 by using

1% (v/v) glacial acetic acid for better ionization. The mobile phase was filtered through 0.45 mm pore size (Millipore) membrane filter followed by sonication to degas the solvent. Whatman syringe filters (NYL 0.45  $\mu\text{m}$ ) were used for the filtration of the extract. The temperature of the column was reserved at 25°C and the input volume was given 20  $\mu\text{L}$ . The total run time was set at 10 minutes. The flow rate was set to 1.0 mL/min, with a maximum wavelength of 230 nm for maximum absorption of the compound. The external calibration method was used to achieve quantitative measurement with Empower 2 software applications. Typical chromatograms of andrographolides standard and an *Andrographis paniculata* extract sample are shown in Figure 5.1.

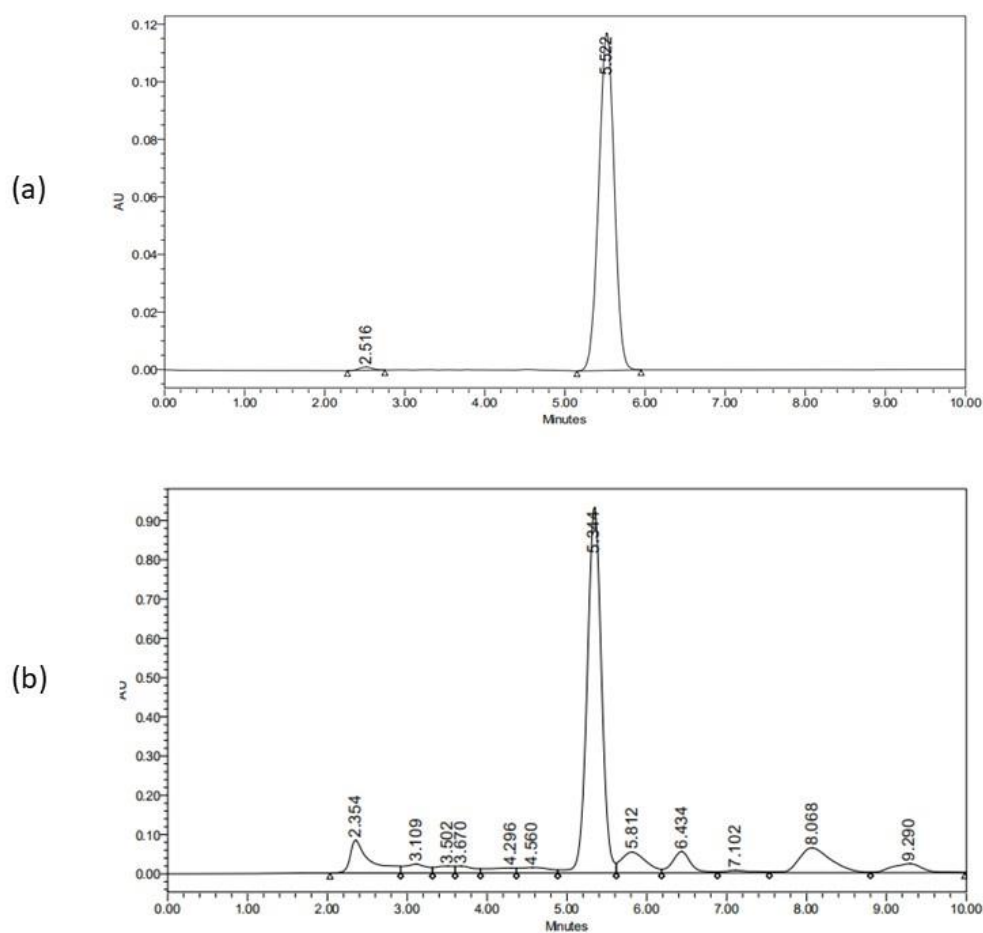


Figure 5.1 HPLC chromatogram of (a) Andrographolides Standard (b) *Andrographis paniculata* extract sample.

#### 5.2.1.2.4 Method validation

The RP-HPLC method was validated on the basis of the International Conference on Harmonization guidelines (ICH Q2(R1) Guideline) (ICH Harmonised Tripartite Guideline, 2005). The retention period of both the standard and test samples was compared to establish

method specificity. Limit of Detection (LOD) and Limit of Quantification (LOQ) were calculated based on the equation:  $LOD = 3.3 \sigma/S$  and  $LOQ = 10 \sigma/S$ , where  $\sigma$  is the residual standard deviation of regression and  $S$  is the slope of the calibration curve. The accuracy of the method was determined as % recovery by the assay of known added amount of analyte in the sample. The samples were spiked with three different concentrations of standard compounds in triplicate. The precision of the analytical method was assessed by measuring six replicates of each of three different concentrations of the reference compounds. The results were represented as %RSD of intra-day and inter-day analysis.

### 5.2.2 Experimental Setup and NIR Spectra Acquisition

A DWARF-Star NIR spectrometer (StellarNet Inc., USA) coupled with an upward looking diffuse reflectance accessory RFX-3D was used to acquire the diffuse reflectance spectra of the medicinal plant samples. The scanning range was from 900 to 1700 nm, and a RS50 (50mm diameter White reflectance standard, halon>97%) was used as a calibration reference. The sample (after drying and grinding) was placed in a standard quartz plate of 1mm thickness at the top of RFX-3D. RFX-3D was integrated with a 5-watt halogen bulb and three fibre connectors to the spectrometer each positioned 120 degrees in a circle to eliminate the need to rotate for coarse grain or non-uniform samples. Each sample was scanned 16 times with integration time of 300ms and then the averaged spectrum was used for analysis. The S/N ratio was 4,000:1, wave-number accuracy was within  $\pm 0.01 \text{ cm}^{-1}$ , and the resolution was set as the resolving resolution of 2.5nm. The temperature was kept at about 25 °C during the whole experiment. Figure 5.2 explains the workflow of the chemical analysis, and the training, and testing steps with NIR spectrum.

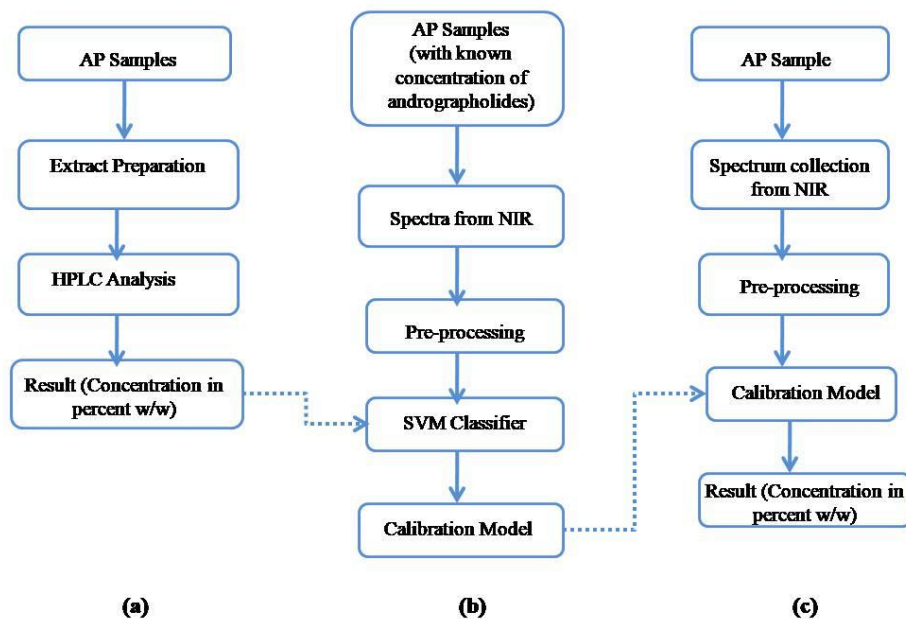


Figure 5. 2 Experimental workflow of (a) chemical analysis (b) training (c) testing.

In the Stellarnet spectrometer used in our study, the data points were collected from 900 nm to 1700.5 nm with a gap of 1.75 nm. Thus, there were  $(1700.5-900)/1.75 = 459$  data points for every spectrum. Fifteen (15) replicates were taken for each *Andrographis paniculata*; therefore,  $459 \times 18 \times 15$  spectral data points were obtained for 18 samples.

## 5.2.3 Result and Discussion

### 5.2.3.1 Interpretation of Spectroscopic Characterization

#### 5.2.3.1.1 Original and preprocessed Spectra

The graphical representation of the wavelength versus absorbance of the raw spectra without any pre-processing is shown in Figure 5.3. The spectra obtained using the dried leaf powder shows absorption peaks at 1200 nm (C-H Second overtone region due to presence of CH<sub>2</sub>, CH) and 1472 nm (O-H second overtone region due to presence of R-OH group) [18].



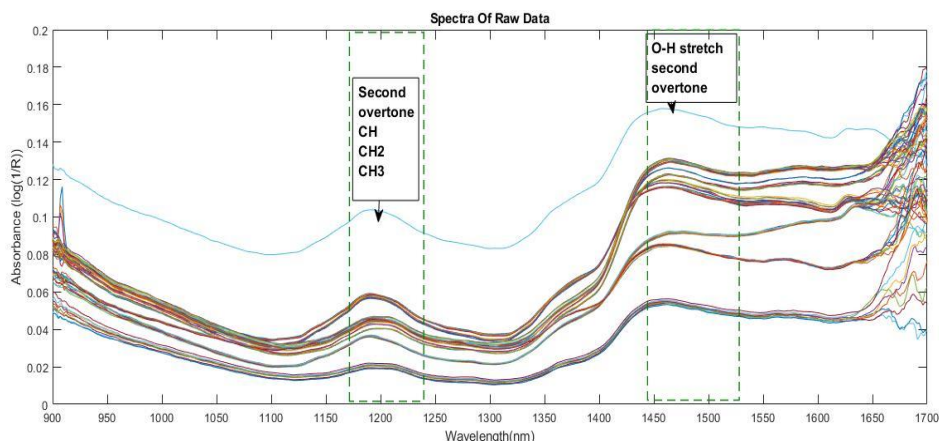


Figure 5.3 Wavelength versus absorbance of the original spectra without any pre-processing.

### 5.2.3.1.2 Loading plot

The loading plot of the spectra is shown in Figure 5.4. The relative contributions of each PC to the explained variation were large for the first few components, with 97.2% of the variation explained by the first four components for andrographolides (PC1 = 55.89%, PC2 = 21.82%, PC3 = 15.94%, and PC4 = 3.56%).

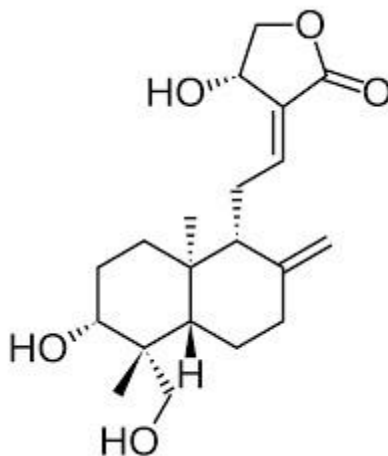


Figure 5.4 Chemical structure of andrographolides.

The first two principal components (PCs) showed strong absorption peaks at 1100 nm and 1300 nm (C-H Second overtone region due to presence of CH<sub>3</sub>). The loading plot of PC2 (Figure 5) showed another absorption peak at 1450 nm (O-H Second overtone region due to presence of R-OH group) and loading plot of PC1 showed another absorption peak at 1650 nm (C-H first overtone region due to presence of CH<sub>3</sub>). The loading plot of PC4 (Figure 5) had major absorption peaks at 1400 nm (O-H second overtone, associated with water) and

1650nm (C-H first overtone region due to presence of CH<sub>3</sub>, CH<sub>2</sub>, CH). These are all related to the most abundant structural groups present in the andrographolides (Figure 5.4).

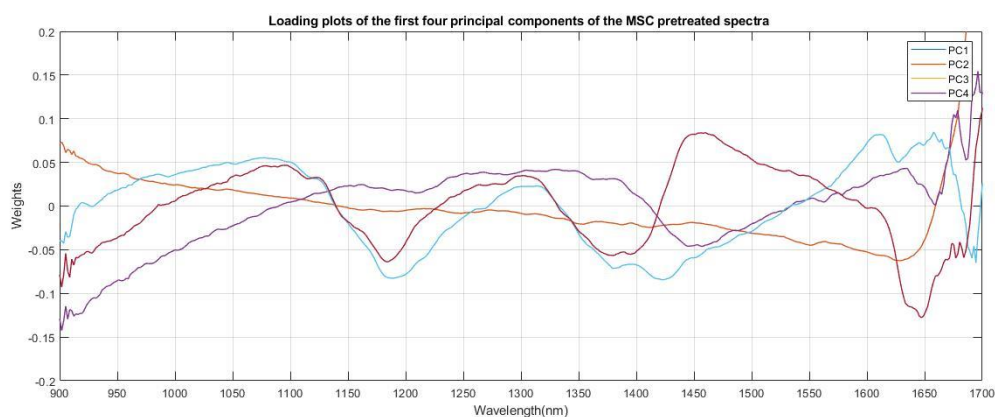


Figure 5.5 Loading plot of the first 4 PCs of MSC preprocessed spectra of *Andrographis paniculata*.

### 5.2.3.2 Plot of PCA

PCA was performed on the raw and preprocessed spectra to examine the qualitative differences among the three varieties of the samples. Figure 5.6 presents the PCA score plot derived from the raw spectra of *Andrographis paniculata* samples. The first and second principal components (PCs) accounted for 90.67% and 7.89% of the total variance, respectively. Samples of the same variety have been observed to appear as clusters, and no overlaps were observed among the three samples.

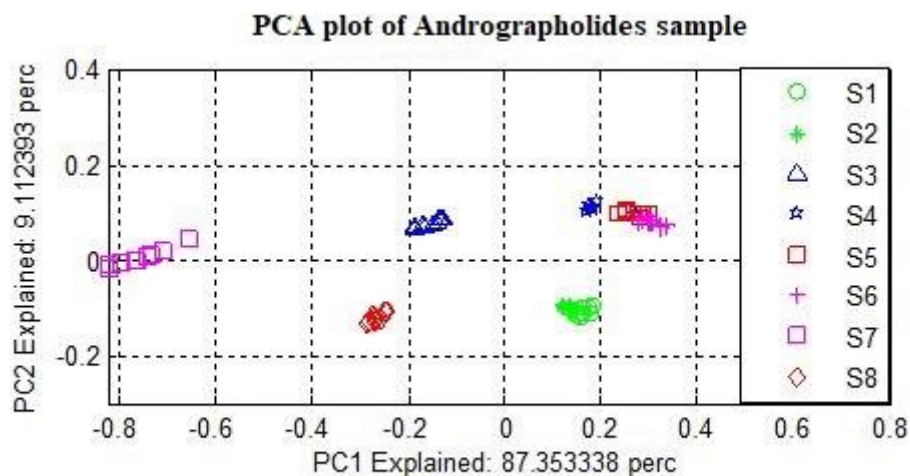


Figure 5.6 PCA plot with first two PC.

### 5.2.3.3 Plot of LDA

Figure 5.7 displays the Linear Discrimination Analysis plot applied to the whole data matrix after preprocessing using Standard Normal Variate (SNV). The discrimination is better than PCA.

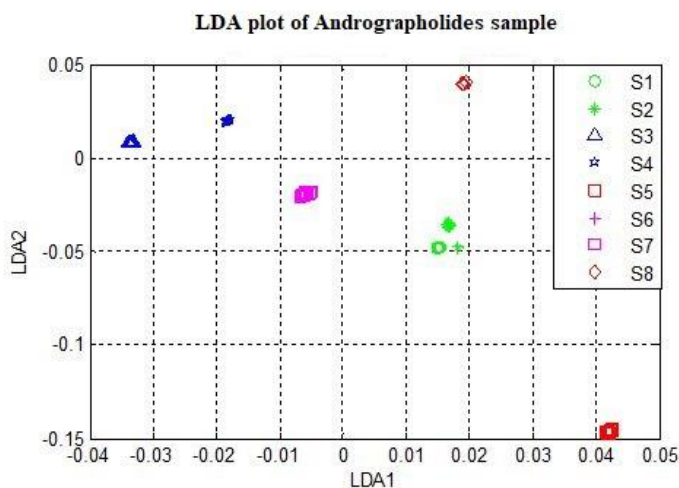


Figure 5.7 LDA plot with first two components.

### 5.2.3.4 SVM model

For analysis on the spectra obtained from the ethanol extracts of 18 samples, the support vector model was used for regression on the data pretreated with SNV data. The results of HPLC analysis, NIR predicted values and the corresponding grades are shown in Table 1. The of correlation coefficients and paired two tailed 't' statistic results of three pairs of among three sets of estimates: NIR estimates of methanol extract, NIR estimates of powdered samples, and the estimates from HPLC analysis, are given in Table 5.1.

Table 5.1 Result of HPLC and NIR for grades of the 18 samples.

Serial No.	Sample Name	HPLC method	Prediction by NIR		Grade
			Extract	Powder	
1	SNPS_NMPB_AP1	2.50	2.45	2.25	II
2	SNPS_NMPB_AP2	2.20	2.10	2.00	II
3	SNPS_NMPB_AP3	1.5	1.45	1.44	II

4	SNPS_NMPB_AP4	0.53	0.47	0.41	III
5	SNPS_NMPB_AP5	0.54	0.54	0.49	III
6	SNPS_NMPB_AP6	0.55	0.50	0.44	III
7	SNPS_NMPB_AP7	0.93	0.90	0.89	III
8	SNPS_NMPB_AP8	2.90	2.89	2.46	I
9	SNPS_NMPB_AP9	2.65	2.62	2.52	I
10	SNPS_NMPB_AP10	1.71	1.70	1.65	II
11	SNPS_NMPB_AP11	2.57	2.54	2.32	I
12	SNPS_NMPB_AP12	2.72	2.62	2.52	I
13	SNPS_NMPB_AP13	2.68	2.31	2.14	I
14	SNPS_NMPB_AP14	2.30	2.28	2.29	II
15	SNPS_NMPB_AP15	1.57	1.80	2.07	II
16	SNPS_NMPB_AP16	1.79	2.24	2.05	II
17	SNPS_NMPB_AP17	1.59	1.54	1.44	II
18	SNPS_NMPB_AP18	2.03	2.13	2.12	II
	Correlation coefficient with respect to HPLC results		0.97	0.94	
	“t” value		0.27	1.78	
	“p” value		0.79	0.09	

Eighteen data patterns were considered for the tenfold cross-validation method. In this method, a total of ten train-test trials were conducted, and the total data set was divided into ten subsets. Out of these ten subsets, one subset (10% of data) was used as the test set, and the other nine subsets (90% of data) were used as the training set. The classification rates were then averaged over these folds for estimating the classifier performance. The classification rate and the total misclassified pattern on 18 NIR data are shown in Table 5.2.

From the results of the tenfold cross-validation method, the average classification rate is found to vary from 75% to 95% and the average accuracy is obtained as 83% with SNV preprocessing. This result is quite encouraging, even though the data set is quite small with respect to the number of classes.

Table 5.2 Result of 10-fold cross-validation method for SNV preprocessed data.

Cross validation folds	%Classification on SNV pre-processed data
1	75
2	95
3	90.5
4	75
5	80
6	90
7	81
8	75
9	81
10	85
<b>Average</b>	<b>83</b>

### 5.3 Experiment II: Qualitative estimation of *Andrographis paniculata* using developed portable NIR spectrometer

#### 5.3.1 Material and methods

##### 5.3.1.1 Plant Material

Plant material (leaves) of *Andrographis paniculata* was collected from West Medinipur, East Medinipur, Purulia, South 24 Parganas, Hooghly, and Kolkata district of West Bengal, India. Plant material were identified and authenticated by Dr. S. Rajan, Field botanist, the medicinal plant collection unit, Ooty, Tamil Nādu, Govt. of India. The voucher specimens of 40 samples were kept at SNPS, Jadavpur University, Kolkata, India for forthcoming reference.

##### 5.3.1.2 NIR spectral data collection

The developed NIR spectrometer in reflectance mode was used to acquire the diffuse reflectance spectra of the *Andrographis paniculata* samples. The scanning range was from 950nm to 1700 nm. A RS50 (50mm diameter White reflectance standard, halon>97%) was used as a calibration reference.

The raw intensity of material was normalized using two reference standards: a white reference intensity and a dark reference intensity, both collected under the identical conditions as the sample intensity. The dark reference intensity was collected by turning off the light source and fully covering the lens with its opaque cap, while the white reference intensity was collected using a white Teflon board with nearly hundred percent reflectivity. The normalized intensity was then determined using the formula below. (Eq. (1)):

$$R = \frac{R_O - R_D}{R_W - R_D} \quad (1)$$

where  $R_O$ -recorded intensity,

$R_D$  -the dark reference intensity (with 0% reflectance), and

$R_W$ -the white reference intensity.

The sample (after drying and grinding) was placed in a standard quartz cuvette on the sample holder. Each sample was scanned 16 times with integration time of 300ms and then the averaged spectrum was used for analysis. The resolution of the instrument was about 2.92 nm. The temperature was kept at about 25 °C during the whole experiment. The experimental workflow is shown in [19]. Fifteen replicates were collected for individual sample *Andrographis paniculata*; therefore, 15×40=600 data points were attained for 40 samples. During experiment the scan average was set at 16 with integration time of 0.1 sec. The details of the samples are shown in table 5.3.

Table 5.3 Statistics about andrographolide content in the *Andrographis paniculata* used for calibration and prediction sets.

Sample sets	Number of samples	Minimum (mg/g)	Maximum (mg/g)	Mean (mg/g)	Median (mg/g)	Standard deviation (mg/g)
<b>Total samples</b>	40	0.53	2.9	1.801	1.895	0.749
<b>Calibration set</b>	32	0.53	2.9	1.806	1.92	0.757
<b>Prediction set</b>	8	0.55	2.81	1.78	1.835	0.721

## 5.3.2 Results and Discussion

### 5.3.2.1 NIR spectra of andrographolides

The wavelength versus absorbance plot of the raw, SNV and MSC pre-processed spectra are shown in Figures 5.8-5.10 respectively. The absorption peaks corresponded to the most abundant structural groups present in andrographolide [19], [20].

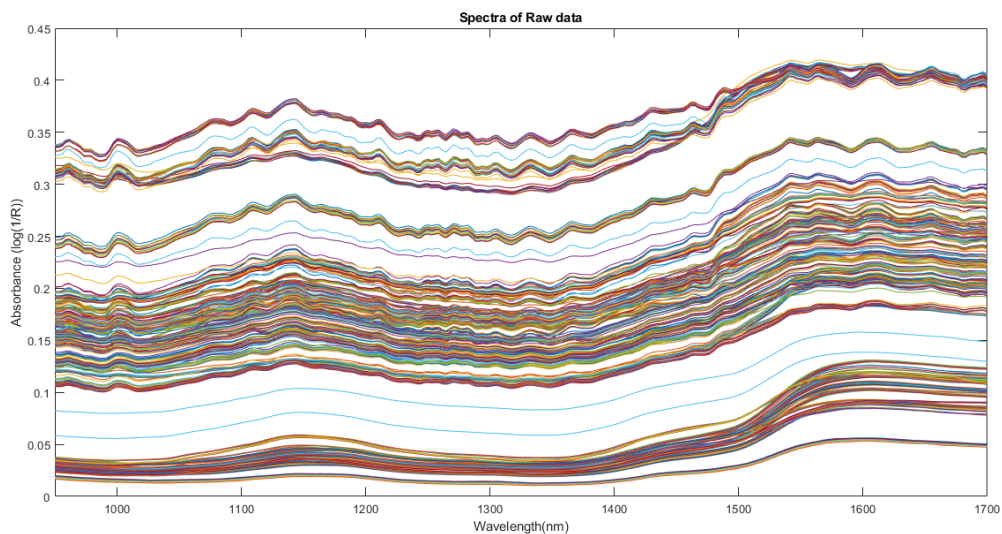


Figure 5.8. Wavelength versus absorbance plot of the raw spectra.

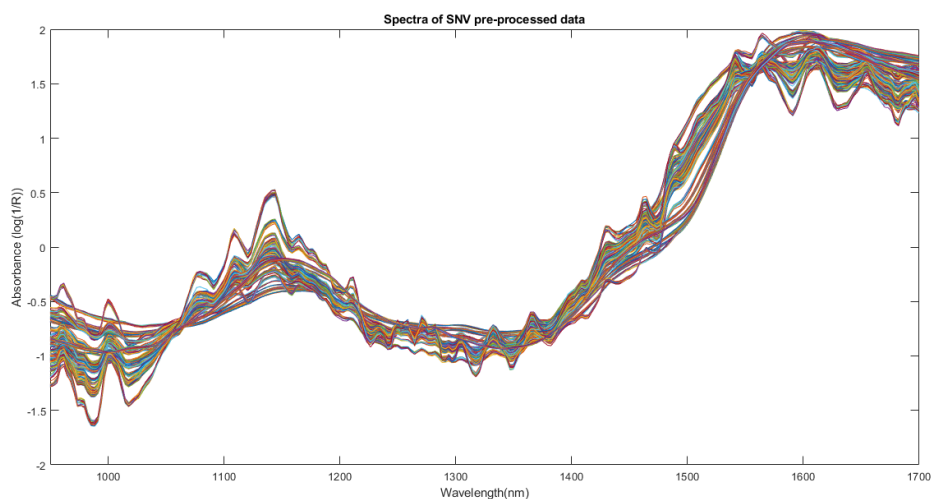


Figure 5.9 Wavelength versus absorbance plot of the SNV pre-processed spectra.



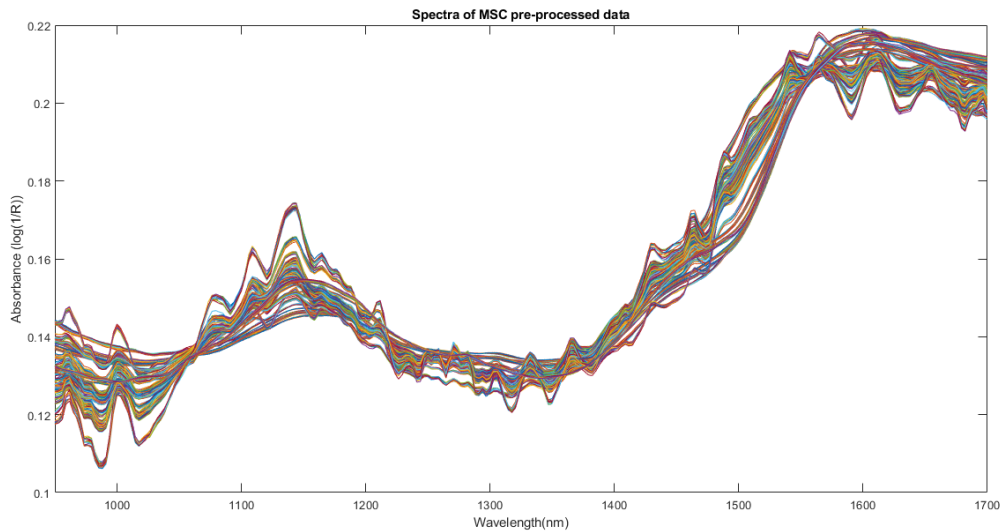


Figure 5.10 Wavelength versus absorbance plot of the MSC pre-processed spectra.

The loading plot of the raw spectral data and SNV pre-processed spectral data is shown in Figure. 5.11 and Figure. 5.12 respectively. The variation explained by the first four principal components for the raw spectral data was 99.99% (PC1=99.59%, PC2=0.35%, PC3=0.03%, PC4=0.02%). The variation explained by the first four principal components for the SNV pre-processed spectral data was 99.37% (PC1=77.72%, PC2=13.56%, PC3=4.22%, PC4=3.87%).

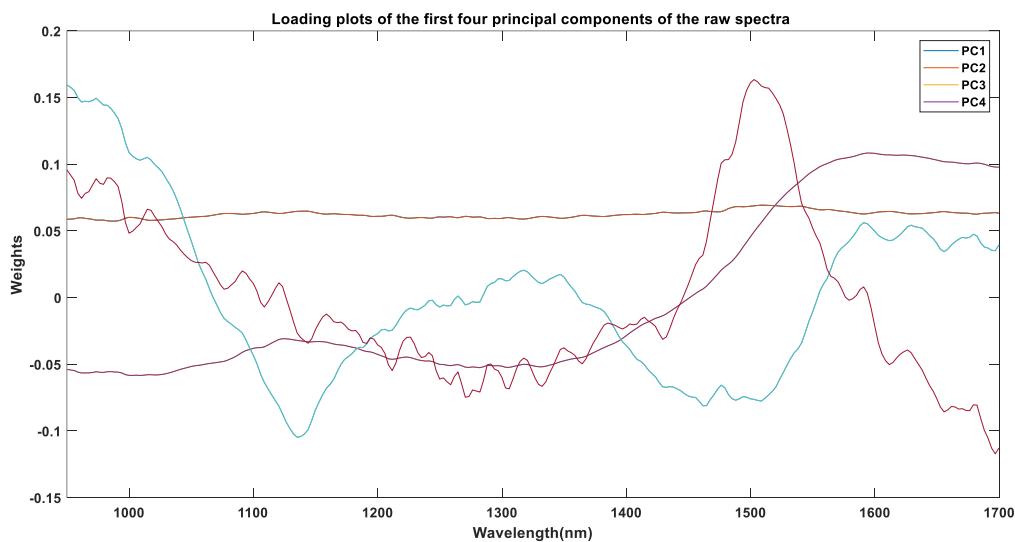


Figure 5.11 Loading plots of the first four principal components of the raw spectra.



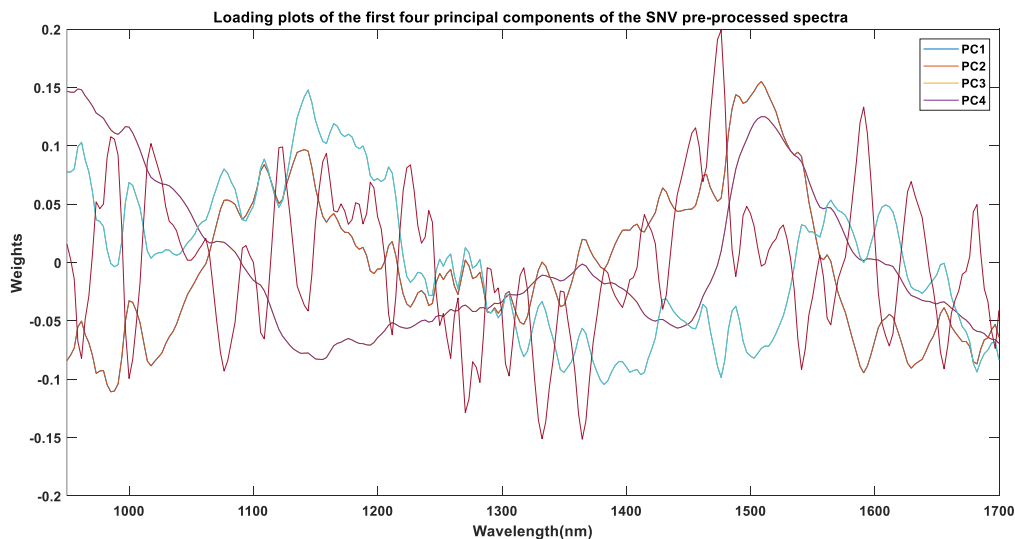


Figure 5.12 Loading plots of the first four principal components of the SNV pre-processed spectra.

### 5.3.2.2 Exploratory Analysis using PCA

PCA analysis (Figure. 5.13) was performed to determine qualitative and quantitative differences of andrographolide in various *Andrographis paniculata* samples. The data reduction was facilitated by PCA. The principal components (PCs): 1st PC and 2<sup>nd</sup>PC accounted for explained variation of 99.7% (PC1=86.47% and PC2=13.23%). The PCA plot reveals a tendency for formation of clusters between *Andrographis paniculata* samples having a certain content of andrographolide thus belonging to a particular category as found in [19].

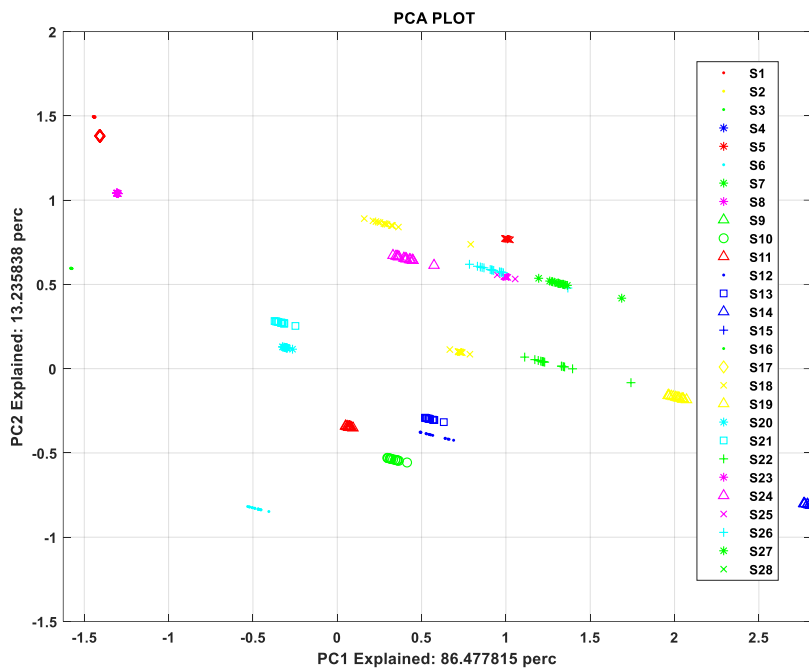


Figure 5. 13 PCA analysis plot.

### 5.3.2.2 Quantitative analysis using PLSR and SVM

#### 5.3.2.2.1 Quantitative analysis using PLSR

RMSECV was used to estimate the optimal number of components in partial least square regression method. The number of components vs. RMSECV plot is has been shown in Figure 5.14. Twelve component number was selected as optimal. The correlation coefficient ( $R^2$ ) and RMSECV were obtained as 0.98 and 0.11 respectively.

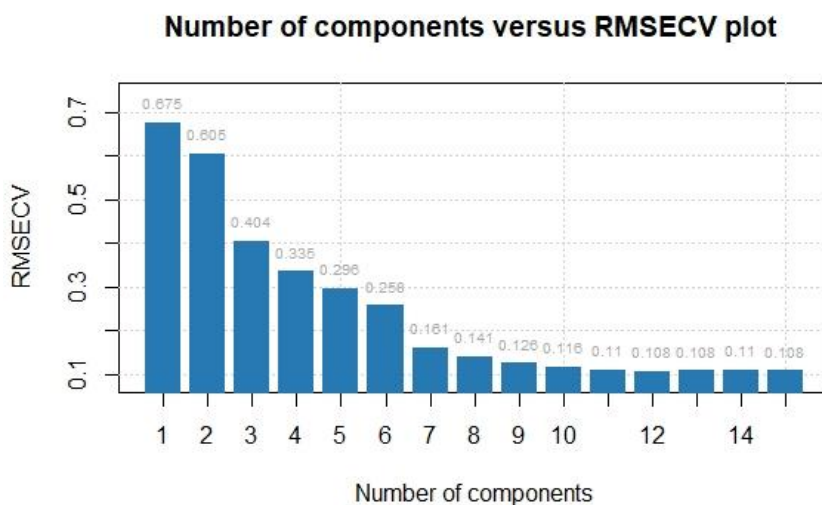


Figure 5.14 RMSECV vs. Number of components plot.

The performance of the PLSR models has been illustrated in table 5.4. The best PLSR model for estimating the andrographolide content *Andrographis paniculata* was developed using the first derivative pre-processed data with  $R^2_P$ , RMSEP and  $RPD_P$  values of 0.99, 0.08 and 8.71 respectively. Normally,  $R^2$  values in the range of 0.82–0.90 indicate good performance for regression models, whereas  $R^2$  values greater than 0.90 imply exceptional performance [21]. Likewise, for residual prediction deviation values below 1.5 are regarded unusable, those between 1.5 and 2.0 are adequate for rough prediction, those between 2.0 and 2.5 are suitable for quantitative predictions, and those between 2.5 and 3.0 are called good and outstanding prediction models [22]. The developed partial least square regression model demonstrated significant result with high values of  $R^2_P$  and  $RPD_P$  for predicting the andrographolide content of *Andrographis paniculata*.

The “two-tailed paired t-test” was carried out between the reference values of andrographolide obtained with chemical analysis of the samples and values predicted by PLS regression. The ‘ $t$ ’ values were obtained as 0.25, and 0.5, and ‘ $p$ ’ values were 0.81, 0.63 for raw and first-derivative pre-processed data respectively, thus satisfying the null hypothesis.

#### 5.3.2.2.2 Quantitative analysis using SVM

Regression analysis using the SVM algorithm was carried out for estimating the andrographolide content *Andrographis paniculata*. In this technique, the constraints (regularization ( $\gamma$ ) and the squared bandwidth of the Gaussian curve ( $\sigma^2$ ) of the model were adjusted to determine the ideal value using search process.

The model performance of SVM with the optimal parameters for each spectral preprocessing has been illustrated in table 5.4. The results indicate that PLSR is slightly superior to SVM for estimating the andrographolide content in *Andrographis paniculata*. The best SVM model for estimating the andrographolide content in *Andrographis paniculata* was developed using the first derivative pre-processed data with  $R^2_P$ , RMSEP and  $RPD_P$  values of 0.97, 0.13 and 5.69 respectively.

In addition, we carried the “two-tailed paired t-test” on the values obtained with chemical analysis of the samples. The  $t$  value values are obtained as 1.04, and 1.2, and  $p$  values are obtained as 0.33, 0.27 for and first derivative pre-processing respectively, satisfying the null hypothesis.

Figure. 5.15 and figure 5.16 show that scatter plots of predicted versus measured andrographolide content in *Andrographis paniculata* samples. For both the models, the samples were distributed closely around the regression line, indicating high correlation between the measured and the reference andrographolide values. These results also confirmed the effectiveness of portable NIR spectrometer for estimating the andrographolide content in *Andrographis paniculata*.

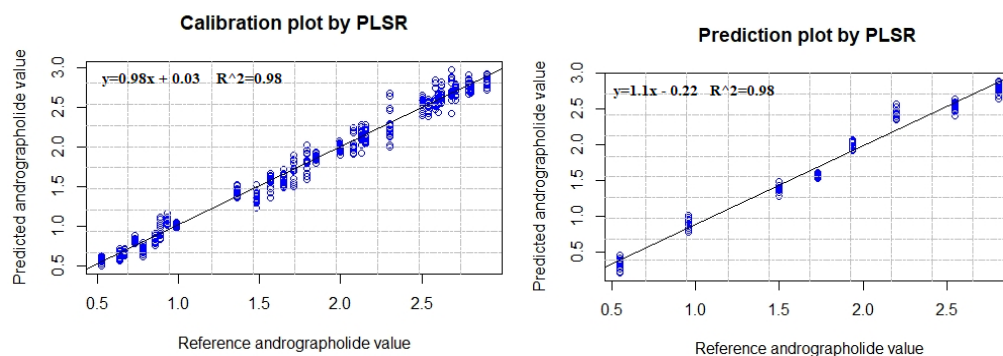


Figure 5.15 Scatter plot of PLSR of raw data.

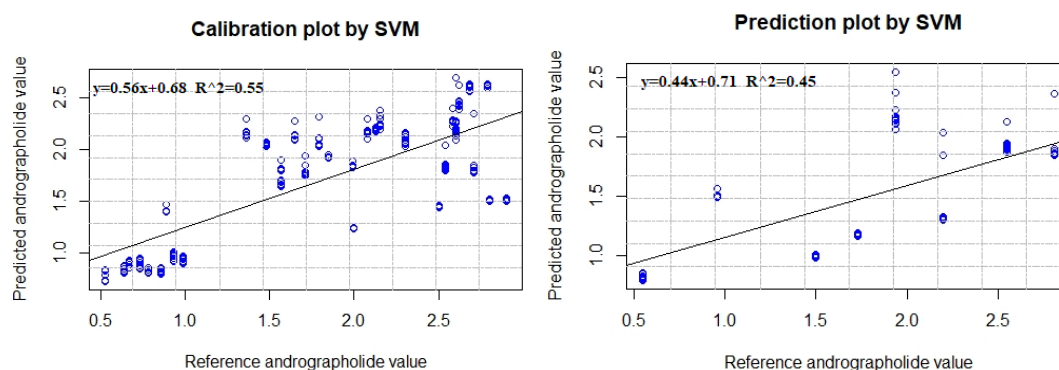


Figure 5.16 Scatter plot of SVM of raw data.

Table 5.4 Performance of partial least square regression (PLSR) and support vector machine (SVM) full-band models using different preprocessing methods for andrographolide content in the *Andrographis paniculata* using developed NIR spectrometer.

Model	Preprocessing	Parameters	Calibration			Prediction		
			$R_c^2$	RMSEC	RPD <sub>c</sub>	$R_p^2$	RMSEP	RPD <sub>p</sub>
PLS	Raw	Latent Variable 12	0.98	0.09	8.03	0.98	0.15	4.9

	SNV	15	0.99	0.07	10.13	0.95	0.16	4.43	
	1d	15	0.99	0.05	13.72	0.99	0.08	8.71	
	2d	15	0.99	0.07	10.54	0.98	0.11	6.53	
		$\gamma$	$\sigma$						
<b>SVM</b>	None	0.004	0.1	0.55	0.52	1.45	0.45	0.6	1.19
	SNV			0.99	0.06	11.82	0.92	0.22	3.3
	1d			0.95	0.06	12.65	0.97	0.13	5.69
	2d			0.99	0.08	9.11	0.95	0.17	4.18

#### 5.4 Comparison study between commercially available spectrometer and our developed spectrometer

From table 5.5, it can be noted that the correlation coefficient ( $R^2$ ) and RPD values were better for predicting the TF values with the developed Raman spectrometer compare to our previous study. Here, RMSEP is less, but average accuracy is better for developed spectrometer with respect to commercially available spectrometer.

Table 5.5 Comparison of evaluation performance between the developed low-cost spectrometer and the spectrometer used by Sing et al. referred above

Type of spectrometer	Average accuracy (%)	$R^2$	RMSEP	RPD
Developed spectrometer	95.8	0.98	0.33	4.52
Spectrometer used by Sing et al. 2021[23]	92.0	0.93	0.13	3.9

In the comparison given in the above table 4(b), the regression technique used in the developed spectrometer was SVM-R while in previous study [23] it was Partial least square regression (PLS-R) and the sample sets used in the two studies were also different.

### 5.5 Conclusion

In this chapter, a methodology has been proposed to grade *Andrographis paniculata* samples using NIR spectroscopy and SVM classifier based on the content of marker molecules, andrographolides. Relative accuracies of estimating the andrographolides by NIR spectra of methanol extracts of the samples, and powdered leaf samples were compared taking the estimates obtained from HPLC analysis as the standard. The accuracy of estimation based on extracts was a little higher than the powder leaf samples. But it did not change the grading pattern of the samples. Support vector machine was used to grade the samples into three classes – Class I (best quality), Class II (intermediate quality) and Class III (poor quality). The average classification accuracy of tenfold cross validation of SVM was obtained as 83%. Thus, NIR based estimation of powdered leaf samples combined with SVM classifier can be a low-cost solution to grade the samples rapidly. A small range portable NIR instrument would serve as a field-lab deployable instrument for gradation of *Andrographis paniculata* samples by the industry.

The second study was conducted for evaluating the application of a portable NIR spectrometer for predicting the andrographolide content using different preprocessing and regression techniques. The portable spectrometer was built using bought out components. *Andrographis paniculata* samples were collected from West Medinipur, East Medinipur, Purulia, South 24 Parganas, Hooghly, and Kolkata districts of West Bengal, India that included different species. The spectral analysis was carried out in the range of 950nm-1700nm on the NIR spectra. The PLSR model developed using first derivative pre-processing was found to be slightly superior to SVM for estimating the andrographolide content in *Andrographis paniculata*. The PLSR model developed using first derivative pre-processed data yielded  $R^2_P$ , RMSEP and RPD<sub>P</sub> values of 0.99, 0.08 and 8.71 respectively. All in all, it may be concluded that NIR spectroscopy promises to be a feasible method for fast and accurate estimation of andrographolide in *Andrographis paniculata*, and prove to be a useful tool for its quality assessment.

Finally, a comparison study was carried out between commercially available and developed NIR spectrometer.

## References

- [1] T. Jayakumar, C. Y. Hsieh, J. J. Lee, and J. R. Sheu, “Experimental and clinical pharmacology of *Andrographis paniculata* and its major bioactive phytoconstituent andrographolide,” *Evidence-based Complementary and Alternative Medicine*, vol. 2013, no. Figure 1, 2013, doi: 10.1155/2013/846740.
- [2] Y. C. Shen, C. F. Chen, and W. F. Chiou, “Andrographolide prevents oxygen radical production by human neutrophils: Possible mechanism(s) involved in its anti-inflammatory effect,” *British Journal of Pharmacology*, vol. 135, no. 2, pp. 399–406, 2002, doi: 10.1038/sj.bjp.0704493.
- [3] N. P. Trivedi and U. M. Rawal, “Hepatoprotective and antioxidant property of *Andrographis paniculata* (Nees) in BHC induced liver damage in mice,” *Indian Journal of Experimental Biology*, vol. 39, no. 1, pp. 41–46, 2001.
- [4] Y. Dai, S. R. Chen, L. Chai, J. Zhao, Y. Wang, and Y. Wang, “Overview of pharmacological activities of *Andrographis paniculata* and its major compound andrographolide,” *Critical Reviews in Food Science and Nutrition*, vol. 59, no. 0, pp. S17–S29, 2019, doi: 10.1080/10408398.2018.1501657.

- [5] T. Jayakumar, C. Y. Hsieh, J. J. Lee, and J. R. Sheu, “Experimental and clinical pharmacology of *Andrographis paniculata* and its major bioactive phytoconstituent andrographolide,” *Evidence-based Complementary and Alternative Medicine*, vol. 2013, no. Figure 1, 2013, doi: 10.1155/2013/846740.
- [6] X. Y. Hu *et al.*, “Correction: *Andrographis paniculata* (ChuānXīnLián) for symptomatic relief of acute respiratory tract infections in adults and children: A systematic review and meta-analysis (PLoS ONE (2018) 12:8 (e0181780) DOI: 10.1371/journal.pone.0181780),” *PLoS ONE*, vol. 13, no. 11, pp. 1–30, 2018, doi: 10.1371/journal.pone.0207713.
- [7] P. K. Mukherjee, S. Bahadur, S. K. Chaudhary, A. Kar, and K. Mukherjee, “Quality Related Safety Issue-Evidence-Based Validation of Herbal Medicine Farm to Pharma,” in *Evidence-Based Validation of Herbal Medicine*, Elsevier Inc., 2015, pp. 1–28. doi: 10.1016/B978-0-12-800874-4.00001-5.
- [8] S. Borraz-Martínez, J. Simó, A. Gras, M. Mestre, and R. Boqué, “Multivariate Classification of *Prunus Dulcis* Varieties using Leaves of Nursery Plants and Near Infrared Spectroscopy,” *Scientific Reports*, vol. 9, no. 1, pp. 1–9, 2019, doi: 10.1038/s41598-019-56274-5.
- [9] A. K. Hazarika *et al.*, “Quality assessment of fresh tea leaves by estimating total polyphenols using near infrared spectroscopy,” *Journal of Food Science and Technology*, vol. 55, no. 12, pp. 4867–4876, 2018, doi: 10.1007/s13197-018-3421-6.
- [10] D. Kusumaningrum, H. Lee, S. Lohumi, C. Mo, M. S. Kim, and B. K. Cho, “Non-destructive technique for determining the viability of soybean (*Glycine max*) seeds using FT-NIR spectroscopy,” *Journal of the Science of Food and Agriculture*, vol. 98, no. 5, pp. 1734–1742, 2018, doi: 10.1002/jsfa.8646.
- [11] H. Cen and Y. He, “Theory and application of near infrared reflectance spectroscopy in determination of food quality,” *Trends Food Sci Technol*, vol. 18, pp. 72–83, 2007, doi: 10.1016/j.tifs.2006.09.003.
- [12] K. M. Lee and T. J. Herrman, “Determination and Prediction of Fumonisin Contamination in Maize by Surface-Enhanced Raman Spectroscopy (SERS),” *Food and Bioprocess Technology*, vol. 9, no. 4, pp. 588–603, 2016, doi: 10.1007/s11947-015-1654-1.



- [13] H. Cho, B. Lee, G. L. Liu, A. Agarwal, and L. P. Lee, "Label-free and highly sensitive biomolecular detection using SERS and electrokinetic preconcentration," *Lab on a Chip*, vol. 9, no. 23, pp. 3360–3363, 2009, doi: 10.1039/b912076a.
- [14] C. Muehlethaler, M. Leona, and J. R. Lombardi, "Towards a validation of surface-enhanced Raman scattering (SERS) for use in forensic science: repeatability and reproducibility experiments," *Forensic Science International*, vol. 268, pp. 1–13, 2016, doi: 10.1016/j.forsciint.2016.09.005.
- [15] P. K. Mukherjee, "Quality Control and Evaluation of Herbal Drugs," Elsevier Science, USA, 2019.
- [16] A. P. Raina, V. Gupta, N. Sivaraj, and M. Dutta, "Andrographis paniculata (Burm. f.) Wall. ex Nees (Kalmegh), a traditional hepatoprotective drug from India," *Genetic Resources and Crop Evolution*, vol. 60, no. 3, pp. 1181–1189, 2013, doi: 10.1007/s10722-012-9953-0.
- [17] A. P. Raina, V. Gupta, N. Sivaraj, and M. Dutta, "Andrographis paniculata (Burm. f.) Wall. ex Nees (Kalmegh), a traditional hepatoprotective drug from India," *Genetic Resources and Crop Evolution*, vol. 60, no. 3, pp. 1181–1189, 2013, doi: 10.1007/s10722-012-9953-0.
- [18] N. O. Reuben, P. A. Perez, M. A. Josiah, and M. M. Abdul, "Towards enhancing sustainable reuse of pre-treated drill cuttings for construction purposes by near-infrared analysis: A review," *Journal of Civil Engineering and Construction Technology*, vol. 9, no. 3, pp. 19–39, 2018, doi: 10.5897/jcect2018.0482.
- [19] D. Sing *et al.*, "Estimation of Andrographolides and Gradation of *Andrographis paniculata* Leaves Using Near Infrared Spectroscopy Together With Support Vector Machine," *Frontiers in Pharmacology*, vol. 12, no. May, pp. 1–8, 2021, doi: 10.3389/fphar.2021.629833.
- [20] S. N. J. and P. K. M. Dilip Sing, Ranajoy Mallik, Sudarshana Ghosh Dastidar , Rajib Bandyopadhyay , Subhadip Banerjee, "Prediction of Andrographolide Content in *Andrographis paniculata* Using NIR Spectroscopy," *IEEE Applied Signal Processing Conference (ASPCON)*, pp. 335–338, 2020.

- [21] A. Puttipipatkajorn and A. Puttipipatkajorn, “Development of calibration models for rapid determination of moisture content in rubber sheets using portable near-infrared spectrometers,” *Journal of Innovative Optical Health Sciences*, vol. 13, no. 02, p. 2050009, 2020.
- [22] K. Williams, P.; Norris, *Near-infrared technology in the agricultural and food industries*. American Association of Cereal Chemists, Inc., 1987.
- [23] D. Sing *et al.*, “Rapid estimation of piperine in black pepper: Exploration of Raman spectroscopy,” *Phytochemical Analysis*, 2021.

## **Chapter 6**

### **Conclusions and Future scopes**

## 6.1 Introduction

Medicinal plant is the most popular alternative medicine in the world enjoyed in many cultures by both rich and poor. But regardless of its wide consumption, consumer awareness in the quality has brought about consumption behavioural pattern changes over time. With the demand of quality medicinal plant in recent years, high standards of assurance and process control during manufacturing has become imperative. Quality estimation and valuation in medicinal plant industry is characterized by the traditional ‘art’ of human and by the elaborate and time consuming ‘science’ of biochemistry. Both of these estimations are done with the finished medicinal plants, i.e., at the end of the entire manufacturing process; thus, do not qualify for on-site inspection and control of the intermediate steps. The consistency and conformity in quality during manufacturing of medicinal plant is entirely operator dependent, and may be prone to human error or slackness.

In the last few decades, the application of computer/electronics to support the human sensory panel in making subjective judgments is a growing area of research. Researchers have explored the non-invasive instrumental techniques to improve quality of the made-medicinal plant following monitoring and control during manufacturing and hence to develop commercially acceptable quality monitoring tools for medicinal plant processing industry. Instrumental methods are guaranteed to produce accurate and reproducible qualitative and quantitative indications of major quality attributes. Therefore, on-site estimation and corrective manipulation of these parameters using appropriate instrumental techniques (especially, Raman and Near Infrared Spectroscopy) would enable us to exercise control over the dynamics of chemical changes during processing of medicinal plant.

The objective of this thesis work was to address this issue; to develop real time electronic sensing technique, i.e., portable Raman and near infrared spectroscopic methodologies for estimation of two key medicinal plant quality parameters viz. piperine in black pepper and andrographolides in *Andrographis paniculata*. It is expected that, successful estimation of key components of biomarker of medicinal plant will open up opportunities of controlling down-stream process conditions, enabling improved product consistency despite variability in raw material, and hence enhanced end product quality.

## 6.2 Summary of findings

### 6.2.1 Development of a portable Raman spectrometer

The design and development of a portable Raman spectrometer with customized GUI is discussed in detail in Chapter 2. During the design of our work, the mechanical, optical, and other components were chosen in such way that the end product becomes a portable and low-cost one. The Raman spectrometer was developed using bought out components from different companies. This work was tedious and took substantial time in our research work. This led to the development of the “portable Raman spectrometer” which drastically reduced the instrument size and cost. The machine could be easily set up at the field of a medicinal plant factory for in situ estimation/inspection. The integrated Raman spectrometer consists of laser power supply, optical head and detector and a customized GUI was developed to estimate the piperine content in black pepper for assessing its quality. The detail of the machine along with the calibration and validation are explained in this chapter.

### 6.2.2 Estimation of piperine in black pepper

In this work, a methodology is proposed for determining the content of piperine in black pepper berries using Raman spectroscopy. In this study, we present a simple, rapid and green analytical method based on Raman spectroscopy for the quantitative assessment of piperine (chapter 3). To assess the potential of the technique, we report the complete vibrational characterisation of the piperine with density functional theory (DFT) calculations. The theoretical peaks were obtained at  $1097\text{ cm}^{-1}$ ,  $1388\text{ cm}^{-1}$ ,  $1528\text{ cm}^{-1}$ ,  $1578\text{ cm}^{-1}$ , and at  $1627\text{ cm}^{-1}$ , and this result was verified in a Raman spectrometer followed by a preliminary experiment. Twenty black pepper samples were analysed using high-performance liquid chromatography (HPLC) and used as reference data for Raman analysis. The Raman shift spectra were analysed using partial least squares (PLS) and good prediction accuracy with correlation coefficient of prediction ( $R_p^2$ ) = 0.93, root mean square error of prediction (RMSEP) = 0.13 and residual prediction deviation (RPD) = 3.9 were obtained.

### 6.2.3 Development of a portable NIR spectrometer

It was discussed in detail in Chapter 4 that, a 3D of NIR model was created during design process using solid works software. Before, finalizing the design, the key factor was the cost

and availability of different optical components in the market. This led to the development of the “portable NIR” which is compact and low cost. The system could be easily set up at the field of a medicinal plant factory for in situ estimation/inspection. The portable NIR has a light source and optical components and detector, and a GUI for the quantitative estimation of andrographolides in *Andrographis paniculata* for its gradation and quality assessment. The detail of the machine along with GUI is explained.

#### **6.2.4 Assessment of andrographolides in *Andrographis paniculata***

In this study, a methodology has been proposed to grade *Andrographis paniculata* samples using NIR spectroscopy and SVM classifier based on the content of marker molecules, andrographolides (chapter 5). Relative accuracies of estimating the andrographolides by NIR spectra of methanol extracts of the samples, and powdered leaf samples were compared taking the estimates obtained from HPLC analysis as the standard. The accuracy of estimation based on extracts was a little higher than the powdered leaf samples. But it did not change the grading pattern of the samples. Support vector machine was used to grade the samples into three classes—Class I (best quality), Class II (intermediate quality) and Class III (poor quality). The average classification accuracy of tenfold cross validation of SVM was obtained as 83%. Thus, NIR based estimation of powdered leaf samples combined with SVM classifier can be a low-cost solution to grade the samples rapidly. A small range portable NIR instrument would serve as a field-lab deployable instrument for gradation of *Andrographis paniculate* samples by the industry.

### **6.3 Limitations during development of instruments and models**

Few shortcomings faced during our research work are listed below:

- The powdered medicinal plant samples contain particles of different sizes, which cause scattering of light. This scattering effect exhibits systematic variations on the baseline and may play a significant role for variability of the spectra from sample to sample. To reduce spectral variability, Standard Normal Variate (SNV) and Multiplicative Scatter Correction (MSC) were used as data pre-processing methods. Further, measurements were taken in triplicate to minimize any error due to light scattering, multi-collinearity and atmospheric influences.

- The NIRS approach necessitates not just a precise reference analysis, but also a big and current calibration data set. Utmost care was taken, with replication of reference biochemical analysis on a large number of medicinal plant samples, to nullify this shortcoming.
- Because near infrared sensors have a limited detection range, they can't be used to analyse chemicals with low concentrations (below 0.1 percent). The minimum concentrations of piperine and andrographolides, considered in our study, were 0.95% and 0.6% respectively.
- The researcher must correct for any interfering ambient circumstances like light and humidity while using near infrared equipment for on-site studies. Precautions were taken to maintain the light, relative humidity and even temperature, constant during data acquisition. Further, multiple readings were taken for each sample, and the average was used during model development.

#### **6.4 Future scopes of research**

- Raman and NIR models for other key biochemicals (responsible for quality) like gallic acid.
- The models developed may be optimized for online measurements during medicinal plant processing.
- Development of low-cost and miniatures Raman and NIR spectrometer with lithium-ion battery.
- Development of low-cost detector for Raman and NIR spectrometer.

With success in such endeavours, the applications of Raman and NIR spectroscopy will become an asset and widely acceptable to Indian medicinal plant industry in near future.

#### **6.5 Final remarks**

Successful estimation and monitoring of key quality parameters of medicinal plants in a medicinal plant factory, during processing and the final product is expected to open up opportunity of controlling down-stream process conditions based on up-stream monitoring. With these controls in place, a range of quality outcomes can be manipulated— enabling improved product consistency despite variability in raw material, and enable overall enhanced end product quality. The portable Raman and NIR machine and methodologies

developed under this thesis work have been demonstrated for rapid estimations of two key quality parameters, piperine in black pepper and andrographolides in *Andrographis paniculata*, but similar methodology can be adopted for other medicinal plant products and it is expected to usher in a new paradigm in the medicinal plant industry.

